MICROBIAL DIVERSITY IN SEDIMENTS AND GAS HYDRATES ASSOCIATED WITH COLD SEEPS IN THE GULF OF MEXICO

A Dissertation
Presented to
the Academic Faculty

By

Heath Jordan Mills

In Partial Fulfillment
of the Requirements for the Degree
Doctor of Philosophy in the
School of Biology

Georgia Institute of Technology
June, 2004

MICROBIAL DIVERSITY IN SEDIMENTS AND GAS HYDRATES ASSOCIATED WITH COLD SEEPS IN THE GULF OF MEXICO

Approved by:

Patricia A. Sobecky (Committee Chair)

Thomas DiChristina

Joseph Montoya

Frank Loeffler

Roger Wartell

Date approved: 7 July, 2004

This dissertation is dedicated to my wife Jennifer. Her patience has allowed me to chase my dreams and accomplish my goals. I can only hope that throughout our life time together, I can find ways to repay her.

ACKNOWLEDGMENTS

I would like to acknowledge the people that have contributed to this work. I thank my advisor, Dr. Patricia Sobecky, for providing me guidance and the opportunity to work in her laboratory. I would like to thank my committee members Drs. Thomas DiChristina, Joseph Montoya, Frank Loeffler and Roger Wartell for their guidance and support. I would also like to thank the numerous graduate and undergraduate members of the Sobecky lab that have worked with me during my years at Georgia Tech. I would like to thank Sandra Story for isolating portions of the RNA used in this study. I would also like to especially thank Cassie Hodges for her continuous support in the Sobecky lab. In addition, I would like to thank the crews of the *R/V Seward Johnson I* and *II*, and the *Johnson Sea Link* for assisting in sample collection. This work was supported by National Science Foundation LExEn grant OCE-0085549. Support for submersible operations was provided by NOAA NURP and DOE NETL.

TABLE OF CONTENTS

LIST OF TABLES

LIST OF FIGURES

LIST OF SYMBOLS or ABBREVIATIONS

AB	Artesian Basin
AC	anaerobic consortium
ACR	Atlantic Ocean continental rise
AD	anaerobic digestor
AOM	anaerobic oxidation of methane
ANAMMOX	anaerobic ammonia oxidation
ANME archaea	anaerobic methane oxidizing archaea
AS	anoxic sediment
BM	benzene mineralizing
BR	bioreactor
CA	contaminated aquifer
CG	contaminated groundwater
CM	Cascadia Margin
crDNA	complementary ribosomal deoxyribonucleic acid
CS	coastal sediments
DAPI	4’,6-Diamidino-2-phenylindole
DC	dechlorinating consortium
DEPC	diethylpyrocarbonate
DGGE	denaturing gradient gel electrophoresis
DNA	deoxyribonucleic acid
DS	deep sea

DSS	deep subsurface
DV	deep-sea volcano
ER	Eel River Basin
FISH	fluorescent *in situ* hybridization
FW	forested wetland
GB	Guaymas Basin
GoM	Gulf of Mexico
HAB	hydrocarbon associated bacteria
HI	Hawaiian islands
HRC	hydrate recovery chamber
HS	hydrocarbon seep
HSC	hydrate stabilization chamber
HV	hydrothermal vent
IH	interior hydrate
JT	Japan Trench
LL	landfill leachate
MA	Mid-Atlantic Ridge
MB	marine bacterium
MC	methanogenic consortium
MF/MOF	Monterey formation
MS	marine sediment
NS	North Sea
NT	Nankai Trough

PCR	polymerase chain reaction
RC	Republic of Congo
RFLP	restriction fragment length polymorphism
RM	rice microcosms
RNA	ribonucleic acid
RP	rhizoplane
rRNA	ribosomal ribonucleic acid
RS	root sediment
RT-PCR	reverse transcription polymerase chain reaction
RuBisCo	ribulose bisphosphate carboxylase-oxygenase
SA	Southern Aegean Sea
SB	Santa Barbara Basin
SC	South China Sea
SEH	sediment entrained hydrate
SM	salt marsh
SO	Sea of Okhotsk
SS	Svalbard sediments
SRB	sulfate reducing bacteria
TCE	trichloroethene contaminated site
Th.	*Thermus*
T-RFLP	terminal restriction fragment length polymorphism
TS	thioautotrophic symbiont II
UM	uranium mine

Un. 1	unclassified *Bacteria* group 1
Un. 2	Unclassified *Bacteria* group 2
Unclass. Eur.	Unclassified *Euryarchaeota*
WW	wastewater
YS	Yellowstone

SUMMARY

A molecular phylogenetic approach was used to characterize the composition of microbial communities from two gas hydrate sedimentary systems in the Gulf of Mexico. Nucleic acids were extracted from three distinct locales on surface breaching gas hydrate mounds, i.e., sediment overlaying gas hydrate, sediment/hydrate interface and sediment-free hydrate, and from three sediment depths, i.e., 0-2, 6-8 and 10-12 cm, in *Beggiatoa* sp. mat-associated sediments located several meters from exposed gas hydrate. Samples were collected from a research submersible (water depth 550-575 m) during two research cruises aboard the *R/V Seward Johnson I* and *II* funded by the NSF Life in Extreme Environments program. The 16S rRNA gene and 16S rRNA were amplified using PCR and reverse transcription-PCR, respectively, from DNA and RNA extracted from the total microbial community. The primers targeted microorganisms at the domain-specific, i.e., *Bacteria* and *Archaea*, and group-specific, i.e., sulfate-reducing bacteria (SRB) and putative anaerobic methane-oxidizing (ANME) archaea, level. Sequence analysis of the *Bacteria* clones revealed that the microbial communities were primarily dominated by *Deltaproteobacteria*. Other *Proteobacteria* classes, including *Epsilon*- and *Gammaproteobacteria*, represented a large fraction of the total microbial community isolated from the sediment overlying hydrate sample and the metabolically active fraction of the 0-2 cm sediment depth sampled from the *Beggiatoa* sp. mat-associated sediments. Sequence analysis indicated the majority of the archaeal clones were most closely related to *Methanosarcinales*, *Methanomicrobiales* and distinct lineages within the ANME

groups. Several novel lineages were identified including a fourth ANME-2 clade, i.e., ANME-2D, and three clades with no closely related previously sequenced 16S rRNA gene clones or isolates, i.e., Unclassified *Bacteria* groups 1 and 2 and Unclassified *Euryarchaeota*. These studies represent the first 16S rRNA gene and 16S rRNA phylogenetic-based description of microbial communities extant in sediment-free gas hydrate and in methane-rich hydrate-associated and *Beggiatoa* sp.-associated sediments from a hydrocarbon seep region in the Gulf of Mexico.

CHAPTER 1

INTRODUCTION

Gas hydrates, ice-like crystalline solids composed of rigid water molecule cages that trap hydrocarbon gas molecules, are projected to become the main source of hydrocarbon-based energy for this century (55). Hydrates are an attractive energy resource because of the immense volume of methane sequestered at shallow sediment depths (< 2000 m) and their wide geographical distribution (86). An estimated 50% of the total organic carbon on earth, twice that of conventional fossil fuels, is trapped within hydrates (84). Estimates of total hydrate-bound methane gas resources in the marine subsurface exceed 10^{16} m^3 (39, 55). The US Exclusive Economic Zone alone potentially contains $>10^{15}$ m^3 of hydrate-bound methane (25), with ~40% localized in the Gulf of Mexico (25, 83). Interestingly, the technologies necessary to harvest methane in this form may not be available until after 2030 (55).

Whereas the geochemistry and economic importance of these Gulf of Mexico (GoM) seep sites is well documented, the ecosystems within these environments, potentially affecting hydrate formation and dissolution, are less understood. In this study, the microbial communities from two GoM seep sites, i.e., GC185 and GC234 (Figure 1.1), were characterized using molecular techniques including cloning of PCR and reverse transcription PCR derived amplicons of 16S rRNA genes and 16S rRNA, respectively, restriction fragment length polymorphism analysis, and DNA sequencing. Characterization of these extreme environment microbial communities can help understand the processes present in GoM cold seeps, but, may also

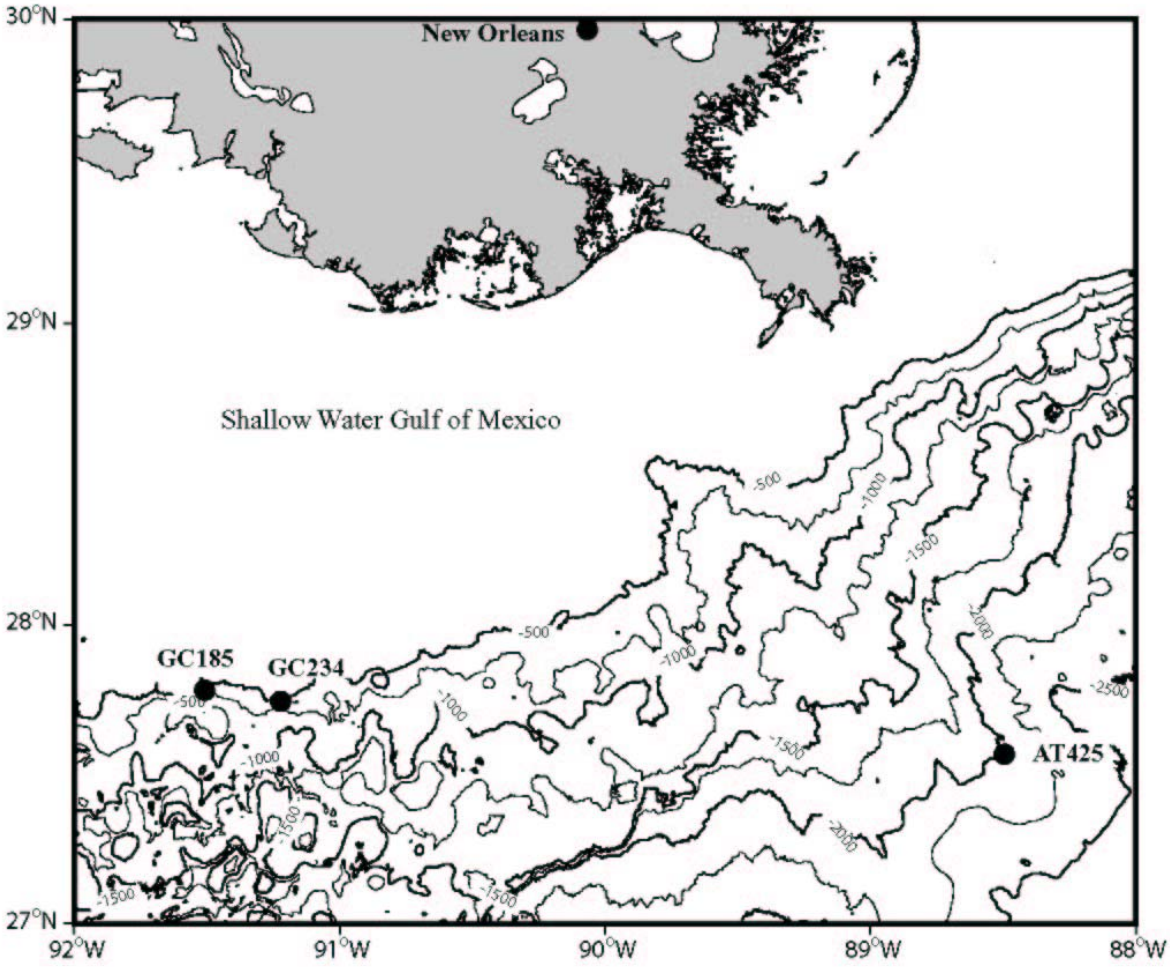
30°N
29°N
28°N
27°N
92°W
91°W
90°W
89°W
88°W
New Orleans
Shallow Water Gulf of Mexico
GC185
GC234
AT425
-500
-1000
-1500
-2000
-2500

increase the accepted boundaries where life is known to exist and potentially identify novel organisms with medical and industrial applications.

1.1 Gulf of Mexico cold seep geology

The seafloor of the Gulf of Mexico (GoM) has been extensively mapped using acoustic based techniques (31, 129, 138, 181) as a result of the continuous search for oil reserves. As a result, numerous features including canyons, mud volcanoes, pockmocks, carbonate encrusted surfaces, and surface breaching gas hydrates have been detected across the northern GoM continental slope. Additionally, ship-based sonar can detect immense gas plumes extending hundreds of meters up into the water column emanating from active vents. A majority of these geologically influenced features can be attributed to the slow rise of subsurface salt diapirs.

1.1.1 Diapirism in the Gulf of Mexico

The constant slow rise of numerous subsurface salt diapirs dominates the active geologic forces present in the GoM (Figure 1.2). The history of GoM diapirism began when crustal rifting led to the formation of many subbasins, during the Late Triassic-Middle Jurassic (140). During the Middle Jurassic, thick Callovian salt (Louann Formation) was deposited (106). Rapid sediment deposition followed during the Cenozoic (181). The sedimentation deformed the Callovain salt into allochthonous sheets (181) providing the basis for future daipir activity (140). The diapirs extend upward from the large salt deposits to depths ranging from several km to over 15

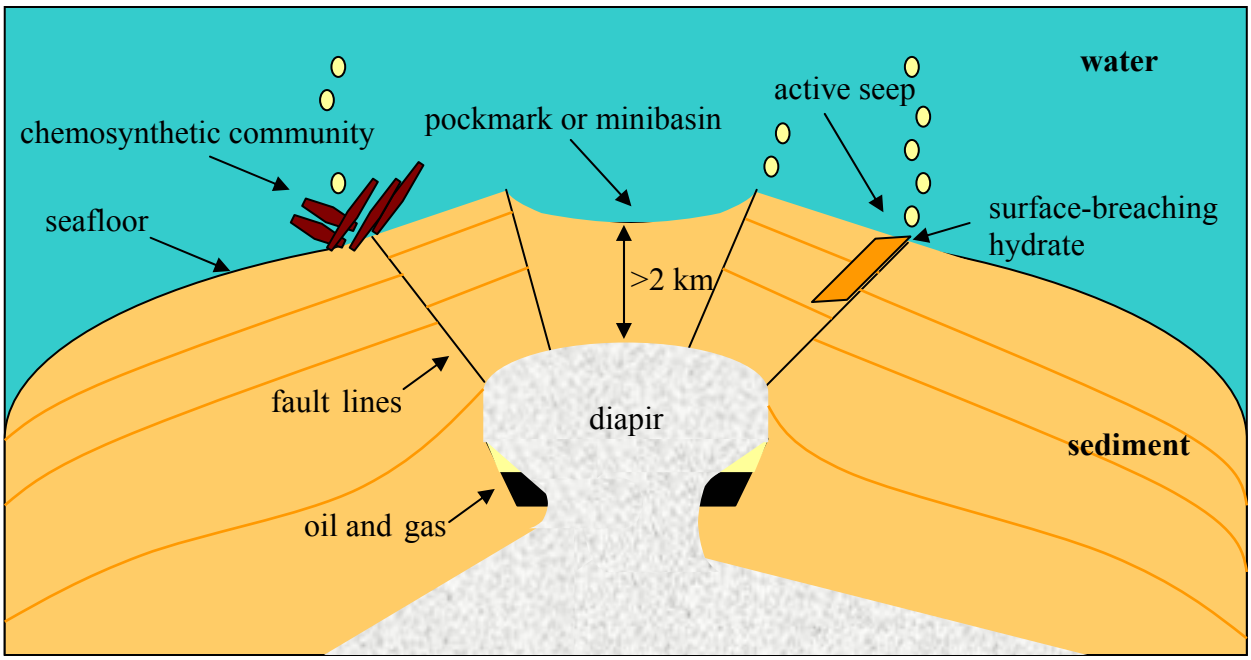

Figure 1.2 Diagram of a subsurface salt diapir. As buoyant salt diapers several km beneath the sediment surface rise, faults form as the overlying sediments fracture (138). These faults act as conduits for subsurface oil and gas deposits to reach the upper sediments (47, 141). As the sediments slump away from the rise center of the salt diapir, pockmarks or minibasins can form (138). The venting gas and oil supports the formation of diverse chemosynthetic communities and gas hydrates (148). Adapted from Ruppel (unpublished).

km beneath the GoM seafloor (138). These rising salt domes can be detected and measured using bathymetric maps, seismic profiles and thermal projections. As the diapir rises, the compression of overlying sediments produces sufficient force to exceed overburden pressures, thus causing the sediment to fracture and form faults and slumps (138). Shallow (2-3 km) Mesozoic oil and gas reserves (79) utilize the faults as conduits to reach the upper sediments (47, 141). Active faults, predominately located near the rims of the minibasins and over salt ridges (142), localize high concentrations of oil and gas, promoting the formation of both chemosynthetic communities and shallow gas hydrates [Figure 1.2; (148)].

1.1.2 Vent gas formation

Active venting of hydrocarbon gas has been reported at numerous locales in the northern GoM (31, 143, 147). Expansive gas and oil reserves in the deeply buried Mesozoic hydrocarbon system (6-10 km) and connecting shallower accumulations (2-3 km) migrate to the surface through diapir-derived faults. In the upper sediment and water column, the venting hydrocarbon gas has been identified as both thermogenic and biogenic in origin. Thermogenic gas, including C_1-C_5 alkanes and CO_2, is produced by long-term exposure of hydrocarbons (oil) to high temperatures and pressures. The majority of evolved thermogenic gasses exit the sediment by venting directly into the water column (142). In contrast to the deep subsurface origin of thermogenic hydrocarbon gas, biogenic gas, predominately methane, is produced by the microbial reduction of carbon compounds at shallow sediment depths. In general, microbes selectively utilize lighter, or lower mass, isotopes in metabolic processes (e.g., ^{12}C is

preferentially utilized before ^{13}C). Therefore, a comparison of hydrocarbon gas isotopic ratios can identify whether the origin of the vent gas is thermogenic (higher ratio of heavy isotopes, $\delta^{13}C = \sim$-43‰) or biogenic (higher ratio of light isotopes, $\delta^{13}C = \sim$70‰) (12). Therefore, vent gas sampled from both GoM sites, GC185 and GC234, having $\delta^{13}C$ values between -42‰ and -46‰ suggest a thermogenic origin (142, 144). Over 90% of the vent gas is composed of methane, with a decreased relative abundance of gases containing increasing carbon numbers, i.e., C_2-C_5 (150). Such hydrocarbon distributions suggest unaltered thermogenic reservoir gas associated with crude oil deposits (71, 149). Similar vent gas isotopic signatures and C_1-C_5 compositions detected at GC185 and GC234 suggest the same Mesozoic subsurface hydrocarbon system as a possible subsurface gas source (142).

1.1.3 Gas hydrates

1.1.3.1 Gas hydrate structural characteristics

Within the sediment, a fraction of the vent gas undergoes a rapid phase change becoming entrapped within solid gas hydrate (150). Clathrate gas hydrates are formed by weak van der Waals interactions between gas and water molecules in an open arrangement that allows the gas to occupy nearly spherical cavities within a water molecule cage [reviewed in (15)]. A majority of the cavities (>70%) must be gas filled to prevent structural destabilization, although a completely gas filled clathrate is not predicted to be found in nature [reviewed in (156)]. During crystallization, vent gas undergoes molecular fractionation to assure optimal molecule size for the structure of the water molecule cage (156). To date, three different structures, i.e., Structure I, II and H

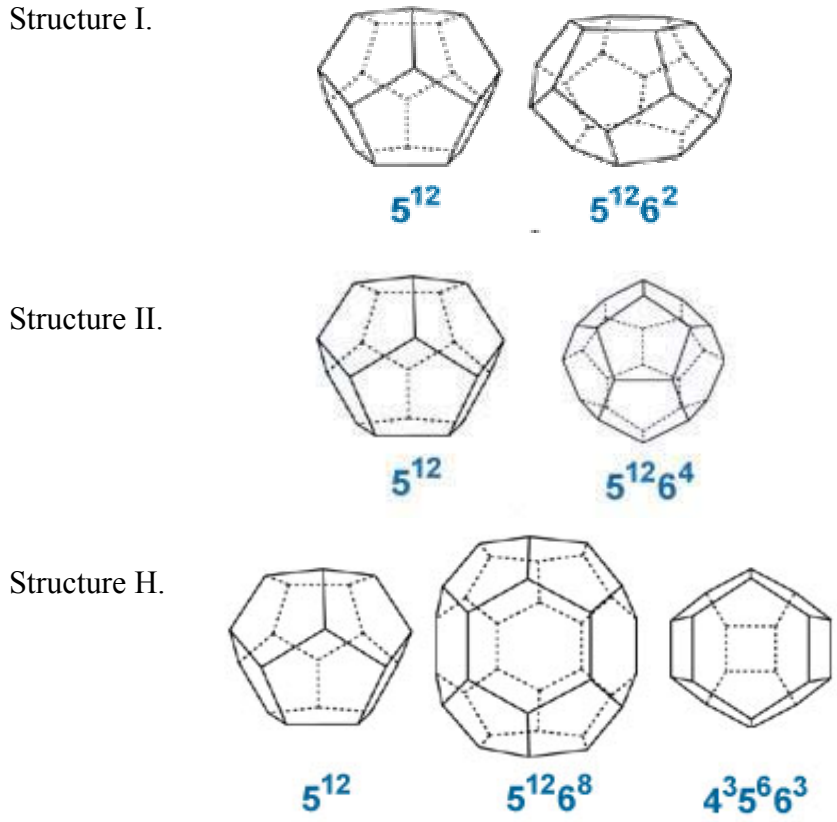

Figure 1.3 Gas hydrate Structures I, II, and H. The 3 known gas hydrate structures are composed of multiple gas filled water molecule cavities. Structure I, the smallest of the three structures, and Structure II form two cavities each with unit cells comprising 46 and 136 water molecules, respectively (177). Structure H has a unit cell of 34 water molecules forming a hexagonal lattice with three cavity types, i.e., pentagonal dodecahedra, a $5^{12}6^8$ and a $4^35^66^3$ (136). The numbers beneath each structure represent the number of water molecules per face, while the superscript values indicate the number of such faces forming that cavity. Therefore, 5^{12} represents 12 pentagonal faces, or a pentagonal dodecahedron cavity.

(Figure 1.3), have been identified in natural environments. Structure I, the most common structure in nature (156), forms a unit cell of two small pentagonal dodecahedron cages and six large tetradecahedral cages, optimally resulting in eight gas molecules trapped per 46 water molecules (72, 93, 156). The size and stability of Structure I cages dictates that a minimum of 90% of the gas-filled cages contain methane (64). Primarily, this methane is biologic in origin (72, 93). Thermogenic Structures II and H are capable of incorporating larger hydrocarbons (C_1-C_5), carbon dioxide and hydrogen sulfide (12, 76, 156). Structure II, first sampled in the GoM at a water depth of 530-560 m (13), has a unit cell consisting of 16 small dodecahedrons and eight large hexakaidecahedral cages, together incorporating 136 water molecules with up to 24 entrapped gas molecules (93). In contrast to the methane concentrations of Structure I, Structure II gas hydrate sampled from GC185 and GC234 is typically composed of 72-86% methane (142). Structure H (hexagonal lattice), first reported occurrence naturally at GC185, incorporates C_1-C_5 gases, although predominantly composed of *i*-C_5 (41.1%) (146) within three cages forming a unit cell of only 34 water molecules (80). However, this structure encloses four times more volume than Structure I (80).

1.1.3.2 Conditions for hydrate formation.

To date, more than 50 thermogenic and biogenic gas hydrate accumulations have been identified in the northwest GoM continental slope margin (440-2400 m water depth) (12, 13, 142, 150). Hydrates form when hydrocarbon gases, mainly C_1-C_5, actively vent through sediment porewater at specific temperatures, pressures and dissolved gas concentrations. Phase equilibrium calculations predict the stability of gas hydrates at

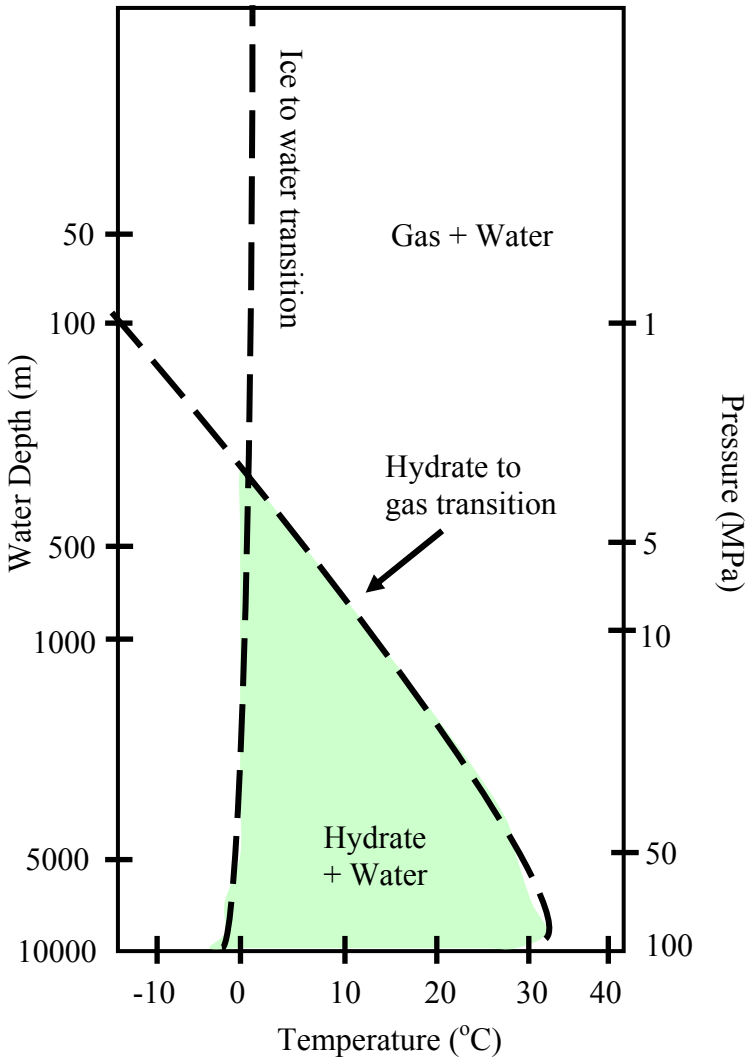

Figure 1.4 Phase diagram showing pressure and temperature boundaries for hydrate stability. The conditions for hydrate formation in this diagram assume pure water. The addition of salts shifts the boundary to the left. The influx of C_2-C_5, CO_2, or H_2S to the methane shifts the boundary to the right. Depth scale assumes lithostatic and hydrostatic pressure gradients of 10.1 kPa m^{-1} (86). Redrawn after Katz et al. (77).

various temperatures, pressures and gas concentrations, thus determining the gas hydrate stability zone (GHSZ) (Figure 1.4) (156, 186). The methane concentration at which saturation is achieved in water decreases with a reduction of temperature and a pressure increase. Over saturation of dissolved gases forces the gases out of the liquid phase, promoting gas hydrate formation. In natural environments, additional factors that facilitate hydrate formation include, but are not limited to dissolved salts (37) and texture and mineralogy of surrounding sediments (23, 58). Ambient water temperatures (~7^{o}C) at the GoM continental shelf sea floor (water depths of ~550 m) (97) support shallow sediment, as well as surface breaching gas hydrate formation. However, the amount of geologic heating in the sediment rises with increased sediment depth, thus creating a lower thermal boundary to the gas hydrate stability zone (187). Thus according to the phase diagram (Figure 1.4), below a certain sediment depth, liquid water and free methane gas would coexist without gas hydrate formation (106). Formation of hydrates at the lower edge of the GHSZ can form a seal blocking the upward migration of gases through the sediments, thus trapping pools of gas (55). The potential disruption of this seal during active drilling represents a significant risk to surface vessels (55). As deepwater oil production continues to increase [e.g., such drilling exceeded shallow water drilling for the first time in 1999 (7)], a greater importance is placed on detecting and identifying hydrate fields.

1.1.3.3 Detection of gas hydrates

The presence of a bottom simulating reflector (BSR) in seismic profiles is a widely recognized indicator of the presence of subsurface gas hydrate. A BSR is created

by an acoustic impedance contrast between solid and vapor phases, typically forming when gas concentrations exceed the saturation point at the base of the gas hydrate stability zone (4, 70). The BSR thus represents the sediment depth at which solid and gaseous phases of methane are at equilibrium, and therefore can vary with temperature and pressure changes (52, 55). The amplitude of the BSR is determined by the hydrate concentration and sediment porosity (19). Although hydrate has been observed in large quantities in the northern GoM slope provinces, acoustic profiles of GoM sediments indicate that BSRs are either absent or in low abundance (105).

1. 2 Gulf of Mexico cold seep chemosynthetic communities

Numerous seep locales in the GoM support diverse biological communities that rely on chemosynthetic bacteria as the energetic basis for the ecosystem (Figure 1.5). Below the photic zone, these primary producers oxidize reduced compounds, i.e., methane and hydrogen sulfide, released at active vent systems, providing the energy necessary to synthesize organic compounds utilized by higher trophic levels. The inundation of crude oil into the upper sediment layers and the presence of surface breaching gas hydrate provide a unique environment for examining biological diversity.

1.2.1 Symbiotic macrofaunal communities

The first biological characterizations of GoM cold seep chemosynthetic communities examined the physiology of vestimentiferan tubeworms and methanotrophic mussels (14, 78, 96). Two main genera of tubeworms have since been classified from the

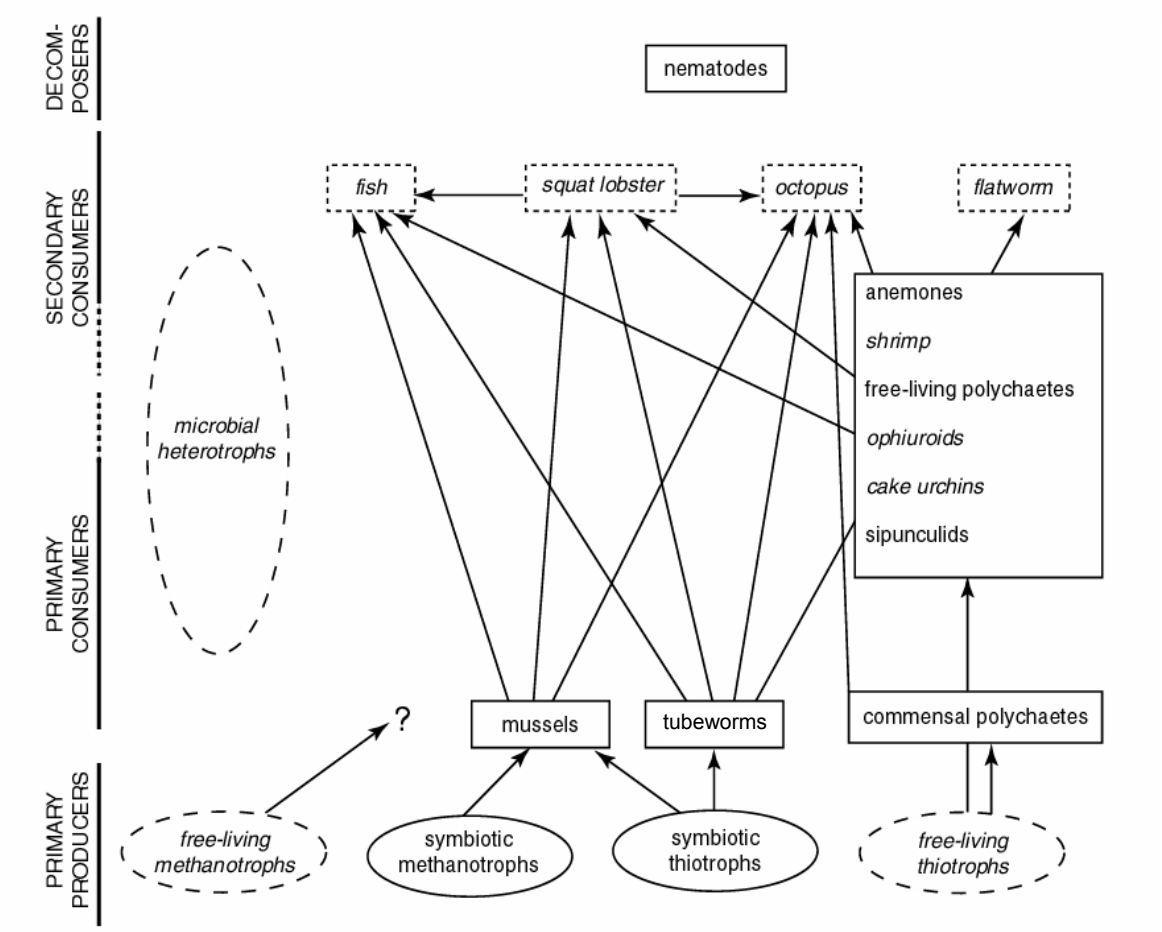

Figure. 1.5 Schematic detailing cold seep chemosynthetic community energetics. Chemoautotrophic methanotrophs and thiotrophs convert inorganic compounds into organic molecules utilizing energy gained from reduced compounds abundant at the cold seeps (i.e., CH_4 and H_2S, respectively). These groups are either directly associated with primary consumers in a symbiotic relationship (22, 43), or are grazed by or provide secondary metabolites to heterotrophic microbes and higher organisms (116). Higher trophic levels acquire their energy from lower trophic levels, providing the energy transfer necessary to sustain a complex chemosynthetic community (142). Adapted from Van Dover (unpublished).

GoM, including *Lamellibrachia* and *Escarpia*, both related to the well characterized hydrothermal vent tubeworm, *Riftia pachyptila* (49). The dominant GoM tubeworm species, *Lamellibrachia* cf. *luymesi* produces relatively straight tubes that extend over a meter into the water column. Aggregations of *L.* cf. *luymesi* can include 500-2000 individuals, while groups of aggregations may involve over 100,000 individuals and encompass 1,600 m^2 (96). Estimates of the *L.* cf. *luymesi* life span suggest these species can live at least 170-250 years (8, 46). Observations of large tubeworm bushes suggest that these genera may provide a matrix which numerous arthropod and gastropod species can utilize as a habitat for survival.

The most common mussel species identified at GoM cold seep environments is *Bathymodiolus childressi*. *B. childressi* has been observed in numerous GoM environments, including surface breaching hydrate sediments at GC234 (119) and in close proximity to brine pools (157). The range of *B. childressi* shell sizes varied across three distinct zones at a brine pool, from 10 to 70 mm with maximum sizes of ~134 mm in the inner zone, to an average size of 115 mm for both the middle and outer zones (157). The size of the mussels sampled from the inner zone was also the most variable across multiple sample dates (157). This zone was also more than three times more densely populated and contained mussels in the best physiological condition compared to the other zones (157). Water geochemistry measurements indicated that the inner zone contained the highest methane and oxygen concentrations and lowest sulfide concentrations in the mussel beds (81, 157). Compared to the brine pool mussels, *B. childressi* identified at GC234 hydrate associated sediments were smaller, grew slower and were generally in poorer physiological condition (119). Interestingly, methane

concentrations were similar between the brine pools and hydrate-associated sediments (119, 157). Smith et al. (157) hypothesize that the increased hydrocarbon (oil) concentrations reduce the growth and fitness of hydrate-associated mussel beds.

Although the two genera of tubeworms and one genus of mussels have different growth characteristics, all require microbial endosymbionts for energy production. Both genera of GoM tubeworms possess thiotrophic bacteria endosymbionts localized within the worm's trophosome (43). The tubeworms take up H_2S from the sediment using their posterior extension or "root" (49, 75) while absorbing oxygen and carbon compounds from the water column using their anterior extension. Digestion of symbiont tissue or adsorption of symbiont released metabolic byproducts provides a nutrient source for the host tubeworm. In contrast to the tubeworm incorporation of thiotrophic bacteria, the mussel species *B. childressi* incorporates methanotrophic endosymbionts within its gill tissue (22). Isotopic signatures of methane carbon incorporated in host tissue support mussel nutrient acquisition from the endosymbionts (22, 44, 160). In addition, juvenile mussels were able to grow using methane as the sole carbon and energy source (17). Therefore, tubeworms and mussels have different isotopic signatures as a result of their thiotrophic and methanotrophic bacteria endosymbionts utilizing different carbon sources, i.e., dissolved CO_2 or methane, respectively, (28, 43, 95).

1.2.2 Cold seep microbial communities

Existing below the photic zone, chemoautotrophs from GoM cold seep environments use readily abundant reduced substrates, i.e., H_2S and CH_4 (28, 75), to provide the energy necessary for organic carbon synthesis. Thiotrophic (H_2S oxidizing)

bacteria utilize inorganic carbon dissolved in the pore water, whereas methanotrophic (CH_4 oxidizing) bacteria use CH_4 (28, 43). These symbiotic organisms, as well as their free-living counterparts, comprise the bulk of the primary producers in the cold seep environment (Figure 1.5). Research on thiotrophic and methanotrophic bacteria in the GoM has described their symbiotic relationship with tubeworms and mussels (49, 157). Although fewer studies have focused on free-living primary producers, thiotrophic orange- and white-pigmented *Beggiatoa* spp. have been well characterized from numerous seep locales (2, 74, 116, 148). Interestingly, no pure cultures of marine *Beggiatoa* spp. have been obtained. Additionally, molecular characterizations of the microbial communities associated with the sediments beneath the *Beggiatoa* sp. mats are lacking.

1.2.2.1 Microbial mats

Numerous reports have characterized the physical and metabolic properties of GoM mat forming, anaerobic sulfur-oxidizing, orange- and white-pigmented *Beggiatoa* spp. (89, 116, 148, 182). The source of the orange pigmentation has yet to be determined, however, similarly pigmented *Beggiatoa* spp. have been described in Monterey Canyon (6). Microscopic observations indicate that GoM *Beggiatoa* spp. range in filament width from 20-200 μm (116, 148, 182) and contain numerous sulfur granules (116). Visible *Beggiatoa* sp. mats generally occur in close proximity to active gas vents, tubeworms and mussels, or covering shallow gas hydrate deposits (43, 56, 96). White- and orange-pigmented *Beggiatoa* spp. have been observed to be spatially separated, suggesting a possible competitive exclusion (96, 116, 146). A single *Beggiatoa* sp. cell is capable of

coupling nitrate reduction to the anaerobic oxidation of H_2S, producing ammonia and sulfate as end products (Figure 1.6). *Beggiatoa* sp. have been reported to migrate from the sediment surface to depths >10 cm, potentially in response to H_2S gradients (116). Ribulose bisphosphate carboxylase-oxygenase (RuBisCo) activities (115) and $\delta^{13}C$ values (148) support the hypothesis that white-pigmented *Beggiatoa* are chemosynthetic, using CO_2 for carbon and H_2S for energy. However, a lack of RuBisCo activity and carbon fixation activity for orange-pigmented species suggests that they are heterotrophic (116). The sediment geochemistry beneath the microbial mats indicates partial bacterial oxidation of oils and C_1-C_5 gases (78, 145), suggesting additional microbial species are active at depth. To date, no studies have examined the metabolically active fraction of the total microbial community, i.e., *Bacteria* and *Archaea*, across a sediment depth profile within and beneath a *Beggiatoa* sp. mat.

1.2.2.2 Anaerobic methane oxidizing archaea

Distinct archaeal lineages common to several cold seep environments, i.e., anaerobic methane oxidizing archaea group 1 (ANME-1) and group 2 (ANME-2) (62, 123), can oxidize CH_4 in anaerobic environments, unlike methanotrophic bacteria. To make anaerobic oxidation of methane (AOM) energetically favorable for the archaea, this process has been hypothesized to be coupled to the reduction of sulfate. The net equation describing the AOM reaction is as follows:

$$SO_4^{2-} + CH_4 \rightarrow H_2S + CO_3^{2-} + H_2O \quad (63, 133)$$

16S rRNA gene phylogenetic analysis of the two archaeal lineages associated with AOM, i.e., ANME-1 and ANME-2, reveals sequence similarity to the methanogenic

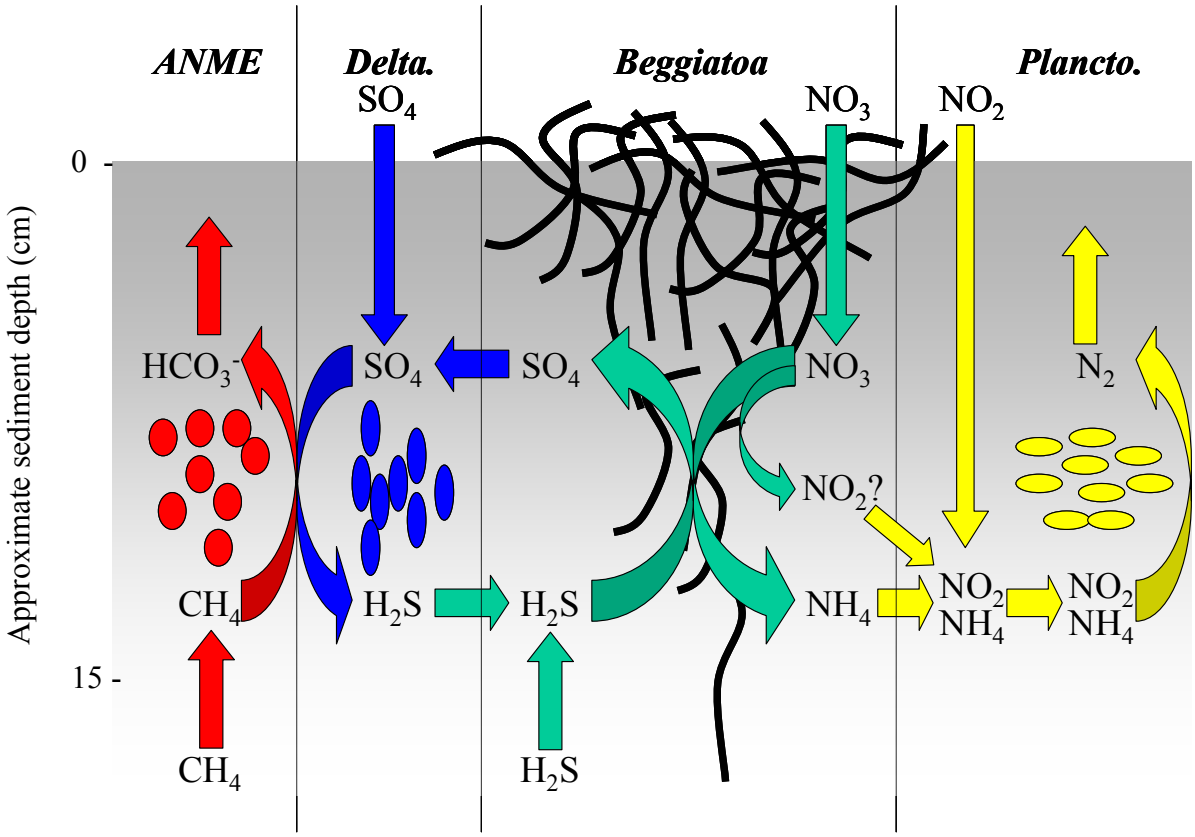

Figure 1.6 Hypothesized microbial utilization of nitrogen, sulfur and carbon down a sediment depth profile in sediments associated with *Beggiatoa* sp. mats. External sources of nitrate, nitrite and sulfate are from the overlying water column. Methane and hydrogen sulfide seep into the sediments from deep subsurface reservoirs. Depth indicators are approximated based on clone data from Mills et al. (109). Adapted from Montoya (unpublished).

orders *Methanomicrobiales* and *Methanosarcinales*. To date, no anaerobic methane oxidizing archaea have been cultivated in pure culture; therefore the complete physiology of these groups is unknown. However, a consortium visualized by fluorescent *in situ* hybridization (FISH) revealed a close spatial interaction between a δ-*Proteobacteria* and an ANME-2 archaea (10, 123). Although the AOM reaction is thermodynamically favorable and FISH images of a δ-*Proteobacteria* and an ANME-2 archaea revealed an apparent consortium of sulfate reducing bacteria and anaerobic methane oxidizing archaea (10), recent reports question this symbiosis (74, 125). In particular, fluctuations in sulfate reduction and AOM rate measurements from GoM sediments appear to be uncoupled suggesting that this tenuous link between sulfate reduction and AOM may not be present at GC234 (74). The debate surrounding the AOM reaction may not be resolved until a successful pure culture of an ANME archaeon is obtained.

1.2.2.3 Sulfate reducing bacteria

The microbial reduction of sulfate in seep environments is one of the dominant heterotrophic microbial processes (30, 53, 102). Restricted to anaerobic sediments, highly energetic sulfate reduction converts sulfate to hydrogen sulfide. Sulfate concentrations in the upper several cm of GoM continental slope sediments ranged from ~25 mM to <5 mM below 10 cm (74). Sulfate reduction rates are several orders of magnitude higher in active seep sites relative to non-seep sediments (1). Sulfate reducing bacteria (SRB), typically from the class δ-*Proteobacteria* and several lineages of *Firmicutes*, are capable of utilizing various carbon compounds including long-chain hydrocarbons within the oil seeping through the sediment (146, 188). A total of 31% of the sulfide produced as an

end product of sulfate reduction in GoM sediments is either utilized by thiotrophs or precipitated as sulfides (1).

1.2.2.4 Microbial metabolic activity within gas hydrates

Solid gas hydrate deposits and microbial mat covered sediments have been the focus of several studies attempting to identify and characterize GoM free-living microbial communities (88, 189). The rapid crystalization and dissolution of solid gas hydrate promotes the formation of faults and fissures, and the inclusion of sediment particles (176). The inclusion of microbes, coupled to the fluid flow through faults and fissures provide a possibility for microbial colonization of the gas hydrate interior (142). Methane trapped within GC185 and GC234 hydrate deposits is enriched in ^{13}C and D relative to associated vent gas, whereas no alterations were observed with C_2-C_5 isotopic concentrations. These data suggested bacterial oxidation of methane within the hydrate (142), because microbes preferentially incorporate ^{12}C and ^{1}H during oxidation of CH_4 (24) and are not able to utilize reduced compounds with carbon-carbon bonds (114). Additional evidence for microbial activity was reported as depletion in CO_2 ^{12}C in trapped hydrate gas relative to vent gas (142).

1.2.2.5 Characterization of GoM cold seep microbial communities

Culture dependent and independent techniques can be used to characterize microbial populations, including the extant microbial members of the GoM cold seep communities. However, current cultivation techniques provide limited information on environmental microbial community structure, with a small percentage (<1%) of the total

population being culturable (3) and the frequency of individual species cultured often misrepresenting the true proportions in the community (178). Culture independent, molecular-based techniques target nucleic acid sequences, stable isotopes and fatty acids rather than rely on the cultivation of isolates. New technological advances have allowed numerous molecular-based techniques to be applied to many microbial communities from extreme environments, but only measurements of phospholipid fatty acids (PLFA), stable carbon isotopes, and PCR-based amplicon clones have been utilized at GoM cold seeps (88, 189). Zhang et al. (189) utilized PLFA and stable carbon isotope analysis to characterize the microbial community in hydrate-associated sediments. Results indicated 16-52% of the total fatty acids identified from the sediments could be attributed to sulfate reducing bacteria (SRB). Similarly, stable carbon isotope analysis indicted an abundance of SRB within the sediment communities. However, the presence or absence of specific SRB lineages cannot be determined using this method.

The first detailed microbial characterization published from a GoM cold seep was by Lanoil et al. (88). Total DNA was extracted from buried hydrate samples obtained from shipboard piston cores at site AT425, a deep-water site (~1000 m) 35 km east of GC185 (Figure 1.1). *Bacteria* and *Archaea* 16S rRNA genes were amplified, cloned and grouped according to restriction fragment length polymorphism (RFLP) patterns. Sequencing of representative clones indicated a large percentage of the bacterial and archaeal libraries were most related to several *Pseudomonas* and non-ANME-2 *Methanosarcinales* lineages. Similar lineage frequencies have not been previously observed at other cold seeps including Cascadia Margin, Eel River and Santa Barbara

Basin (62, 123). Therefore, additional detailed characterizations of the microbial communities associated with gas hydrates are required to confirm these results.

The northern Gulf of Mexico is a geologically dynamic extreme environment containing vast oil and gas reserves under the constant influence of rising salt diapirs. Ambient bottom temperatures and pressures, in association with upward fluxes of thermogenic and biogenic gases, predominately methane, support the formation of massive surface breaching gas hydrates mounds. Numerous reports have characterized the macrofauna, i.e., tubeworms, mussels (18, 38, 82, 98), around the gas vents and hydrate mounds, however detailed molecular characterizations of the free-living microbial communities in these habitats is lacking. Reported herein is one of the first molecular characterization of total microbial populations and the first characterization of the apparent metabolically active fraction of the populations from three distinct layers on surface breaching gas hydrate mounds, i.e., sediment overlying gas hydrate, sediment entrained hydrate, and interior hydrate. In addition, this study reports the first molecular characterizations of the metabolically active fraction of the microbial community extant across a depth profile in sediments associated with orange- and white-pigmented microbial mats.

CHAPTER 2

MICROBIAL DIVERSITY IN SEDIMENTS ASSOCIATED WITH SURFACE BREACHING GAS HYDRATE MOUNDS IN THE GULF OF MEXICO

2.1 Abstract

A molecular phylogenetic approach was used to characterize the composition of microbial communities from two gas hydrate sedimentary systems in the Gulf of Mexico. Nucleic acids, extracted from sediments directly overlaying surface-breaching gas hydrate mounds collected from a research submersible (water depth 550-575 m), were amplified with nine different 16S rRNA gene primer sets. The PCR primers targeted microorganisms at the domain-specific (*Bacteria* and *Archaea*) and group-specific [sulfate reducing bacteria (SRB) and putative anaerobic methane oxidizing archaea] level. Amplicons were obtained with five of the nine primer sets including two of the six SRB groups (SRB Group 5 and Group 6) and used to generate five different clone libraries. Analysis of 126 clones from the *Archaea* library revealed that the sediments associated with naturally occurring gas hydrate harbored a low diversity. Sequence analysis indicated the majority of archaeal clones were most closely related to *Methanosarcinales*, *Methanomicrobiales* and distinct phylogenetic lineages within the anaerobic methane oxidation (ANME) groups. The most frequently recovered phylotypes in the ANME library were related to either ANME-2 or *Methanomicrobiales*. In contrast to the two archaeal libraries, *Bacteria* diversity was higher with the majority of the 126 bacterial clones most closely related to uncultured clones dominated by the δ- and ε-

Proteobacteria. Interestingly, while 82% of the clones in the SRB Group 5 library were affiliated with δ-*Proteobacteria*, the vast majority (83%) of clones in the SRB Group 6 library was affiliated with the *Firmicutes*. This is the first phylogenetic-based description of microbial communities extant in methane-rich hydrate associated sediments from a hydrocarbon seep region in the Gulf of Mexico.

2.2. Introduction

The northern continental slope of the Gulf of Mexico, a hydrocarbon seep region, contains vast reservoirs of oil and gas deposits, areas of active gas venting and gas hydrate mounds occurring as seafloor outcroppings and in the shallow (i.e., < 6 m) subsurface (12, 97, 105, 106). The ice-like gas hydrate, composed of water and hydrocarbon gas molecules (predominately methane), requires suitable gas, temperature and pressure conditions for formation and stability (reviewed in (15)). Although such conditions occur globally, with gas hydrates distributed in many marine (active and passive continental margins) and terrestrial locales (85), focused seep locations in the shallow Gulf of Mexico (GoM) basin provide a unique access to abundant gas hydrate mounds and associated sediments at the seafloor. Gas hydrates have become the subject of intense investigation owing to their potential use as an alternative energy resource (84), possible effect on sea-floor stability (127, 137), change in climatic conditions (87, 91, 98, 117, 118, 128) and presence on other planets and satellites (5, 94, 185).

In marine methane seeps with naturally occurring hydrates an increasing number of geochemical-based studies (e.g., (69, 74)) demonstrate significant contributions of

sulfate reduction and anaerobic methane oxidation activities to the cycling of methane. Such gas hydrate-bearing marine sediments have recently become the focus of numerous studies characterizing the extant microbial communities. Specifically, a number of groups have reported the phylogenetic diversity of microorganisms in hydrate-containing sediments collected from seep locales in the Cascadia margin off the Oregon coast (9, 100), and the California continental margin including Eel River (62, 122), and Santa Barbara Basins (122) where sulfate reduction (SR) and anaerobic oxidation of methane (AOM) processes predominate. Although it has been proposed that AOM is mediated by a syntrophic coupling between archaeal (i.e., ANME-1 or ANME-2 groups) and sulfate reducing bacterial (i.e., *Desulfosarcina sp.*) partners (123), recent evidence suggests that such a specific association may not always be necessary for AOM (125). This particular microbial consortia, however, has been repeatedly detected either directly [i.e., FISH; (10, 123, 124)] or indirectly [16S rRNA gene sequences; (62, 170, 172)] in methane-rich sediments, cold methane seeps, hydrothermally active sediments and within the methane-sulfate transition zone of near-shore sediments. In contrast, there remains a considerable lack of knowledge regarding the phylogenetic diversity of *Bacteria* and *Archaea* within GoM methane-rich cold seep sediments associated with gas hydrates.

In this present study, sediments and gas hydrate were sampled by deploying a custom-made hydrate drill from a manned research submersible at two different GoM cold seep locations (550-575 m water depth) to obtain discrete sediment/hydrate samples at gas hydrate mound outcrops. The objective was to characterize the sediment microbial community in direct contact with surface breaching gas hydrates. Total nucleic acids were extracted from the sediment samples and subjected to PCR amplification with nine

different primer sets representing microorganisms at the domain and group-specific level. This is among the first 16S rRNA gene surveys to be conducted on free-living GoM seep sediment microbial communities directly associated with surface-breaching gas hydrate mounds.

2.3 Materials and methods

2.3.1 Gulf of Mexico site description, sample collection and preservation

The study sites sampled are located in the northern GoM continental slope province. The sites, GC185 (Bush Hill; 550 m depth) and GC234 (575 m depth) are located at 27°46'N, 91°30'W and 27°44'N, 91°13'W, respectively (Figure 1.1). These locales were selected for study as both sites have visible oil and gas seepage with gas hydrates occurring as exposed hydrate breaching the sediment-water interface and buried hydrate covered by a layer of sediment that is centimeters to meters thick. Multiple core samples (2.9 cm OD, 12-15 cm average length) containing overlaying sediments in direct contact with hydrate outcroppings and intact hydrate were collected during July 2001. Cores were collected with a custom-made rotary drilling device fitted for the Johnson Sea Link manned submersible. To prevent solid gas hydrate samples from decomposing during submersible operations and recovery, samples were immediately placed into a hydrate recovery chamber (HRC) that maintains bottom water pressure and temperature (50 atm, 7°C). Onboard ship, the HRC was immediately transferred to a refrigerated van (4°C) and intact cores were removed from the HRC and placed into a hydrate stabilization container (HSC). The HSC is an ethanol-sterilized metal tray (29.8 x 20.3 x

12.7 cm) insulated with styrofoam and maintained between -30 to -35°C with a continuously chilled ethanol bath. Aliquots of gas hydrate and sediments were removed aseptically and immediately transferred to N_2 purged glass containers and held at –20°C until DNA extraction. Direct cell counts were performed on aliquots (0.5 g wet wt) of overlaying sediment, sediment-hydrate interface and sediment-free hydrate samples as previously described in Powers et al. (131).

2.3.2 Nucleic acid extraction and PCR amplification

DNA was extracted from 0.5 g (wet weight) sediment aliquots sectioned from the interface directly in contact with gas hydrate as previously described (107). Three to five separate DNA extractions per sampling site were performed and samples were pooled. The crude pooled DNA extract was purified according to the method of Tebbe and Vahjen (168) with ion-exchange columns (Qiagen-Tip 500). Primers were synthesized by Integrated DNA Technologies, Inc. (Coralville, IA) and sequences are listed in Table 2.1. Aliquots of marine sediment community DNA (1 µl, corresponding to the DNA recovered from approximately 5-10 mg sediment) were PCR-amplified in reaction mixtures containing (as final concentrations) 1 × PCR buffer (Stratagene, CA, USA), 1.5 mM $MgCl_2$, 200 µM of each deoxynucleoside triphosphate, 1 pmol of each forward and reverse primer, and 0.025 U μl^{-1} *TaKaRa Taq*™ (TaKaRa, Japan). Reaction mixtures were incubated in a model 2700 GeneAmp thermal cycler (Applied Biosystems, CA, USA) initially at 95˚C for 2-5 min, followed by amplification according to recommended conditions as previously described for each primer set (Table 2.1) (29, 33, 73, 172). Amplified products were analyzed on 1.0% agarose gels run in TBE buffer, stained with

Table 2.1
Oligonucleotide primer pairs used and amplicons obtained.

Primers	Specificity	Annealing temperature (^{o}C)	Product size (bp)	Sequence (5'-3')	Reference	Amplification products obtained from site:	
						GC185	GC234
27F[a] 1522R	Domain *Bacteria*	52	1495	AGAGTTTGATCCTGGCTCAG AAGGAGGTGATCCARCCGCA	(73)	+	+
Ar21F Ar958R	Domain *Archaea*	55	937	TTCCGGTTGATCCYGCCGGA YCCGGCGTTGAMTCCAATTT	(33)	+	+
DFM140 DFM842	SRB Group1	58	702	TAGMCYGGGATAACRSYKG ATACCCSCWWCWCCTAGCAC	(29)	-	-
DBB121 DBB1237	SRB Group 2	66	1116	CGCGTAGATAACCTGTCYTCATG GTAGKACGTGTGTAGCCCTGGTC	(29)	-	-
DBM169 DBM1006	SRB Group 3	64	837	CTAATRCCGGATRAAGTCAG ATTCTCARGATGTCAAGTCTG	(29)	-	-
DSB127 DSB1273	SRB Group 4	60	1146	GATAATCTGCCTTCAAGCCTGG CYYYYYGCRRAGTCGSTGCCCT	(29)	-	-

Table 2.1 (continued)

DCC305 DCC1165	SRB Group 5	65	860	GATCAGCCACACTGGRACTGACA GGGGCAGTATCTTYAGAGTYC	(29)	+	+
DSV230 DSV838	SRB Group 6	61	608	GRGYCYGCGTYYCATTAGC CYCCGRCAYCTAGYRTYCATC	(29)	+	+
ANMEF 907R	ANME	57	817	GGCUCAGUAACACGUGGA CCGTCAATTCCTTTRAGTTT	(172)	+	+

[a] F and R denote forward and reverse, respectively

ethidium bromide, and UV illuminated. Amplicons were subsequently pooled from three to five reactions and purified with the Qiaquick gel extraction kit (Qiagen, CA, USA).

2.3.3 Cloning, RFLP grouping and 16S rRNA gene sequence analysis

Purified pooled amplicons were cloned into vector pCR2.1 according to manufacturer's instructions (Invitrogen, CA, USA). Inserts were PCR-amplified as described above with primers listed in Table 2.1. To prevent amplification of *Escherichia coli* host 16S rRNA genes, M13F/R primers (Table 2.1) were used to amplify inserts from clones obtained with 27F and 1522R primers. Products from the *Archaea*, *Bacteria*, anaerobic methane oxidizing archaea (ANME) and sulfate reducing bacteria (SRB) libraries were digested with *MspI* and *HhaI* (Promega, WI, USA). Clones were grouped according to restriction fragment length polymorphism (RFLP) banding patterns, unique clones identified and sequenced. Multiple representative clones were sequenced from RFLP groups containing five or more members. Sequencing was performed at the Georgia Tech core DNA facility using a BigDye Terminator v3.1 Cycle sequencing kit on an automated capillary sequencer (model 3100 Gene Analyzer, Applied Biosystems). Inserts were sequenced multiple times on each strand.

2.3.4 Phylogenetic and rarefaction analysis

Multiple sequences of individual inserts were initially aligned using the program 'BLAST 2 Sequences' (167) available through the National Center for Biotechnology Information and assembled with the program BioEdit v5.0.9 (57). Sequences were checked for chimeras using Chimera Check from Ribosomal Database Project II (99).

Sequences from this study and reference sequences, as determined by BLAST analysis, were subsequently aligned using CLUSTALX v1.81 (171). Neighbor-joining trees were created from the alignments using CLUSTALX v1.81 (171). An average of 600 (i.e., SRB Group 6 clones) to 1,300 (i.e., *Bacteria* clones) nucleotides were included in the phylogenetic analyses. The bootstrap data represents a percentage of 1,000 samplings. The final trees were viewed using NJPlot (130) and TreeView v1.6.6 available at http://taxonomy.zoology.gla.ac.uk/rod/treeview.html. Rarefaction analysis was performed using equations as described in Heck et al. (60).

2.3.5 Nucleotide sequence accession numbers

The 108 16S rRNA gene nucleotide sequences have been deposited in the GenBank database under accession numbers AY211657-AY211765.

2.4 Results and Discussion

2.4.1 RFLP and rarefaction analyses of 16S rRNA gene libraries

Nine different PCR primer sets (Table 2.1) specific to microorganisms at the domain and group-specific level were applied to total nucleic acids extracted from sediments directly overlaying gas hydrate mounds at two different GoM locations (Figure 1.1). Direct microscopy cell counts for sediment-free hydrate, sediment/hydrate interface and sediment overlaying hydrate were 2.0×10^6, 2.8×10^7 and 5.8×10^8 respectively. Amplicons from GC185 and GC234 DNA samples were obtained with five of the nine primer sets tested (Table 2.1) and subsequently used to construct 16S rRNA gene

libraries. A total of 126 *Bacteria*, 126 *Archaea*, 127 putative sulfate reducing bacteria (SRB) Group 5, 138 putative SRB Group 6 and 138 putative ANME archaea clones were grouped according to RFLP patterns.

Rarefaction analysis was applied to determine if sufficient numbers of clones were screened to estimate diversity within each of the clone libraries sampled (Figure 2.1). A caveat being that primer bias, cell lysis, and nucleic acid extraction and recovery can contribute to an underestimation of overall microbial diversity. For those clones obtained with *Archaea*, ANME and SRB Group 6 specific primers, the curves indicated saturation. Thus, a sufficient number of clones were sampled representative of the diversity of these particular microorganisms in each respective library (Figure 2.1). Numerically dominant RFLP groups, ranging from 12 to 22% of all clones, were obtained for each of these three libraries (Table 2.2 and Table 2.3). In contrast, curves generated for rRNA gene clones obtained with *Bacteria* and SRB Group 5 primer sets did not indicate saturation (Figure 2.1). Although additional sampling of clones would be needed to reveal the full extent of the diversity, numerically dominant RFLP groups were obtained (Table 2.2). Specifically, one dominant group of clones from each of the *Bacteria* (represented by clone GoM GC185 507E) and SRB Group 5 (represented by clone GoM GC234 014S5) libraries comprised 16 and 13% of all clones, respectively (Table 2.2).

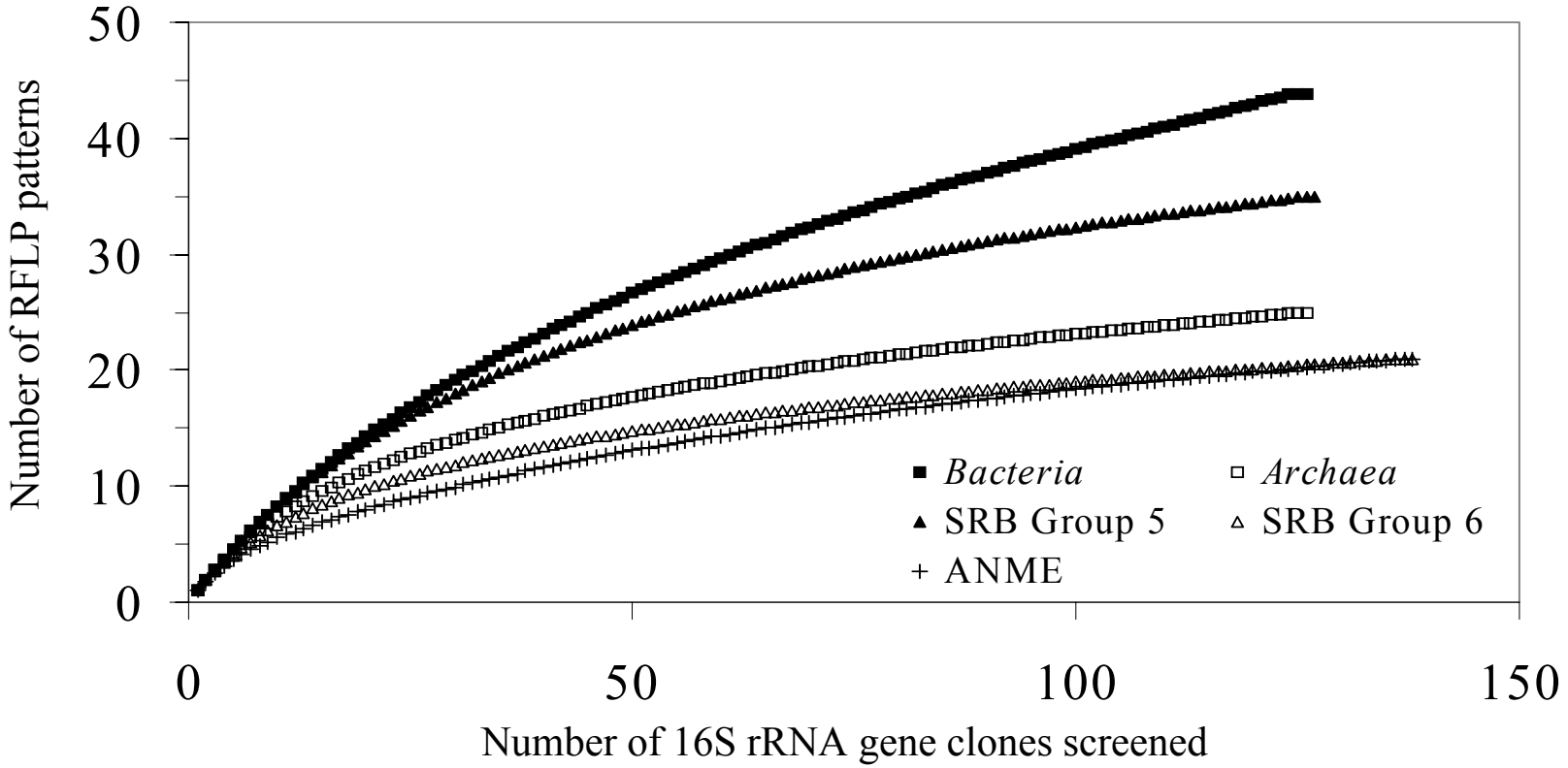

Figure 2.1 Rarefaction curves determined for the different RFLP patterns of 16S rRNA gene clones in the *Bacteria* (■), *Archaea* (□), ANME (+) and SRB Group 5 (▲) and Group 6 (△) 16S rRNA gene libraries. The number of different RFLP patterns was determined after digestion with restriction endonucleases *Hha*I and *Msp*I. Rarefaction analysis was performed using equations reported by Heck et al. (60).

Table 2.2

Summary of 16S rRNA gene sequences from *Bacteria*, SRB Group 5 and SRB Group 6 clone libraries.

	Representative Sequence	Number of Related Clones	Site Clones Acquired	Nearest Relative	Phylogenetic Group	Similarity (%)
Bacteria	GoM GC185 523E	3	GC185	DC Clone SHA-28	GNS Bacteria	92
	GoM GC185 546E	4	GC185, GC234	HS Clone GCA112	GNS Bacteria	92
	GoM GC234 019E	4	GC185, GC234	HS Clone GCA025	*Firmicutes*	97
	GoM GC234 602E	1	GC234	HS Clone GCA025	*Firmicutes*	97
	GoM GC234 616E	2	GC234	JT Clone JTB215	*Firmicutes*, Low G+C	98
	GoM GC185 507E	20	GC185, GC234	DV Clone 33 FL49B99	ε-*Proteobacteria*	98
	GoM GC234 030E	8	GC185, GC234	DV Clone 33 FL39B00	ε-*Proteobacteria*	97
	GoM GC185 538E	6	GC185	NT Clone NKB11	ε-*Proteobacteria*	96
	GoM GC234 615E	5	GC185, GC234	*Sulfurospirillum arcachonese*	ε-*Proteobacteria*	96
	GoM GC234 613E	4	GC234	HV Clone PVB OTU2	ε-*Proteobacteria*	95
	GoM GC234 005E	3	GC234	HV Clone PVB OTU6	ε-*Proteobacteria*	91
	GoM GC234 035E	2	GC234	HV Clone CS B016	ε-*Proteobacteria*	95
	GoM GC185 503E	8	GC185, GC234	ER Clone Eel-Be1A3	δ-*Proteobacteria*	96
	GoM GC234 618E	4	GC185, GC234	ER Clone Eel-Be1A3	δ-*Proteobacteria*	97
	GoM GC185 515E	2	GC185	ER Clone Eel-Be1A3	δ-*Proteobacteria*	98
	GoM GC185 524E	4	GC185	NS Clone SRB mXyS1	δ-*Proteobacteria*	97
	GoM GC234 610E	3	GC185, GC234	*Syntrophus gentianae*	δ-*Proteobacteria*	93
	GoM GC185 508E	1	GC185	*Syntrophus gentianae*	δ-*Proteobacteria*	90
	GoM GC234 007E	3	GC185, GC234	*Aeromarinobacter lutacensis*	γ-*Proteobacteria*	96
	GoM GC234 022E	5	GC185, GC234	CS Clone EI2	α-*Proteobacteria*	99

Table 2.2 (continued)

SRB-5	GoM GC234 058S5	3	GC234	*Acidaminobacter hydrogenoformans*	*Firmicutes*, Low G+C	89
	GoM GC185 538S5	4	GC185, GC234	CS Clone MERTZ 0CM 115	*Firmicutes*, Low G+C	89
	GoM GC234 014S5	17	GC185, GC234	HS Clone GCA017	δ-*Proteobacteria*	98
	GoM GC234 683S5	9	GC185, GC234	HS Clone GCA017	δ-*Proteobacteria*	95
	GoM GC234 676S5	9	GC234	HS Clone GCA017	δ-*Proteobacteria*	96
	GoM GC185 542S5	9	GC185, GC234	HS Clone GCA017	δ-*Proteobacteria*	96
	GoM GC234 094S5	8	GC185, GC234	HS Clone GCA017	δ-*Proteobacteria*	99
	GoM GC185 510S5	7	GC185, GC234	HS Clone GCA017	δ-*Proteobacteria*	99
	GoM GC185 580S5	6	GC185, GC234	HS Clone GCA017	δ-*Proteobacteria*	94
	GoM GC185 585S5	5	GC185, GC234	HS Clone GCA017	δ-*Proteobacteria*	99
	GoM GC234 629S5	4	GC185, GC234	HS Clone GCA017	δ-*Proteobacteria*	97
	GoM GC234 634S5	2	GC234	HS Clone GCA017	δ-*Proteobacteria*	95
	GoM GC234 069S5	2	GC185, GC234	HS Clone GCA017	δ-*Proteobacteria*	99
	GoM GC234 601S5	2	GC234	HS Clone GCA017	δ-*Proteobacteria*	97
	GoM GC234 681S5	3	GC234	CG Clone 12-2	δ-*Proteobacteria*	90
	GoM GC234 054S5	2	GC185, GC234	MC Clone UASB-TL9	δ-*Proteobacteria*	89
	GoM GC234 613S5	2	GC234	Isolate EbS7	δ-*Proteobacteria*	94
	GoM GC234 631S5	7	GC185, GC234	HV Clone C1 B013	γ-*Proteobacteria*	96
	GoM GC234 662S5	2	GC185, GC234	HV Clone C1 B013	γ-*Proteobacteria*	96
	GoM GC234 071S5	2	GC234	*Hyphomicrobium sp. Ddeep-1*	γ-*Proteobacteria*	99
SRB-6	GoM GC185 515S6	24	GC185, GC234	RM Clone PBS-III-27	*Firmicutes*	94
	GoM GC185 610S6	5	GC185, GC234	RM Clone PBS-III-27	*Firmicutes*	89
	GoM GC234 023S6	3	GC234	RM Clone PBS-III-27	*Firmicutes*	92
	GoM GC234 051S6	2	GC234	RM Clone PBS-III-27	*Firmicutes*	89

Ta**ble 2.2** (continued)

GoM GC185 543S6	16	GC185, GC234	MC Clone BA143	*Firmicutes*	90
GoM GC234 676S6	2	GC234	MC Clone BA143	*Firmicutes*	87
GoM GC185 608S6	29	GC185, GC234	AB Clone R35	*Firmicutes,* Low G+C	95
GoM GC234 612S6	16	GC185, GC234	AB Clone Y36	*Firmicutes,* Low G+C	94
GoM GC185 601S6	7	GC185, GC234	*Caloranaerobacter azorensis*	*Firmicutes, Low G+C*	92
GoM GC185 503S6	2	GC185, GC234	*Clostridium botulinum*	*Firmicutes, Low G+C*	88
GoM GC234 694S6	8	GC185, GC234	ER Clone Eel-BE1B1	δ-*Proteobacteria*	98
GoM GC185 619S6	8	GC185, GC234	ER Clone Eel-BE1B1	δ-*Proteobacteria*	94
GoM GC234 615S6	5	GC234	BR Clone SHA-42	δ-*Proteobacteria*	92
GoM GC234 680S6	2	GC234	ER Clone Eel-BE1D3	δ-*Proteobacteria*	98

Table 2.3

Summary of 16S rRNA gene sequences from *Archaea* and ANME clone libraries.

	Representative sequence	Number of Related Clones	Site Clones Acquired	Nearest Relative	Phylogenetic Group	Similarity (%)
Archaea	GoM GC234 621R	1	GC234	HV Clone pMC2A15	*Crenarchaeota*	89
	GoM GC234 626R	9	GC185, GC234	MA Clone VC2.1	*Crenarchaeota*	91
	GoM GC234 001R	3	GC185, GC234	MA Clone VC2.1	*Crenarchaeota*	89
	GoM GC234 007R	2	GC234	SA Clone AEGEAN 71	*Thermoplasmales*	83
	GoM GC234 643R	1	GC234	AD Clone 101B	*Thermoplasmales*	83
	GoM GC234 024R	4	GC185, GC234	ER Clone TA1f2	*Thermoplasmales*	95
	GoM GC234 030R	1	GC234	ER Clone BA2e8	ANME-1	96
	GoM GC234 609R	18	GC185, GC234	ER Clone TA2e12	ANME-1	97
	GoM GC234 614R	5	GC234	ER Clone BA2e8	ANME-1	96
	GoM GC234 616R	1	GC234	SB Isolate SB-17a1A11	ANME-1	94
	GoM GC234 015R	2	GC234	SM Clone 2C174	*Methanomicrobales*	93
	GoM GC234 026R	3	GC234	SM Clone 2C174	*Methanomicrobales*	96
	GoM GC234 003R	13	GC234	HV Clone CSR002	*Methanomicrobales*	96
	GoM GC234 633R	17	GC234	GoM AT425 ArC3	*Methanosarcinales*	99
	GoM GC234 619R	1	GC234	GoM AT425 ArC3	*Methanosarcinales*	99
	GoM GC234 033R	1	GC234	GoM AT425 ArC3	*Methanosarcinales*	98
	GoM GC185 517R	3	GC185	ER Clone BA2H11fin	ANME-2A	95
	GoM GC234 606R	2	GC234	HV Clone G72 C12	ANME-2D	94
	GoM GC185 520R	15	GC185, GC234	ER Clone Eel-36a2E1	ANME-2C	98
	GoM GC185 505R	4	GC185, GC234	ER Clone Eel-36a2E1	ANME-2C	98
	GoM GC234 622R	2	GC234	ER Clone TA1a4	ANME-2C	97

Table 2.3 (continued)

	GoM GC185 503R	8	GC185, GC234	GoM AT425 ArD2	ANME-2C	98
	GoM GC234 021R	8	GC185, GC234	HV Clone C1 R019	ANME-2C	97
	GoM GC234 019R	1	GC234	HV Clone C1 R019	ANME-2C	99
ANME	GoM GC234 011A	4	GC234	ER Clone TA1f2	*Thermoplasmales*	96
	GoM GC185 601A	3	GC185, GC234	ER Clone TA1f2	*Thermoplasmales*	96
	GoM GC234 045A	2	GC234	ER Clone TA1f2	*Thermoplasmales*	96
	GoM GC234 610A	2	GC234	ER Clone TA2e12	ANME-1	99
	GoM GC234 009A	11	GC234	*Methanospirillum hungatei*	*Methanomicrobales*	90
	GoM GC185 624A	3	GC185	HV Clone CS-R002	*Methanomicrobales*	97
	GoM GC234 033A	11	GC185, GC234	HV Clone CS-R002	*Methanomicrobales*	96
	GoM GC234 022A	30	GC185, GC234	HV Clone CS-R002	*Methanomicrobales*	97
	GoM GC185 618A	2	GC185, GC234	HV Clone G72 C12	ANME-2D	94
	GoM GC185 623A	23	GC185, GC234	HV Clone G72 C12	ANME-2D	94
	GoM GC234 046A	3	GC234	HV Clone G72 C12	ANME-2D	94
	GoM GC185 626A	2	GC185, GC234	HV Clone G72 C12	ANME-2D	94
	GoM GC185 620A	31	GC185, GC234	HV Clone G72 C12	ANME-2D	94

2.4.2 Phylogenetic diversity of *Bacteria*

Analysis of the 126 *Bacteria* clones revealed a greater diversity relative to the *Archaea* clone library (Figure 2.1) and included predominately uncultured bacterial lineages. A total of 45 distinct RFLP patterns representing six phylogenetic lineages were detected (data not shown). A considerable majority of the clones (78 of 126) were representative of the phylum *Proteobacteria* (Figure 2.2). Of these, 62% were related to the ε class of *Proteobacteria*, including the most numerically dominant phylotype represented by clone GoM GC185 507E (16% of the total clone library; Table 2.2). This phylotype, present at GC185 and GC234 (Figure 1.1 and 2.2), was most closely related (98% similar) to a non-cultured microorganism (DV Clone 33 FL49B99; (65)) obtained from a deep-sea volcano in the northern Pacific. The second most dominant phylotype was most closely related to the δ class of *Proteobacteria* (17% of all clones; Table 2.2). Similar to the ε-proteobacterial clones, the δ-proteobacterial clones are most closely related to non-cultured microorganisms, except for two phylotypes related to *Syntrophus gentianae* (Figure 2.2). Although a high degree of bacterial diversity was observed, the majority (i.e., 60%) of the *Bacteria* 16S rRNA gene sequences belonged to δ- and ε-*Proteobacteria*. While no phylotypes related to β-*Proteobacteria* were detected, multiple clones were obtained from GC185 and GC234 related to α- and γ-*Proteobacteria*. The phylotype representatives belonging to the α- (GoM GC234 022E; Table 2.2) and γ-*Proteobacteria* (GoM GC234 007E; Table 2.2) were most related to CS Clone EI2 (169), obtained from continental shelf sediments off the New England coast, and to *Aeromarinobacter lutacensis*, respectively. Additionally, 14 of the 126 clones, representing five phylotypes, were identified as either green nonsulfur bacteria- or

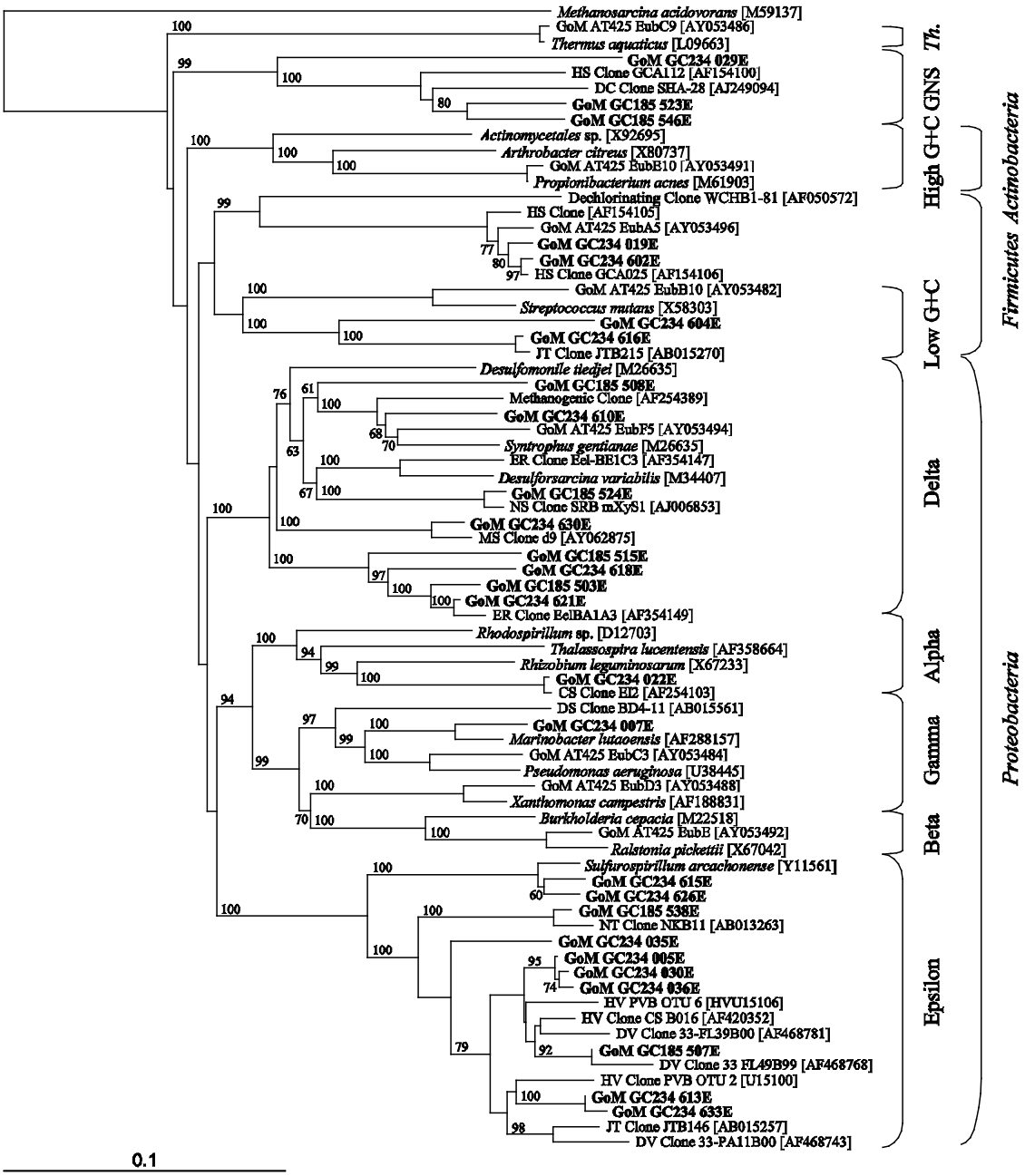
Methanosarcina acidovorans [M59137]
GoM AT425 BubC9 [AY053486]
Thermus aquaticus [L09663]
GoM GC234 029E
HS Clone GCA112 [AF154100]
DC Clone SHA-28 [AJ249094]
GoM GC185 523E
GoM GC185 546E
Actinomycetales sp. [X92695]
Arthrobacter citreus [X80737]
GoM AT425 BubE10 [AY053491]
Propionibacterium acnes [M61903]
Dechlorinating Clone WCHB1-81 [AF050572]
HS Clone [AF154105]
GoM AT425 BubA5 [AY053496]
GoM GC234 019E
GoM GC234 602E
HS Clone GCA025 [AF154106]
GoM AT425 BubB10 [AY053482]
Streptococcus mutans [X58303]
GoM GC234 604E
GoM GC234 616E
JT Clone JTB215 [AB015270]
Desulfomonile tiedjei [M26635]
GoM GC185 508E
Methanogenic Clone [AF254389]
GoM GC234 610E
GoM AT425 BubF5 [AY053494]
Syntrophus gentianae [M26635]
ER Clone Eel-BE1C3 [AF354147]
Desulforsarcina variabilis [M34407]
GoM GC185 524E
NS Clone SRB mXyS1 [AJ006853]
GoM GC234 630E
MS Clone d9 [AY062875]
GoM GC185 515E
GoM GC234 618E
GoM GC185 503E
GoM GC234 621E
ER Clone EelBA1A3 [AF354149]
Rhodospirillum sp. [D12703]
Thalassospira lucentensis [AF358664]
Rhizobium leguminosarum [X67233]
GoM GC234 022E
CS Clone EI2 [AF254103]
DS Clone BD4-11 [AB015561]
GoM GC234 007E
Marinobacter lutaoensis [AF288157]
GoM AT425 BubC3 [AY053484]
Pseudomonas aeruginosa [U38445]
GoM AT425 BubD3 [AY053488]
Xanthomonas campestris [AF188831]
Burkholderia cepacia [M22518]
GoM AT425 BubB [AY053492]
Ralstonia pickettii [X67042]
Sulfurospirillum arcachonense [Y11561]
GoM GC234 615E
GoM GC234 626E
GoM GC185 538E
NT Clone NKB11 [AB013263]
GoM GC234 035E
GoM GC234 005E
GoM GC234 030E
GoM GC234 036E
HV PVB OTU 6 [HVU15106]
HV Clone CS B016 [AF420352]
DV Clone 33-FL39B00 [AF468781]
GoM GC185 507E
DV Clone 33 FL49B99 [AF468768]
HV Clone PVB OTU 2 [U15100]
GoM GC234 613E
GoM GC234 633E
JT Clone JTB146 [AB015257]
DV Clone 33-PA11B00 [AF468743]
0.1
High G+C GNS Th.
Low G+C
Delta
Alpha
Gamma
Beta
Epsilon
Firmicutes Actinobacteria
Proteobacteria

Figure 2.2 Phylogenetic tree of relationships of 16S rRNA gene bacterial clone sequences, as determined by distance Jukes-Cantor analysis, from Gulf of Mexico GC185 and GC234 seep sediments overlaying surface-breaching gas hydrate mounds (in boldface) to selected cultured isolates and environmental clones. Abbreviation *Th* denotes *Thermus*. Designations of environmental clone sequences are CS, continental slope; DC, dechlorination consortia; DS, deep sea; DV, deep-sea volcano; ER, Eel River Basin; HS, hydrocarbon seep; HV, hydrothermal vent; JT, Japan Trench; MS, marine sediment; NS, North Sea; NT, Nankai Trough. Genbank accession numbers are in parentheses. One thousand bootstrap analyses were conducted and percentages greater than 50% are reported. *Methanosarcina acidovorans* was used as the outgroup. The scale bar represents the expected number of changes per nucleotide position.

Firmicutes-related (Table 2.2). These phylotypes were most related to non-cultured environmental clone sequences from diverse niches.

2.4.3 Phylogenetic diversity of sulfate reducing bacteria

Degenerate PCR primer sets, previously shown to be specific for six phylogenetic groups of sulfate reducing bacteria (29), were used to identify potentially dominant benthic Gram-negative and Gram-positive SRB populations in GoM sediment-gas hydrate microbial communities. The rationale for further elucidating these SRB assemblages is supported by the recent findings of Zhang et al. (189). Specifically, the authors reported that more than 50% of total phospholipid fatty acids extracted from GoM site GC234 hydrate-containing sediments belonged to branched-chain lipids indicative of SRB. However, to be able to identify specific SRB populations and for determining phylogenetic relatedness a 16S rRNA gene-based approach is required. Our study thus represents the first report of 16S rRNA gene sequence analysis for SRB populations in the GoM.

Of the six SRB subgroup primers tested (29), we obtained amplicons only with primers detecting the *Desulfococcus-Desulfonema-Desulfosarcina*-like and *Desulfovibrio-Desulfomicrobium*-like suprageneric Groups 5 and 6, respectively. Although Daly et al. (29) reported the need to perform 'nested PCR' on some environmental DNA samples we were able to amplify both of these subgroups directly from extracted nucleic acids suggesting their numerical abundance in this extreme environment. However, PCR amplicons were not observed either by nested PCR (data

not shown) or direct amplification of environmental DNA, with primers for SRB subgroups 1-4 from either GC185 or GC234.

A total of 35 distinct RFLP patterns were observed (data not shown) from 127 clones obtained with SRB Group 5 primers. The majority of sequenced representative clones (92%; Table 2.2), present at GC185 and GC234, were most closely related to δ-*Proteobacteria*. A vast majority of δ-*Proteobacteria*-related clones (80 of 97) were most similar (>94%) to a clone designated HS clone GCA017 isolated from hydrocarbon seep sediments. Interestingly, these clones form a distinct clade which we have denoted GoM G5 (Figure 2.3). SRB Group 5 clones most related to γ-*Proteobacteria* and to *Firmicutes* (>96% and >89% similarity, respectively) were also detected. The γ-*Proteobacteria*-related clones showed high similarity to *Hyphomicrobium* sp. Ddeep-1 (99% similar; (132)), isolated from deep-sea waters in the northwest Pacific Ocean, and to a thioautotrophic symbiont environmental clone found in the gills of the hydrothermal vent clam, *Maorithyas hadalis* (96% similar; (51)).

In contrast to SRB Group 5, the Group 6 library (138 clones) contained fewer (21) RFLP patterns (data not shown). The 18 δ-*Proteobacteria*-related Group 6 clones (Table 2.2) grouped into three phylotypes and exhibited similarity to nucleotide sequences obtained from Eel River Basin, a cold seep site on the California continental margin (122). These GoM phylotypes formed a clade separate from previously determined SRB Group 6 isolates (Figure 2.3) (29). The vast majority of SRB Group 6 sequences were however, most closely related to the *Firmicutes* (82%; Table 2.2. and Figure 2.3). Among the numerically dominant sequences occurring at GC185 and GC234 was the phylotype GoM GC234 608S6, related to an Artesian Basin clone (AB Clone R35; unpublished;

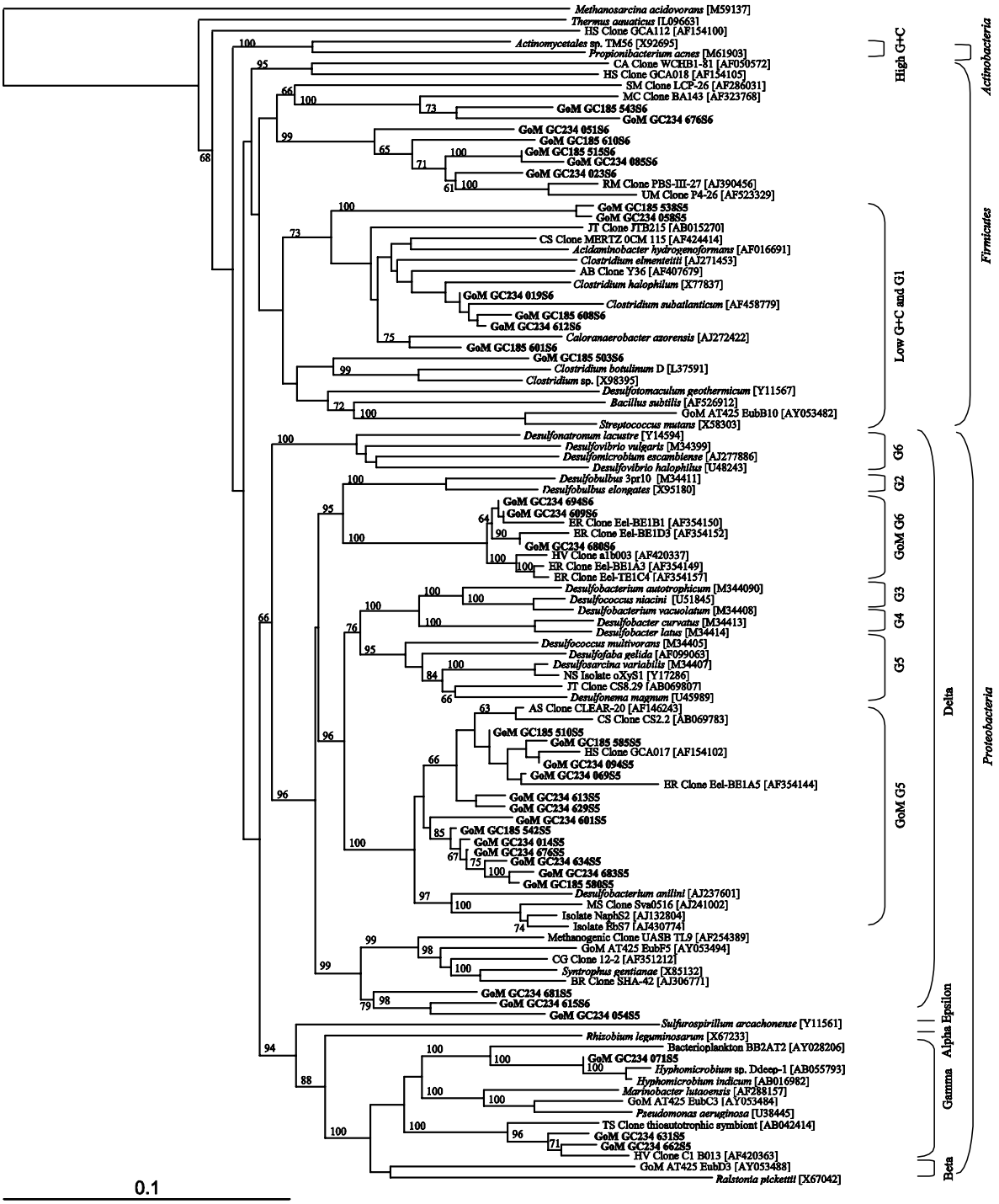
Methanosarcina acidovorans [M59137]
Thermus aquaticus [L09663]
HS Clone GCA112 [AF154100]
Actinomycetales sp. TM56 [X92695]
Propionibacterium acnes [M61903]
CA Clone WCHB1-81 [AF050572]
HS Clone GCA018 [AF154105]
SM Clone LCP-26 [AF286031]
MC Clone BA143 [AF323768]
GoM GC185 543S6
GoM GC234 676S6
GoM GC234 051S6
GoM GC185 610S6
GoM GC185 515S6
GoM GC234 085S6
GoM GC234 023S6
RM Clone PBS-III-27 [AJ390456]
UM Clone P4-26 [AF523329]
GoM GC185 538S5
GoM GC234 058S5
JT Clone JTB215 [AB015270]
CS Clone MERTZ 0CM 115 [AF424414]
Acidaminobacter hydrogenoformans [AF016691]
Clostridium elmentetiti [AJ271453]
AB Clone Y36 [AF407679]
Clostridium halophilum [X77837]
GoM GC234 019S6
Clostridium subatlanticum [AF458779]
GoM GC185 608S6
GoM GC234 612S6
Caloranaerobacter azorensis [AJ272422]
GoM GC185 601S6
GoM GC185 503S6
Clostridium botulinum D [L37591]
Clostridium sp. [X98395]
Desulfotomaculum geothermicum [Y11567]
Bacillus subtilis [AF526912]
GoM AT425 EubB10 [AY053482]
Streptococcus mutans [X58303]
Desulfonatronum lacustre [Y14594]
Desulfovibrio vulgaris [M34399]
Desulfomicrobium escambiense [AJ277886]
Desulfovibrio halophilus [U48243]
Desulfobulbus 3pr10 [M34411]
Desulfobulbus elongates [X95180]
GoM GC234 694S6
GoM GC234 609S6
ER Clone Eel-BE1B1 [AF354150]
ER Clone Eel-BE1D3 [AF354152]
GoM GC234 680S6
HV Clone a1b003 [AF420337]
ER Clone Eel-BE1A3 [AF354149]
ER Clone Eel-TE1C4 [AF354157]
Desulfobacterium autotrophicum [M344090]
Desulfococcus niacini [U51845]
Desulfobacterium vacuolatum [M34408]
Desulfobacter curvatus [M34413]
Desulfobacter latus [M34414]
Desulfococcus multivorans [M34405]
Desulfofaba gelida [AF099063]
Desulfosarcina variabilis [M34407]
NS Isolate oXyS1 [Y17286]
JT Clone CS8.29 [AB069807]
Desulfonema magnum [U45989]
AS Clone CLEAR-20 [AF146243]
CS Clone CS2.2 [AB069783]
GoM GC185 510S5
GoM GC185 585S5
HS Clone GCA017 [AF154102]
GoM GC234 094S5
GoM GC234 069S5
HR Clone Eel-BE1A5 [AF354144]
GoM GC234 613S5
GoM GC234 629S5
GoM GC234 601S5
GoM GC185 542S5
GoM GC234 014S5
GoM GC234 676S5
GoM GC234 634S5
GoM GC234 683S5
GoM GC185 580S5
Desulfobacterium anilini [AJ237601]
MS Clone Sva0516 [AJ241002]
Isolate NaphS2 [AJ132804]
Isolate EbS7 [AJ430774]
Methanogenic Clone UASB TL9 [AF254389]
GoM AT425 EubP5 [AY053494]
CG Clone 12-2 [AF351212]
Syntrophus gentianae [X85132]
BR Clone SHA-42 [AJ306771]
GoM GC234 681S5
GoM GC234 615S6
GoM GC234 054S5
Sulfurospirillum arcachonense [Y11561]
Rhizobium leguminosarum [X67233]
Bacterioplankton BB2AT2 [AY028206]
GoM GC234 071S5
Hyphomicrobium sp. Ddeep-1 [AB055793]
Hyphomicrobium indicum [AB016982]
Marinobacter lutaoensis [AF288157]
GoM AT425 EubC3 [AY053484]
Pseudomonas aeruginosa [U38445]
TS Clone thioautotrophic symbiont [AB042414]
GoM GC234 631S5
GoM GC234 662S5
HV Clone C1 B013 [AF420363]
GoM AT425 EubD3 [AY053488]
Ralstonia pickettii [X67042]
0.1
High G+C
Low G+C and G1
G6
G2
GoM G6
G3
G4
G5
GoM G5
Delta
Alpha
Epsilon
Gamma
Beta
Actinobacteria
Firmicutes
Proteobacteria

Figure 2.3 Phylogenetic tree of relationships of 16S rRNA gene sulfate reducing Group 5 and Group 6 bacterial clone sequences, as determined by distance Jukes-Cantor analysis, from GoM seep sediments overlaying surface-breaching gas hydrate mounds (in boldface) to selected cultured isolates and environmental sequences. Designations of environmental clone sequences are AB, Artesian Basin; AS, anoxic sediment; BR, bioreactor; CA, contaminated aquifer; CG, contaminated groundwater; CS, continental slope; ER, Eel River Basin; HS, hydrocarbon seep; HV, hydrothermal vent; JT, Japan Trench; MC, methanogenic consortium; MS, marine sediment; NS, North Sea; RM, rice microcosms; SM, salt marsh; TS, thioautotrophic symbiont II; UM, uranium mine. Genbank accession numbers are in parentheses. One thousand bootstrap analyses were conducted and percentages greater than 50% are reported. *Methanosarcina acidovorans* was used as the outgroup. The scale bar represents the expected number of changes per nucleotide position.

GenBank accession no. AF407679). In addition, a number of clones exhibited similarity to a second environmental rRNA gene sequence obtained from the Artesian Basin (AB Clone Y36), and a methanogenic consortium bacterium (MC Clone BA143; (184)) (Table 2.1). A total of four distinct *Firmicutes*-related phylotypes, representing 27% of the SRB Group 6 clones, exhibited similarity (>89%) to the same environmental clone from a rice microcosm (RM Clone PBS-III-27; (34)). The detection of a considerable number of *Firmicutes*-related sequences may be explained in part by the cross-reactivity of the forward Group 6 primer, DSV230, and the DSV687 oligonucleotide probe (35) to culturable Gram-positive SRB isolates including *Desulfotomaculum* spp. In addition, our Group 6 *Firmicutes*-like clones contain 14 of 16 nucleotides of the conserved region (5' AGGAGTGAAATCCGTA 3') targeted by the DSV687 probe. However, as our *Firmicutes*-like environmental clones are only 88% and 89% similar to the sulfate reducing *Desulfotomaculum geothermicum* (159) and *Clostridium subatlanticum* respectively, we cannot ascertain definitively whether or not they dissimilate sulfur compounds. Although the sulfur metabolism capabilities of *Clostridium subatlanticum* have not been reported, strain Lup 21^T designated *Clostridium thiosulfatireducens* sp. nov. (61), and *C. peptidivorans* (104) have been shown to reduce thiosulfate to sulfide. Therefore, in addition to an SRB partner coupling with an aceticlastic methanogen as has been reported for other cold seep habitats (10, 62, 122, 124, 170, 172), we hypothesize that fermentative thiosulfate reducing bacteria could thus potentially play an important role in the anaerobic oxidation of methane in GoM hydrocarbon seep sediments.

2.4.4 Phylogenetic diversity of *Archaea*

A total of 126 *Archaea* clones from GC185 and GC234 were grouped into 25 RFLP patterns (data not shown) and representative clones from all patterns were sequenced (Figure 2.4). The 25 RFLP groups encompassed five phylogenetic lineages including the *Crenarcheota* and four groups of *Euryarchaeota* (i.e., *Thermoplasmales*, *Methanomicrobiales*, *Methanosarcinales*, and ANME-1). Although a small percentage of clones from the *Bacteria* library were most closely related to cultured isolates, none of the archaeal clone sequences exhibited such similarity as the library was dominated by the as yet to be cultured groups ANME-1 and ANME-2. Similar findings have recently been reported for other hydrocarbon seep systems (62, 122, 134, 170). In *Archaea* assemblages associated with one sediment-free gas hydrate sample collected by piston coring in the GoM [AT425, 1920 m water depth (Figure 1.1)] significantly fewer RFLP groups (n=8) were observed (88).

The majority of the *Archaea* clones (84%; Table 2.3) are related to methanogens (i.e., the orders *Methanosarcinales and Methanomicrobiales*) as well as to ANME-1. A total of 43 clones associated with the order *Methanosarcinales* branch within the cluster to form a distinct clade known as ANME-2. Members of this cluster, as well as those related to ANME-1, are frequently and often exclusively detected in methane seep environments with sediment profiles indicative of anaerobic methane oxidation activity (62, 88, 122, 169). As reported by Orphan et al. (122), the ANME-2 cluster can be divided into three distinct subgroups designated A, B and C. A total of 41 clones from our study can be assigned to either the A or C subgroups (Table 2.3), with none of the GoM clones being related to the ANME-2 subgroup B. In addition to these subgroups, a

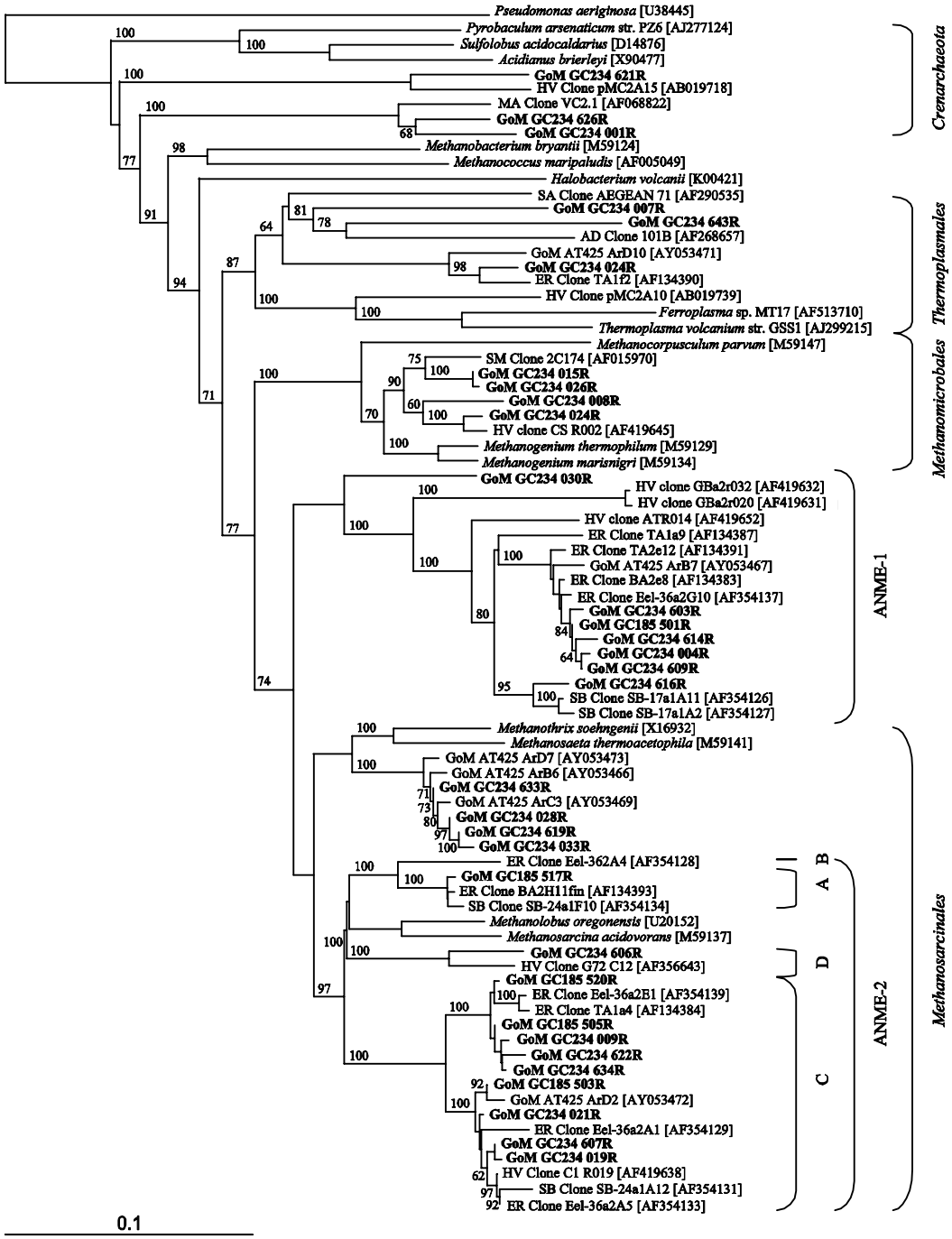
Pseudomonas aeriginosa [U38445]
Pyrobaculum arsenaticum str. PZ6 [AJ277124]
Sulfolobus acidocaldarius [D14876]
Acidianus brierleyi [X90477]
GoM GC234 621R
HV Clone pMC2A15 [AB019718]
MA Clone VC2.1 [AF068822]
GoM GC234 626R
GoM GC234 001R
Methanobacterium bryantii [M59124]
Methanococcus maripaludis [AF005049]
Halobacterium volcanii [K00421]
SA Clone AEGEAN 71 [AF290535]
GoM GC234 007R
GoM GC234 643R
AD Clone 101B [AF268657]
GoM AT425 ArD10 [AY053471]
GoM GC234 024R
ER Clone TA1f2 [AF134390]
HV Clone pMC2A10 [AB019739]
Ferroplasma sp. MT17 [AF513710]
Thermoplasma volcanium str. GSS1 [AJ299215]
Methanocorpusculum parvum [M59147]
SM Clone 2C174 [AF015970]
GoM GC234 015R
GoM GC234 026R
GoM GC234 008R
GoM GC234 024R
HV clone CS R002 [AF419645]
Methanogenium thermophilum [M59129]
Methanogenium marisnigri [M59134]
GoM GC234 030R
HV clone GBa2r032 [AF419632]
HV clone GBa2r020 [AF419631]
HV clone ATR014 [AF419652]
ER Clone TA1a9 [AF134387]
ER Clone TA2e12 [AF134391]
GoM AT425 ArB7 [AY053467]
ER Clone BA2e8 [AF134383]
ER Clone Eel-36a2G10 [AF354137]
GoM GC234 603R
GoM GC185 501R
GoM GC234 614R
GoM GC234 004R
GoM GC234 609R
GoM GC234 616R
SB Clone SB-17a1A11 [AF354126]
SB Clone SB-17a1A2 [AF354127]
Methanothrix soehngenii [X16932]
Methanosaeta thermoacetophila [M59141]
GoM AT425 ArD7 [AY053473]
GoM AT425 ArB6 [AY053466]
GoM GC234 633R
GoM AT425 ArC3 [AY053469]
GoM GC234 028R
GoM GC234 619R
GoM GC234 033R
ER Clone Eel-362A4 [AF354128]
GoM GC185 517R
ER Clone BA2H11fin [AF134393]
SB Clone SB-24a1F10 [AF354134]
Methanolobus oregonensis [U20152]
Methanosarcina acidovorans [M59137]
GoM GC234 606R
HV Clone G72 C12 [AF356643]
GoM GC185 520R
ER Clone Eel-36a2B1 [AF354139]
ER Clone TA1a4 [AF134384]
GoM GC185 505R
GoM GC234 009R
GoM GC234 622R
GoM GC234 634R
GoM GC185 503R
GoM AT425 ArD2 [AY053472]
GoM GC234 021R
ER Clone Eel-36a2A1 [AF354129]
GoM GC234 607R
GoM GC234 019R
HV Clone C1 R019 [AF419638]
SB Clone SB-24a1A12 [AF354131]
ER Clone Eel-36a2A5 [AF354133]
0.1
Crenarchaeota
Thermoplasmales
Methanomicrobales
ANME-1
ANME-2
Methanosarcinales
A
B
C
D

Figure 2.4 Phylogenetic tree of relationships of 16S rRNA gene archaeal clone sequences, as determined by distance Jukes-Cantor analysis, from GoM seep sediments overlaying surface-breaching gas hydrate mounds (in boldface) to selected cultured isolates and environmental clones. Designations of environmental clone sequences are AD, anaerobic digester; ER, Eel River; HV, hydrothermal vent; MA, Mid-Atlantic Ridge; SA, South Aegean; SB, Santa Barbara Basin; SM, salt marsh. Genbank accession numbers are in parentheses. One thousand bootstrap analyses were conducted and percentages greater than 50% are reported. *Pseudomonas aeruginosa* was used as the outgroup. The scale bar represents the expected number of changes per nucleotide position.

fourth lineage, ANME-2 subgroup D, was identified (Figure 2.4) to incorporate those clones represented by GoM GC234 606R (Table 2.3). The remaining clones associated with *Methanosarcinales* are most closely related to environmental clones from the GoM (>98% similarity) (88) and the cultured isolate *Methanothrix soehngenii* (40) (>91% similarity). A total of 25 of the 126 clones were related to the ANME-1 clade (Table 2.3). With the exception of one phylotype (GoM GC234 633R), all ANME-1-related clones were >93% similar to 16S rRNA gene clones derived from nucleic acids extracted from other methane seep sediments (62, 88, 122, 170). In the present study, clones related to *Methanomicrobiales* comprised 14% of the total *Archaea* library (Table 2.3). As observed with ANME-1 and *Methanosarcinales*-related clones, these particular clones were most closely related to non-cultured phylotypes [Figure 2.4; (112, 170)].

The remaining 16% of the *Archaea* clones were either related to non-methanogenic *Euryarchaeota* (i.e., *Thermoplasmales*; n=7) or to *Crenarchaeota* (n=13). The four clones represented by GoM GC234 024R are most related to environmental clones (>94% similar) isolated from methane-rich seep sediments (62) and sediment-free hydrate from the GoM (88) and only distantly related to cultured *Thermoplasmales* sp. (75% similar). In addition, the three clones represented by phylotypes GoM GC234 007R and GoM GC234 643R are also only distantly related (78% similar) to other previously identified environmental clones [Figure 2.4; (110)]. As observed with the *Thermoplasmales*-related clones, the *Crenarchaeota*-related clones are most closely related (>92% similar) to marine environmental clones (135, 166). This is the first report of *Methanomicrobiales*-related (14% of total library) and *Crenarchaeota*-related (10% of

total library) sequences obtained from the GoM hydrate-sedimentary system (Table 2.3 and Figure 2.4).

2.4.5 Phylogenetic diversity of ANME archaea

To better elucidate the members of the ANME-1 and ANME-2 phylotypes, we constructed 16S rRNA gene libraries based on primer sets for putative anaerobic methane oxidizing *Archaea* (172). A total of 138 ANME clones grouped into 22 RFLP patterns and representatives were sequenced (Table 2.3). The most frequently recovered phylotypes (n=116) were related to either the ANME-2 (44% of all clones; Table 2.3) or *Methanomicrobiales* (40% of all clones). In contrast to the *Archaea* library (ANME-1; n=25), the resulting GoM ANME library contained few ANME-1 clones (n=2), whereas 7% of the clones were related to *Thermoplasmales* (Figure 2.5). Instead, as much as 44% of the clone sequences were most closely related to the ANME-2 group. Although ANME-2-related sequences are indeed frequently present in *Archaea* libraries from other high-flux methane-rich cold seep sediment systems (10, 62, 122) and coastal marine habitats (112), we cannot rule out the possibility that the ANME primer set used to construct our GoM ANME library is biased against ANME-1-related groups.

Sequences of ANME-2-related clones were most similar (>94%) to HV Clone G72_C12 (unpublished, GenBank accession no. AF356643) isolated from nucleic acids recovered from the Guaymas Basin (Figure 2.5). While our *Archaea* library lacks clones related to ANME-2 subgroup B, clones related to both ANME-2 subgroups A and C were present (122). Interesting, our GoM ANME library contained ANME-2 related sequences solely represented by members in a yet to be described clade we are designating ANME-

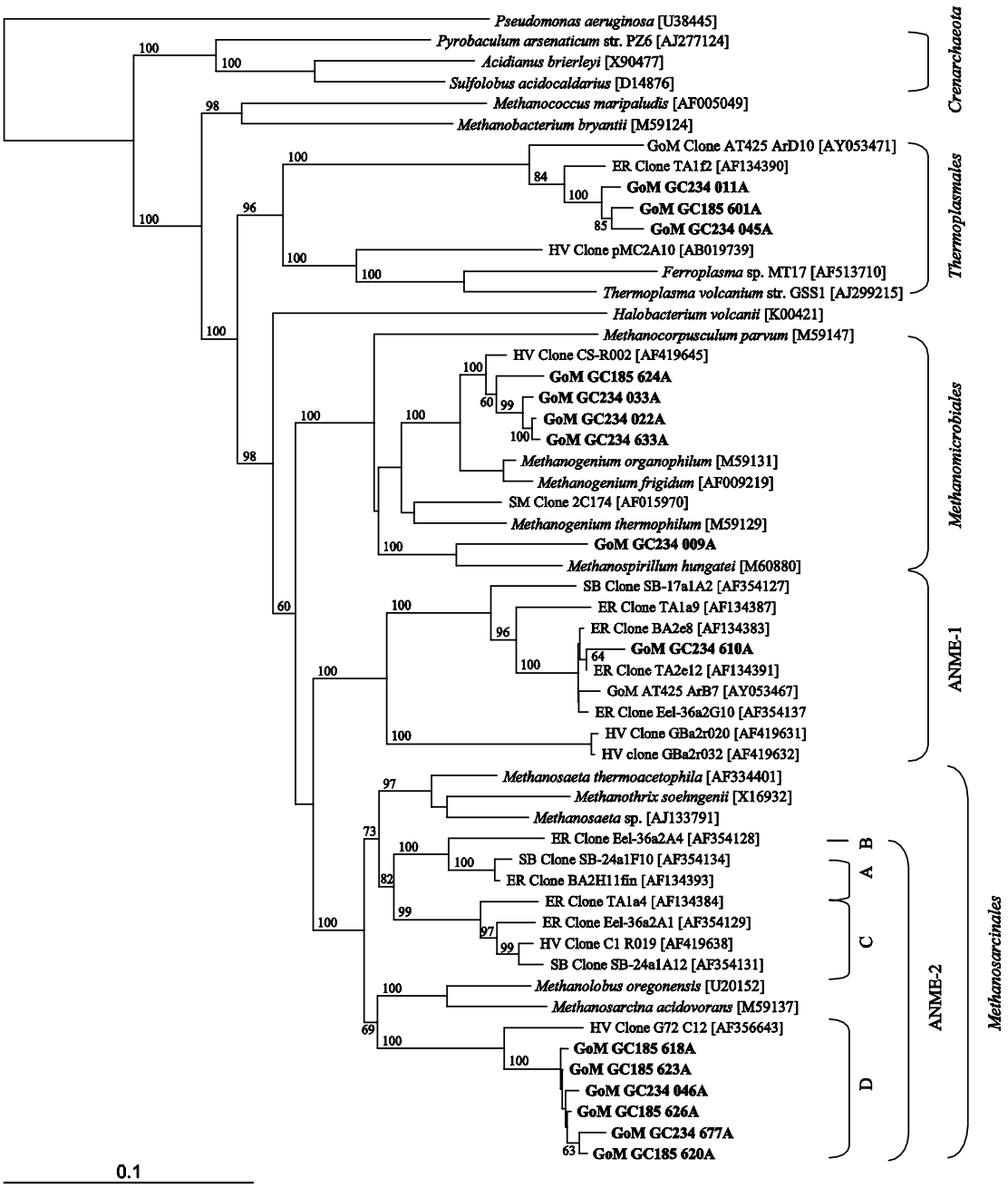
Pseudomonas aeruginosa [U38445]
Pyrobaculum arsenaticum str. PZ6 [AJ277124]
Acidianus brierleyi [X90477]
Sulfolobus acidocaldarius [D14876]
Methanococcus maripaludis [AF005049]
Methanobacterium bryantii [M59124]
GoM Clone AT425 ArD10 [AY053471]
ER Clone TA1f2 [AF134390]
GoM GC234 011A
GoM GC185 601A
GoM GC234 045A
HV Clone pMC2A10 [AB019739]
Ferroplasma sp. MT17 [AF513710]
Thermoplasma volcanium str. GSS1 [AJ299215]
Halobacterium volcanii [K00421]
Methanocorpusculum parvum [M59147]
HV Clone CS-R002 [AF419645]
GoM GC185 624A
GoM GC234 033A
GoM GC234 022A
GoM GC234 633A
Methanogenium organophilum [M59131]
Methanogenium frigidum [AF009219]
SM Clone 2C174 [AF015970]
Methanogenium thermophilum [M59129]
GoM GC234 009A
Methanospirillum hungatei [M60880]
SB Clone SB-17a1A2 [AF354127]
ER Clone TA1a9 [AF134387]
ER Clone BA2e8 [AF134383]
GoM GC234 610A
ER Clone TA2e12 [AF134391]
GoM AT425 ArB7 [AY053467]
ER Clone Eel-36a2G10 [AF354137
HV Clone GBa2r020 [AF419631]
HV clone GBa2r032 [AF419632]
Methanosaeta thermoacetophila [AF334401]
Methanothrix soehngenii [X16932]
Methanosaeta sp. [AJ133791]
ER Clone Eel-36a2A4 [AF354128]
SB Clone SB-24a1F10 [AF354134]
ER Clone BA2H11fin [AF134393]
ER Clone TA1a4 [AF134384]
ER Clone Eel-36a2A1 [AF354129]
HV Clone C1 R019 [AF419638]
SB Clone SB-24a1A12 [AF354131]
Methanolobus oregonensis [U20152]
Methanosarcina acidovorans [M59137]
HV Clone G72 C12 [AF356643]
GoM GC185 618A
GoM GC185 623A
GoM GC234 046A
GoM GC185 626A
GoM GC234 677A
GoM GC185 620A
0.1
Crenarchaeota
Thermoplasmales
Methanomicrobiales
ANME-1
ANME-2
A
B
C
D
Methanosarcinales

Figure 2.5 Phylogenetic tree of relationships of 16S rRNA gene putative anaerobic methane oxidizing archaeal clone sequences, as determined by distance Jukes-Cantor analysis, from GoM seep sediments overlaying surface-breaching gas hydrate mounds (in boldface) to selected cultured isolates and environmental sequences. Designations of environmental clone sequences are ER, Eel River Basin; HV, hydrothermal vent; SB, Santa Barbara Basin; SM, salt marsh. *Pseudomonas aeruginosa* was used as the outgroup. Genbank accession numbers are in parentheses. One thousand bootstrap analyses were conducted and percentages greater than 50% are reported. The scale bar represents the expected number of changes per nucleotide position.

2D. Again, while primer bias may occur it is important to note that clones related to ANME-2D clade were also obtained in our *Archaea* library. Although no cultivated isolates were closely related to this tightly branching ANME-2D clade, the same environmental clone, HV Clone G72_C12 from Guaymas Basin was most closely related (94% similarity) to clone sequences from the GoM *Archaea* and ANME libraries. Interestingly, clones from this phylotype were less then 86% similar to previously identified ANME-2 subgroups A, B and C (122).

As previously seen with ANME-2, the majority of the clones (44 of 55) related to *Methanomicrobiales* were most similar to rRNA gene sequences from Guaymas Basin hydrothermal sediments [Figure 2.5; (170)]. The remaining 11 *Methanomicrobiales*-related clones are most similar to *Methanospirillum hungatei* (>91%), one of the few cultured members of the family *Methanospirillaceae* reported to date (11). The *Methanomicrobiales*-related clones comprise 40% of the total ANME library, however this cluster has not previously been linked to anaerobic methane oxidation. Although such clones may be due to primer bias, *Methanomicrobiales* share common physiological traits with *Methanosarcinales* and thus may contain ANME related phylotypes. Due to the lack of sequence information and cultivated ANME isolates to compare, we cannot rule out that this group may represent an additional cluster of anaerobic methane oxidizing archaea.

2.5 Conclusion

To date, few studies have addressed the microbial ecology of the hydrocarbon-rich GoM seep sediments and associated gas (i.e., methane) hydrate habitats. The composition of these communities, as determined by our 16S rRNA gene analyses, lends further support to recent geochemical findings (74, 189) indicating that anaerobic methane oxidation is a predominate microbial process in the GoM gas hydrate ecosystem. A recent molecular characterization of microbes extant in a single gas hydrate sample recovered from piston-cored sediment collected from a deep water site also located in the GoM (AT425, 1,920 m; Figure 1.1) resulted in vastly different dominant *Bacteria* and *Archaea* populations (88). Lanoil et al. (88) observed a surprisingly low percentage of δ-*Proteobacteria* (5%) and failed to detect any ε-*Proteobacteria*. Instead, their libraries were dominated by sequences related to *Actinobacteria* (26%), γ-*Proteobacteria*, non-ANME-2 *Methanosarcinales* (30%) and ANME-1 (17%) groups. This is in contrast to our results and other seep sediment studies (62, 122, 170) in which δ- and ε-*Proteobacteria* and ANME-2-related sequences dominated. Such differences serve to highlight the diversification and potential specialization of microbial communities associated with GoM gas hydrate and associated sedimentary niches.

2.6 Acknowledgements

This work was supported by National Science Foundation LExEn grant OCE-0085549 (to PAS), the National Undersea Research Center, University of North Carolina

at Wilmington and the Department of Energy National Energy Technology Laboratory. We thank Captains R. van Hoek and G. Gunther and the other officers and crews of the DSRV *Johnson Sea-Link*, the R/V *Seward Johnson I* and the R/V *Seward Johnson II* for their invaluable assistance in sample collections. We also thank C. Ruppel for bathymetry map assistance and C. Fisher for helpful insights on sampling and study sites.

CHAPTER 3

CHARACTERIZATION OF MICROBIAL COMMUNITY STRUCTURE IN GULF OF MEXICO GAS HYDRATES: A COMPARATIVE ANALYSIS OF DNA- AND RNA-DERIVED CLONE LIBRARIES

3.1 Abstract

A molecular phylogenetic approach was used to characterize the metabolically active fraction of the microbial communities extant at the sediment/hydrate interface and in sediment-free hydrate from active cold seeps in the northern Gulf of Mexico. Samples were obtained using a specialized hydrate chipper designed for use on the manned-submersible *Johnson Sea Link* (water depth approximately 550 m). Geochemical analysis and extracted RNA and DNA concentrations indicated increased metabolic activity at the sediment/hydrate interface relative to the sediment-free hydrate. Phylogenetic analysis of RNA- and DNA-derived clones indicated more diversity at the sediment/hydrate interface. Numerous phylotypes were isolated exclusively from a single sample type indicating a potential niche specialization for some lineages. A majority of clones obtained from the metabolically active fraction of the microbial community were most related to putative sulfate reducing bacteria and anaerobic methane oxidizing archaea. Several novel bacterial and archaeal phylotypes with no previously identified closely related cultured isolates were detected in both RNA- and DNA-derived clone libraries. This study represents the first phylogenetic analysis of the metabolically active fraction

of the microbial community extant at the sediment/hydrate interface and in sediment-free hydrate.

3.2 Introduction

Marine gas hydrates, ice-like crystalline solids, are composed of rigid water molecules with trapped gas molecules, primarily methane and other hydrocarbons. In addition to their potential use as a fossil fuel energy source (55), the estimated global occurrence of submarine methane hydrates exceeds 10^{16} m^3 (39, 55), highlighting the impact of hydrates on global carbon cycling, climate conditions, and seafloor stability (86, 91, 127, 143, 150). Gas hydrate reservoirs are distributed in the sediments of active and passive continental slope margins as well as terrestrial (i.e., permafrost) regions (156). The stable formation of gas hydrates is dependent upon suitable gas, temperature and pressure conditions (reviewed in (15)). Geological and chemical conditions in the northern continental slope of the Gulf of Mexico (GoM) promote the formation of gas hydrates where seepage of hydrocarbon gases form extensive surface-breaching mounds on the seafloor as well as vast vein-filling hydrates in hemi-pelagic sediments (122).

Geochemical characterizations, including gas composition and isotopic ratios of surface breaching hydrate in the GoM have been well documented (13, 145, 146, 156). The growth and dissolution of GoM hydrate mounds has also been observed with changes in mound size and shape evident over a period of months (97). Such hydrate growth patterns would increase fluid and solid (i.e., sediment) inclusions as well as increase the frequency of interconnecting flaws and fissures (176). Thus, Sassen et al.

(150) have proposed that rapidly growing hydrate crystals on the outer layers of hydrate mounds, such as those found in the GoM (144), can be colonized by microorganisms. While rate measurements indicate that active microbial populations are present in the distinct layers of solid gas hydrate (121), information regarding the composition of the corresponding metabolically active fraction of the microbial communities extant in these hydrate environments is lacking. Thus, the characterization of microbial assemblages within solid hydrate, especially those that may be physiologically active under *in situ* hydrate conditions, is essential to gain a better understanding of the effects and contributions of microbial activities on GoM hydrate ecosystems.

In the present study, nucleic acids (DNA and RNA) were extracted from samples representing two distinct layers of a gas hydrate environment. One layer denoted 'interior hydrate' refers to the solid materials collected from within the interior portion of solid gas hydrate (> 5 cm from the outside surface) entirely devoid of sediment particles. The second layer, denoted 'sediment-entrained hydrate' refers to materials collected at the interface between the interior portion of the hydrate (IH) and the sediment directly in contact with hydrate. Sediment-entrained hydrate (SEH) samples were mainly composed of solid gas hydrate with less than 5% of the mix composed of sediment particles. The primary objective of this study was to characterize the metabolically active fraction of the microbial communities present in these distinct hydrate layers. Total rRNA was extracted from the IH and SEH layers and subjected to reverse transcription-polymerase chain reaction (RT-PCR) with primers specific for the *Bacteria* and *Archaea* domains. Co-extracted DNA was also amplified with *Bacteria* and *Archaea* domains so that comparisons to the RNA-derived 16S rRNA gene libraries could be made. This study is

the first phylogenetic analysis of interior hydrate-associated microbial communities from surface-breaching GoM gas hydrate mounds and the first report of the metabolically active fraction of IH- and SEH-associated microbial communities.

3.3 Materials and methods

3.3.1 Gulf of Mexico site description and sample collection

The study site, GC 234 (575 m depth) is located in the Green Canyon area in the northern Gulf of Mexico (GoM) continental slope province at 27°44'N, 91°13'W. A detailed site description has recently been reported in Orcutt et al. (121). This area contained oil and gas seepage with extensive (i.e., meters thick) surface breaching gas hydrate mounds and displaced sediments colonized by chemosynthetic tube worms, mussels and polychaete ice worms (45, 49, 157). Samples of solid gas hydrate with overlying sediment drape were collected from visible gas hydrate mounds during multiple dives of the *Johnson Sea Link* manned submersible in July 2002. Recovery, preservation and storage of solid gas hydrate samples and shipboard manipulations have been described in detail in Mills et al. (108). Solid gas hydrate with overlying, entrained sediment was aseptically divided into i) sediment-entrained solid hydrate (SEH) and ii) interior solid hydrate (IH). SEH samples were composed of solid gas hydrate with generally no more than 5% of the mix being sediment particles. IH samples were composed of interior solid hydrate devoid of any sediment, acquired by aseptically cutting and paring away the outer sediment-entrained layers of intact solid gas hydrate (12 cm diameter). Multiple aliquots (150-250 g) of SEH and IH were subsequently stored

in liquid N_2. Direct cell counts were performed on unfrozen aliquots (0.5 g wet wt) of displaced, overlying sediment, SEH and IH samples as previously described (131). Replicate samples were processed for geochemistry (i.e., gas composition and anion concentrations) and microbial activity rate measurements of sulfate reduction and methane oxidation. Relevant geochemical and rate data was included in Table 3.1 and a description of the (geo)chemistry of these samples has been reported (121).

3.3.2 Preparation of reagents and materials used for RNA extraction

Prior to nucleic acid extraction, RNases were removed from solutions and solids by treating stock solutions and water with 0.1% diethylpyrocarbonate (DEPC) overnight at 37^{o}C and autoclaving. All glassware and non-plastics were baked at 250^{o}C for 24 h. All surfaces and plastics were cleaned with RNase Erase (ICN, Aurora, OH) to remove contaminating RNases during shipboard and laboratory manipulations.

3.3.3 RNA and DNA isolation

Total nucleic acids from triplicate samples of SEH and IH aliquots (50-100 g) were extracted as described in Hurt et al. (66). In brief, SEH and IH samples stored in liquid N_2 were repeatedly thawed by physical grinding in the presence of a denaturing solution (4 M guanidine isothiocyanate, 10 mM Tris-HCl [pH 7.0], 1 mM EDTA, 0.5% 2-mercaptoethanol) and refrozen by immersion in liquid N_2. The SEH and IH samples were incubated 30 min at 65^{o}C in pH 7.0 extraction buffer (100 mM sodium phosphate [pH 7.0], 100 mM Tris-HCl [pH 7.0], 100 mM EDTA [pH 8.0], 1.5 M NaCl, 1% hexadecyltrimethylammonium bromide [CTAB], and 2% SDS) and centrifuged (1,800 ×

Table 3.1

Biogeochemical profile of sediment/hydrate interface and sediment-free hydrate samples

Sample Type	Cells g^{-1}	RNA ($\mu g\ g^{-1}$)	DNA ($\mu g\ g^{-1}$)	RNA:DNA	Sulfate (mM) [b]	AOM [a] (nmol cm^{-3} day^{-1}) [b]	SR [a] (nmol cm^{-3} day^{-1}) [b]
Sediment overlying hydrate	$4.3 \times 10^8 \pm 4.8 \times 10^7$ [c]	ND[d]	ND	ND	12.3 ± 1.4	0.60 ± 0.2	76.2 ± 20.8
Sediment-entrained hydrate	$2.0 \times 10^7 \pm 4.2 \times 10^6$	11.4	11.5	0.99	9.5 ± 1.0	0.13 ± 0.1	23.0 ± 1.0
Interior hydrate	$4.3 \times 10^6 \pm 2.1 \times 10^6$	0.9	3.6	0.25	3.2 ± 2.1	0.28 ± 0.3	3.2 ± 4.1

[a] abbreviations: AOM, anaerobic oxidiation of methane; SR, sulfate reduction

[b] previously reported in Orcutt et al. (121) from the same samples as used in this study

[c] previously reported in Mills et al. (108) from samples acquired at GC234 in July 2001

[d] not determined

g for 10 min). The supernatants from three separate extractions were pooled, extracted with 24:1 (v/v) chloroform-isoamyl alcohol and centrifuged (1,800 × g for 20 min). The nucleic acids were precipitated at room temperature with isopropanol (30 min), pelleted by centrifugation (16,000 × g for 20 min), resuspended in DEPC-treated water and subsequently purified by ion exchange chromatography (66, 158) into DNA- and RNA-only aliquots.

3.3.4 Reverse transcription of ribosomal RNA

Aliquots of ribosomal RNA were reverse transcribed (RT) with MMLV reverse transcriptase according to manufacturer's instructions (Invitrogen, CA). Purified RNA was initially denatured by heating (65^{o}C) for 10 min. The RT reaction mix consisted of 5 μM of a 16S rRNA reverse primer amplifying either domain-specific *Bacteria*, i.e., DXR518 (5'-CGTATTACCGCGGCTGCTGG-3') (120) or *Archaea*, i.e., Ar958r (5'-YCCGGCGTTGAMTCCAATTT-3') (33), 50-100 ng of denatured RNA and 200 μM dNTPs. The mix was incubated for 5 min at 65^{o}C and 2 min at 4^{o}C followed by the addition of 1 × 1st Strand Buffer (50 mM Tris-HCl [pH 8.3], 75 mM KCl, 3 mM $MgCl_2$) and 75 U RNase inhibitor and heating at 37^{o}C for 2 min. MMLV (200 U) was added prior to a 50 min incubation at 37^{o}C that resulted in transcription of the RNA into crDNA. The crDNA end product was used as template for a standard PCR reaction. DNA contamination of RNA templates was routinely monitored by PCR amplification of aliquots of RNA that were not reverse transcribed. No contaminating DNA was detected in any of these reactions. The primers used for standard PCR amplification included the above reverse primers and 16S rRNA gene forward domain-specific *Bacteria*, i.e., 27F

(5'-AGAGTTTGATCCTGGCTCAG-3'), and *Archaea*, i.e., A341f (5'-CCTAIGGGGIGCAICAG-3') (179) primers. The PCR reaction mix contained 10-50 ng crDNA, 1× PCR buffer (Stratagene, CA), 1.5 mM $MgCl_2$, 200 μM of each dNTP, 1 pmol of each forward and reverse primer, and 0.025 U μl^{-1} *TaKaRa Taq*™ (TaKaRa, Japan). Amplicons were analyzed on 1.0% agarose gels run in TBE buffer, stained with ethidium bromide and UV illuminated.

3.3.5 Environmental clone library construction.

Aliquots of purified DNA (1 μl, corresponding to the DNA recovered from approximately 0.5-1.0 g sample) were PCR amplified as previously described (108). 16S amplicons, derived from SEH and IH DNA (e.g., 16S rRNA gene) and RNA (e.g., 16S crDNA) samples, were subsequently pooled from three to five reactions, purified with the Qiaquick gel extraction kit (Qiagen, CA) and cloned into the TOPO TA cloning vector pCR2.1 according to manufacturer's instructions (Invitrogen, CA). Cloned inserts were amplified from lysed colonies with the following primers specific for either the vector, i.e., M13F (5'-GTAAAACGACGGCCAG-3') and M13R (5'-CAGGAAACAGCTATGAC-3') or the *Archaea* amplicons, i.e, A341f (179) and Ar958r (33). The M13F/R primers were used to amplify inserts from bacterial clones to prevent amplification of the *Escherichia coli* host 16S rRNA gene. PCR products of bacterial clones were digested (2 h, 37°C) with *Msp*I and *Hha*I and with *Hha*I and *Rsa*I for archaeal clones. Clones were grouped according to restriction fragment length polymorphism (RFLP) patterns and representative clones sequenced as previously described (108). Representative clones from all phylotypes in each library, with the

exception of the DNA-derived bacteria library constructed from the SEH samples, were sequenced. Phylotypes from the SEH DNA library having more than one clone member and a random selection of phylotypes with a single clone representative were sequenced. Sequencing was performed at the Georgia Institute of Technology core DNA facility using a BigDye Terminator v3.1 Cycle sequencing kit on an automated capillary sequencer (model 3100 Gene Analyzer, Applied Biosystems**).** Inserts were sequenced multiple times on each strand. Prior to comparative sequence analysis, vector sequences flanking bacterial 16S rRNA gene and crDNA inserts were manually removed. A total of 97 sequences representing 374 *Bacteria* and *Archaea* clones were obtained in this study.

3.3.6 Phylogenetic and statistical analyses.

Sequence analysis was preformed as previously described in Mills et al. (108, 109). Multiple sequences of individual inserts were initially aligned using the program 'BLAST 2 Sequences' (167) available through the National Center for Biotechnology Information and assembled with the program BioEdit v5.0.9 (57). Sequences were checked for chimeras using Chimera Check from Ribosomal Database Project II (99). Sequences from this study and reference sequences, as determined by BLAST analysis, were subsequently aligned using CLUSTALX v1.81 (171). An average of 500 (*Bacteria* clones) to 600 (*Archaea* clones) nucleotides were included in the final phylogenetic analyses. Neighbor-Joining trees were created from the shortened sequence alignments. The bootstrap data represented 1,000 samplings. The final trees were viewed using NJPlot (130) and TreeView v1.6.6 available at http://taxonomy.zoology.gla.ac.uk/rod/treeview.html. Rarefaction analysis was

performed using equations as described in Heck et al. (60). Standard calculations were used to produce the rarefaction curve using the total number of clones obtained compared to the number of clones representing each unique RFLP pattern. Sorensen's index and Shannon-Weiner index were calculated using standard equations. Species richness was determined by the EstimateS (20, 26, 27). Additional statistical estimators, including gene (113) and nucleotide (113, 165) diversity, $\theta(\pi)$ (165), F_{ST} (155) and P tests (101), were calculated using Arlequin (154). Lineage-per-time plots were constructed from TreePuzzle (http://www.tree-puzzle.de) pairwise alignments assuming a molecular clock.

3.3.7 Nucleotide sequence accession numbers

The 97 16S rRNA gene and 16S crDNA nucleotide sequences have been deposited in the GenBank database under accession numbers AY542171-AY542267.

3.4 Results

The composition of the *Bacteria* and *Archaea* community in a gas hydrate environment in the GoM was determined by 16S rRNA gene phylogenetic analyses of clone libraries derived from RNA and DNA extracted from sediment-entrained hydrate (SEH) and interior hydrate (IH). The purified RNA was of sufficient quality and quantity to be reverse transcribed. The concentration of recovered RNA and DNA and the corresponding RNA:DNA ratios were significantly higher in the SEH layer compared to the IH layer (Table 3.1). Quantification of microbial cell numbers in the overlying sediment indicated a one- to two-order of magnitude higher cell count relative to either

the SEH or IH layers (Table 3.1). A similar trend was observed in sulfate reduction (SR) rates where the highest rates were measured in the overlying sediment and the lowest rates in the IH layer (Table 3.1). Higher rates of anaerobic oxidation of methane (AOM) were detected in the IH layer relative to the SEH (Table 3.1). The highest rate of AOM (0.60 ± 0.2 nmol cm^{-3} day^{-1}) was measured in the overlying sediment.

3.4.1 RFLP and statistical analyses of 16S rRNA-based libraries

Four different 16S rRNA-based libraries were constructed representing a total of 99 *Bacteria* 16S rRNA gene clones (DNA-derived), 97 *Bacteria* 16S complementary rDNA clones (RNA-derived, denoted crDNA), 100 *Archaea* 16S rRNA gene clones and 97 16S crDNA clones from IH and SEH layers. All clones were grouped according to restriction fragment length polymorphism (RFLP) patterns and subjected to rarefaction and percent coverage analysis to determine if a sufficient number of clones from each of the libraries were sampled to estimate library diversity (54). Curves reached saturation for *Archaea* clones obtained from either DNA or RNA (data not shown). The percent coverage for the *Archaea* clone libraries was greater than 92% with the exception of the DNA-derived library from the SEH (82%; Table 3.2). All *Archaea* clones libraries had significant ($P<0.05$) F_{ST} and P tests (data not shown) while lineage-per-time plots were similar to plots indicative of constant birth and deaths (data not shown) (101). Greater gene and nucleotide diversity, and $\theta(\pi)$ values were observed in IH DNA-derived libraries, whereas these indices were higher in the SEH layer RNA-derived libraries (Table 3.2).

Table 3.2

Statistical analysis of *Bacteria* and *Archaea* 16S rRNA gene clone libraries using standard ecological and molecular estimates of sequence diversity

Domain	Nucleic Acid Sampled	Sample Layer	No. of Clones Screened	No. of OTUs	Percent Coverage (%)	Species Richness	Sorensen's Index	Shannon-Weiner Index	Gene Diversity	Nucleotide Diversity	$\theta(\pi)$
Bacteria	DNA	SEH	34	35	42.9	69 (57, 81)[a]		2.785	0.95 ± 0.02[b]	0.22 ± 0.11[b]	85.0 ± 41.7[b]
		IH	46	26	64.0	45 (38, 53)		2.762	0.93 ± 0.02	0.24 ± 0.12	97.5 ± 47.4
		Total	80	55	60.6	77 (71, 82)	0.238	3.168	0.95 ± 0.01	0.23 ± 0.11	96.0 ± 46.2
	RNA	SEH	48	18	81.3	37 (14, 60)		2.591	0.93 ± 0.02	0.17 ± 0.08	82.0 ± 39.9
		IH	49	22	75.5	39 (30, 47)		2.811	0.94 ± 0.02	0.17 ± 0.08	76.8 ± 37.3
		Total	97	30	83.5	50 (44, 57)	0.500	2.946	0.94 ± 0.01	0.17 ± 0.08	83.0 ± 39.9
Archaea	DNA	SEH	50	12	82.0	33 (22, 45)		1.675	0.72 ± 0.05	0.08 ± 0.04	23.3 ± 11.6
		IH	50	14	92.0	15 (14, 16)		2.375	0.91 ± 0.02	0.21 ± 0.10	58.9 ± 28.7
		Total	100	20	94.0	24 (22, 27)	0.519	2.527	0.90 ± 0.02	0.17 ± 0.08	46.4 ± 22.5
	RNA	SEH	49	6	95.9	7 (4, 10)		1.301	0.69 ± 0.04	0.08 ± 0.04	44.7 ± 21.9
		IH	48	4	97.9	4 (4, 4)		0.897	0.49 ± 0.07	0.04 ± 0.02	23.3 ± 11.6
		Total	97	7	96.9	9 (4, 14)	0.600	1.293	0.69 ± 0.02	0.07 ± 0.03	38.3 ± 18.6

[a] parenthesis indicate 95% confidence intervals
[b] standard deviation

Rarefaction curves generated for *Bacteria* 16S rRNA gene and crDNA clones did not indicate saturation (data not shown). The percent coverage for the RNA-derived clones libraries ranged from 76% for the IH to 81% for the SEH layer. Both of these DNA-derived *Bacteria* libraries had a percent coverage less than 64% (Table 3.2). F_{ST} and P tests were insignificant (P>0.05) for all *Bacteria* libraries (data not shown). In addition, little difference was observed for gene and nucleotide diversity, Shannon-Weiner indices and $\theta(\pi)$ values calculated for the four *Bacteria* libraries (Table 3.2). In contrast to the *Archaea* libraries, *Bacteria* lineage-per-time plots were indicative of populations with an excess of highly divergent lineages (data not shown) (101).

3.4.2 *Bacteria* community structure based on 16S rRNA gene sequence analyses

Analysis of the 16S rRNA gene *Bacteria* clones obtained from the SEH and IH layers revealed the greatest phylogenetic diversity relative to the other clone libraries (Table 3.2). The vast majority of *Bacteria* clones obtained were most related to as yet uncultured lineages (Table 3.3). A total of 53 RFLP patterns (data not shown) representing eight distinct lineages and 55 phylotypes were detected. Representatives from 37 phylotypes, i.e., 13 phylotypes comprising more than one clone and 24 phylotypes incorporating a single clone, were sequenced and analyzed. All frequency calculations are based on the number of clones represented by phylotypes that have been sequenced (n = 80). No one lineage was numerically dominant in these DNA-derived

Table 3.3

Summary of 16S rRNA gene sequences from sediment entrained hydrate and interior hydrate *Bacteria* clone libraries.

Clone	Total Number of Related Clones	Sediment Entrained Hydrate	Interior Hydrate	Nearest Relative	Phylogenetic Group	Similarity (%)
GoM IDB-15	4	4	0	HS Clone GCA017	*Deltaproteobacteria*	95
GoM HDB-20	3	0	3	HS Clone GCA017	*Deltaproteobacteria*	99
GoM HDB-32	2	0	2	GoM Clone AT425 EubF5	*Deltaproteobacteria*	93
GoM IDB-43	1	1	0	GoM Clone AT425 EubF5	*Deltaproteobacteria*	91
GoM IDB-01	1	1	0	CM Clone Hyd89-52	*Deltaproteobacteria*	98
GoM HDB-12	1	0	1	CM Clone Hyd89-52	*Deltaproteobacteria*	98
GoM HDB-06	2	0	2	MB Clone NaphS2	*Deltaproteobacteria*	92
GoM IDB-47	2	1	1	FW Clone FW117	*Deltaproteobacteria*	90
GoM IDB-21	1	1	0	WW Clone SR FBR E86	*Deltaproteobacteria*	89
GoM IDB-33	1	1	0	GoM GC234 610E	*Deltaproteobacteria*	97
GoM HDB-02	11	4	7	GB Clone C1 B011	*Epsilonproteobacteria*	98
GoM HDB-15	1	0	1	GoM GC185 036E	*Epsilonproteobacteria*	96
GoM HDB-07	3	0	3	GoM GC185 546E	*Chloroflexi*	99
GoM HDB-31	1	0	1	GoM GC185 546E	*Chloroflexi*	99
GoM IDB-24	2	2	0	GB Clone C1 B004	*Chloroflexi*	97
GoM HDB-03	2	0	2	HS Clone GCA112	*Chloroflexi*	94
GoM HDB-23	1	0	1	WW Clone CARB ER2 5	*Chloroflexi*	89
GoM HDB-37	1	0	1	DSS Clone t0.6.f	*Chloroflexi*	90
GoM IDB-09	1	1	0	HV Clone P. palm A11	*Chloroflexi*	85
GoM IDB-35	1	1	0	MC Clone Eub 6	*Chloroflexi*	87
GoM IDB-50	1	1	0	TS Clone O1aA2	*Chloroflexi*	90
GoM HDB-21	7	2	5	GoM GC234 604E	*Firmicutes*	97
GoM HDB-18	1	0	1	GoM GC234 604E	*Firmicutes*	88

Table 3.3 (continued)

GoM HDB-46	1	0	1	GoM GC234 604E	*Firmicutes*	95
GoM IDB-10	1	1	0	GoM GC234 604E	*Firmicutes*	95
GoM IDB-30	1	1	0	GoM GC234 604E	*Firmicutes*	95
GoM IDB-40	1	1	0	GoM GC234 604E	*Firmicutes*	96
GoM IDB-03	2	1	1	*Clostridium* sp.	*Firmicutes*	87
GoM HDB-19	1	0	1	RC Isolate DSM 44180	*Verrucomicrobales*	89
GoM HDB-48	1	0	1	*Verrucomicrobia* Clone LD1-PA26	*Verrucomicrobales*	86
GoM HDB-08	1	0	1	SO Clone OHKB16.85	*Actinomycetales*	94
GoM IDB-04	1	1	0	TCE Clone ccslm2126	*Spirochaetales*	83
GoM HDB-04	13	5	8	HS Clone GCA025	HAB	99
GoM IDB-08	3	3	0	HS Clone GCA018	HAB	98
GoM HDB-09	1	0	1	GoM GC185 546E	HAB	99
GoM HDB-22	1	0	1	CM Clone Hyd24-12	Un. 1	95
GoM IDB-27	1	1	0	RP Clone P2D6	Un. 2	94

clone libraries (Table 3.3). Five of the eight lineages detected, i.e., δ - and ε–*Proteobacteria*, *Chloroflexi*, *Firmicutes* and Hydrocarbon-Associated Bacteria (Figure 3.1 and 3.2), comprised between 15 and 23% of the total 16S rRNA gene library (Table 3.3). A majority of the proteobacterial-related clones (18 of 30) were most similar to the δ-*Proteobacteria* and grouped into 10 different phylotypes (Table 3.3). The phylotype denoted GoM IDB-15 was one of five δ-related phylotypes detected only in the SEH layer (Table 3.3). Although only one of the 10 δ-related phylotypes, GoM IDB-47, was detected in both hydrate layers, comparable percentages of δ-related clones were observed in the SEH- (27%) and IH-derived (20%) libraries (Figure 3.3). The remaining 12 *Proteobacteria*-related clones, 15% of the total *Bacteria* 16S rRNA gene library, were related to the class ε–*Proteobacteria* (Table 3.3, Figure 3.1). One phylotype, GoM HDB-02, represented the majority of the ε–related sequences detected (Table 3.3).

A majority of the 16S rRNA gene *Bacteria* clones (63%; Table 3.3) were related to 4 non-*Proteobacteria* lineages including *Chloroflexi*, *Firmicutes*, *Verrucomicrobiales*, and *Spirochaetales*, and three as yet uncharacterized groups designated Hydrocarbon Associated Bacteria, Unclassified *Bacteria* group 1 and Unclassified *Bacteria* group 2 (Figure 3.2). The second most frequently detected group of phylotypes (21% of all rRNA gene clones; Table 3.3) was most closely related to the Hydrocarbon Associated Bacteria (HAB), a distinct clade within the phylum *Chloroflexi* (Figure 3.2). The HAB-related phylotype GoM HDB-04 was the most numerically abundant phylotype in the *Bacteria* library (16%; Table 3.3). Nine distinct *Chloroflexi*-related phylotypes were detected (Table 3.3), however none of these phylotypes co-occurred in the SEH and IH layers.

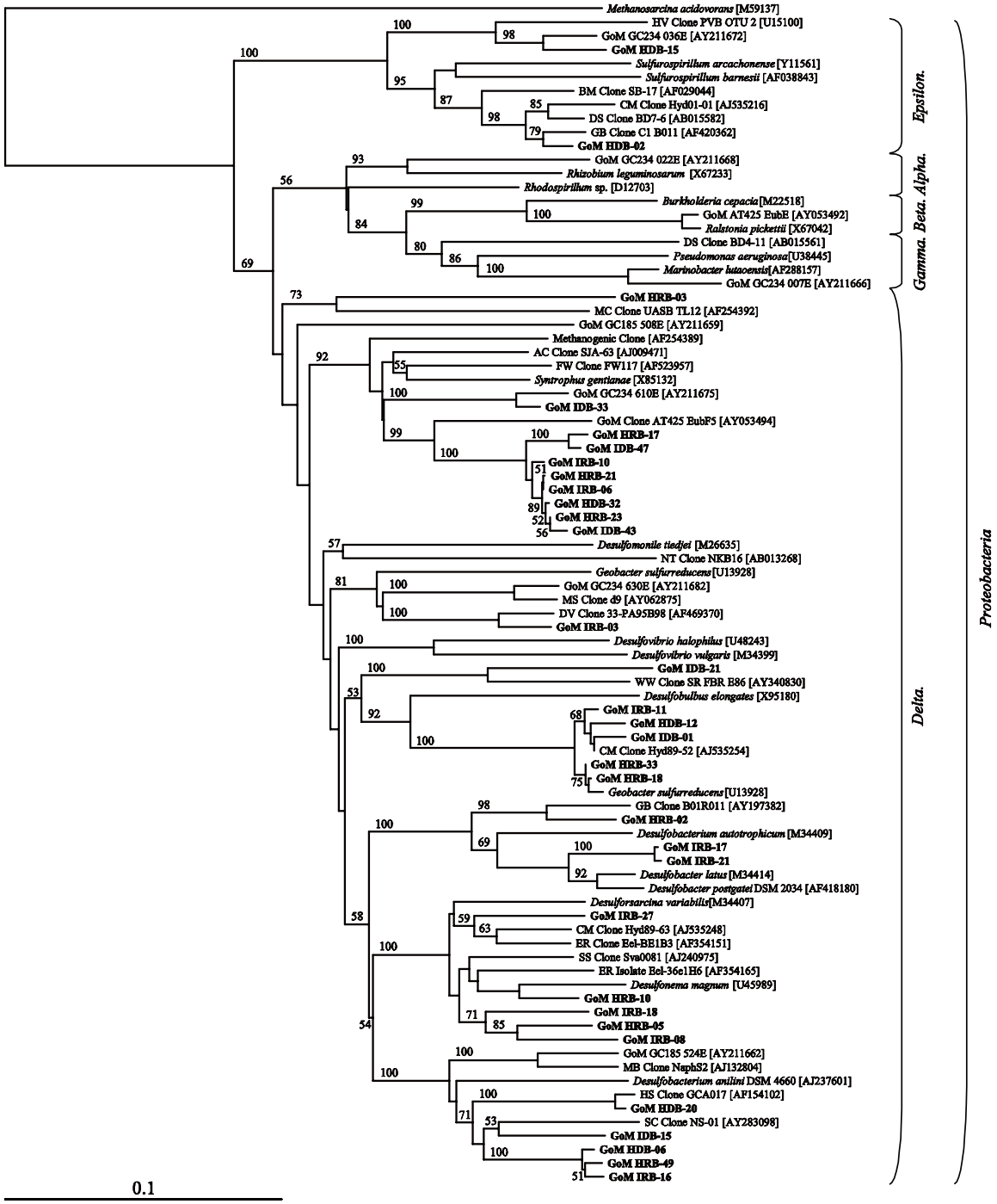
Methanosarcina acidovorans [M59137]
HV Clone PVB OTU 2 [U15100]
GoM GC234 036E [AY211672]
GoM HDB-15
Sulfurospirillum arcachonense [Y11561]
Sulfurospirillum barnesii [AF038843]
BM Clone SB-17 [AF029044]
CM Clone Hyd01-01 [AJ535216]
DS Clone BD7-6 [AB015582]
GB Clone C1 B011 [AF420362]
GoM HDB-02
GoM GC234 022E [AY211668]
Rhizobium leguminosarum [X67233]
Rhodospirillum sp. [D12703]
Burkholderia cepacia [M22518]
GoM AT425 EubE [AY053492]
Ralstonia pickettii [X67042]
DS Clone BD4-11 [AB015561]
Pseudomonas aeruginosa [U38445]
Marinobacter hutaoensis [AF288157]
GoM GC234 007E [AY211666]
GoM HRB-03
MC Clone UASB TL12 [AF254392]
GoM GC185 508E [AY211659]
Methanogenic Clone [AF254389]
AC Clone SJA-63 [AJ009471]
FW Clone FW117 [AF523957]
Syntrophus gentianae [X85132]
GoM GC234 610E [AY211675]
GoM IDB-33
GoM Clone AT425 BubF5 [AY053494]
GoM HRB-17
GoM IDB-47
GoM IRB-10
GoM HRB-21
GoM IRB-06
GoM HDB-32
GoM HRB-23
GoM IDB-43
Desulfomonile tiedjei [M26635]
NT Clone NKB16 [AB013268]
Geobacter sulfurreducens [U13928]
GoM GC234 630E [AY211682]
MS Clone d9 [AY062875]
DV Clone 33-PA95B98 [AF469370]
GoM IRB-03
Desulfovibrio halophilus [U48243]
Desulfovibrio vulgaris [M34399]
GoM IDB-21
WW Clone SR FBR B86 [AY340830]
Desulfobulbus elongates [X95180]
GoM IRB-11
GoM HDB-12
GoM IDB-01
CM Clone Hyd89-52 [AJ535254]
GoM HRB-33
GoM HRB-18
Geobacter sulfurreducens [U13928]
GB Clone B01R011 [AY197382]
GoM HRB-02
Desulfobacterium autotrophicum [M34409]
GoM IRB-17
GoM IRB-21
Desulfobacter latus [M34414]
Desulfobacter postgatei DSM 2034 [AF418180]
Desulforsarcina variabilis [M34407]
GoM IRB-27
CM Clone Hyd89-63 [AJ535248]
ER Clone Eel-BE1B3 [AF354151]
SS Clone Sva0081 [AJ240975]
ER Isolate Eel-36e1H6 [AF354165]
Desulfonema magnum [U45989]
GoM HRB-10
GoM IRB-18
GoM HRB-05
GoM IRB-08
GoM GC185 524E [AY211662]
MB Clone NaphS2 [AJ132804]
Desulfobacterium anilini DSM 4660 [AJ237601]
HS Clone GCA017 [AF154102]
GoM HDB-20
SC Clone NS-01 [AY283098]
GoM IDB-15
GoM HDB-06
GoM HRB-49
GoM IRB-16
0.1
Epsilon.
Gamma. Beta. Alpha.
Delta.
Proteobacteria

Figure 3.1 Phylum *Proteobacteria* phylogenetic tree of relationships of 16S rRNA gene and 16S crDNA bacterial clone sequences, as determined by distance Jukes-Cantor analysis, from GoM GC234 SEH and IH samples (in boldface) to selected cultured isolates and environmental clones. Genbank accession numbers are in parentheses. One thousand bootstrap analyses were conducted and percentages greater than 50% are reported. *Methanosarcina acidovorans* was used as the outgroup. The scale bar represents the expected number of changes per nucleotide position.

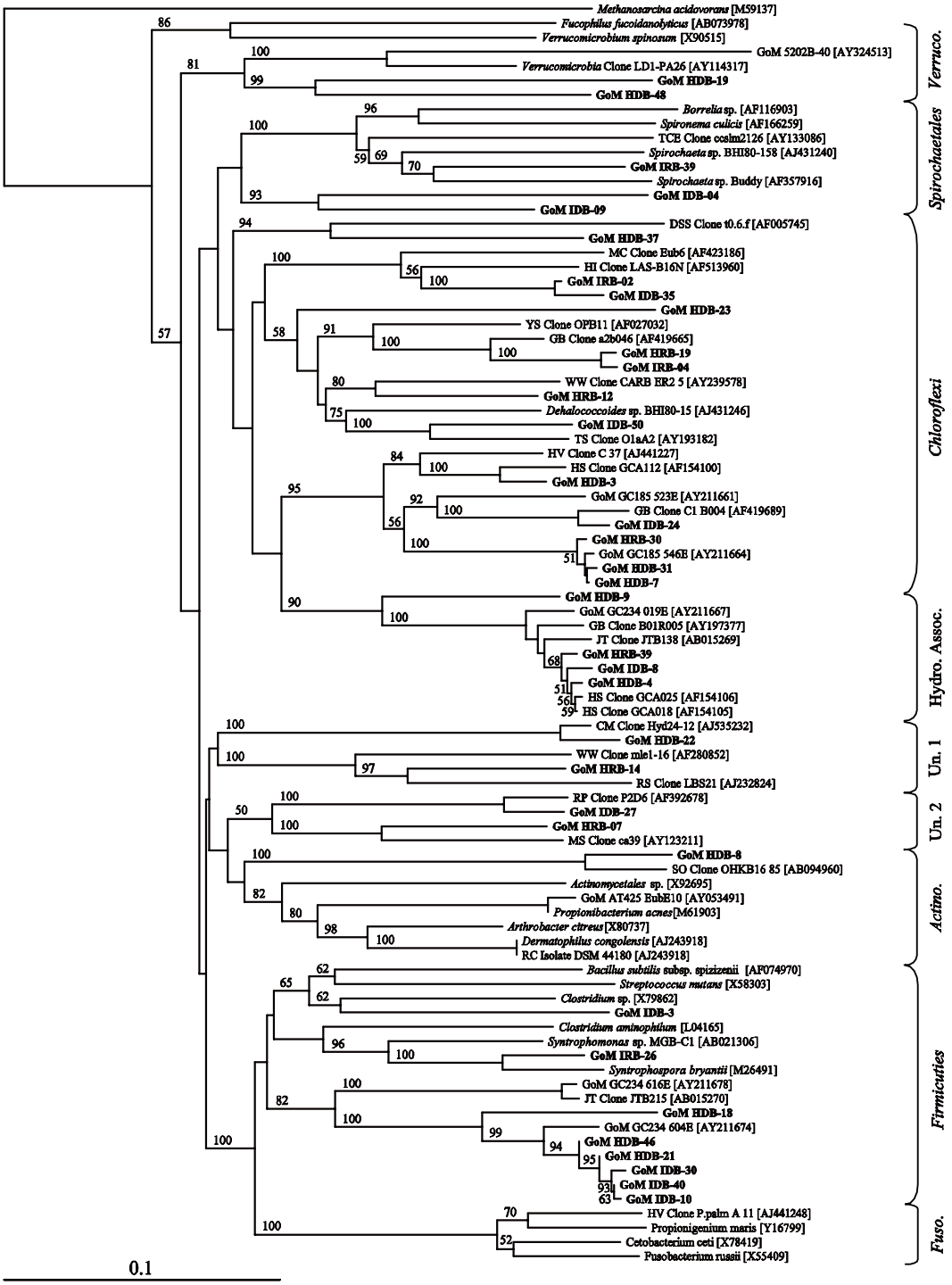
Methanosarcina acidovorans [M59137]
Fucophilus fucoidanolyticus [AB073978]
Verrucomicrobium spinosum [X90515]
GoM 5202B-40 [AY324513]
Verrucomicrobia Clone LD1-PA26 [AY114317]
GoM HDB-19
GoM HDB-48
Verruco.
Borrelia sp. [AF116903]
Spironema culicis [AF166259]
TCE Clone ccslm2126 [AY133086]
Spirochaeta sp. BHI80-158 [AJ431240]
GoM IRB-39
Spirochaeta sp. Buddy [AF357916]
GoM IDB-04
GoM IDB-09
Spirochaetales
DSS Clone t0.6.f [AF005745]
GoM HDB-37
MC Clone Bub6 [AF423186]
HI Clone LAS-B16N [AF513960]
GoM IRB-02
GoM IDB-35
GoM HDB-23
YS Clone OPB11 [AF027032]
GB Clone a2b046 [AF419665]
GoM HRB-19
GoM IRB-04
WW Clone CARB ER2 5 [AY239578]
GoM HRB-12
Dehalococcoides sp. BHI80-15 [AJ431246]
GoM IDB-50
TS Clone O1aA2 [AY193182]
HV Clone C 37 [AJ441227]
HS Clone GCA112 [AF154100]
GoM HDB-3
GoM GC185 523E [AY211661]
GB Clone C1 B004 [AF419689]
GoM IDB-24
GoM HRB-30
GoM GC185 546E [AY211664]
GoM HDB-31
GoM HDB-7
Chloroflexi
GoM HDB-9
GoM GC234 019E [AY211667]
GB Clone B01R005 [AY197377]
JT Clone JTB138 [AB015269]
GoM HRB-39
GoM IDB-8
GoM HDB-4
HS Clone GCA025 [AF154106]
HS Clone GCA018 [AF154105]
Hydro. Assoc.
CM Clone Hyd24-12 [AJ535232]
GoM HDB-22
Un. 1
WW Clone mle1-16 [AF280852]
GoM HRB-14
RS Clone LBS21 [AJ232824]
RP Clone P2D6 [AF392678]
GoM IDB-27
GoM HRB-07
MS Clone ca39 [AY123211]
Un. 2
GoM HDB-8
SO Clone OHKB16 85 [AB094960]
Actinomycetales sp. [X92695]
GoM AT425 BubE10 [AY053491]
Propionibacterium acnes [M61903]
Arthrobacter citreus [X80737]
Dermatophilus congolensis [AJ243918]
RC Isolate DSM 44180 [AJ243918]
Actino.
Bacillus subtilis subsp. spizizenii [AF074970]
Streptococcus mutans [X58303]
Clostridium sp. [X79862]
GoM IDB-3
Clostridium aminophilum [L04165]
Syntrophomonas sp. MGB-C1 [AB021306]
GoM IRB-26
Syntrophospora bryantii [M26491]
GoM GC234 616E [AY211678]
JT Clone JTB215 [AB015270]
GoM HDB-18
GoM GC234 604E [AY211674]
GoM HDB-46
GoM HDB-21
GoM IDB-30
GoM IDB-40
GoM IDB-10
Firmicuties
HV Clone P.palm A 11 [AJ441248]
Propionigenium maris [Y16799]
Cetobacterium ceti [X78419]
Fusobacterium russii [X55409]
Fuso.
0.1

Figure 3.2 Non-*Proteobacteria* phyla phylogenetic tree of relationships of 16S rRNA gene and 16S crDNA bacterial clone sequences, as determined by distance Jukes-Cantor analysis, from Gulf of Mexico GC234 SEH and IH samples (in boldface) to selected cultured isolates and environmental clones. Genbank accession numbers are in parentheses. One thousand bootstrap analyses were conducted and percentages greater than 50% are reported. *Methanosarcina acidovorans* was used as the outgroup. The scale bar represents the expected number of changes per nucleotide position.

Sediment-Entrained Hydrate

Interior Hydate

DNA-derived

A.

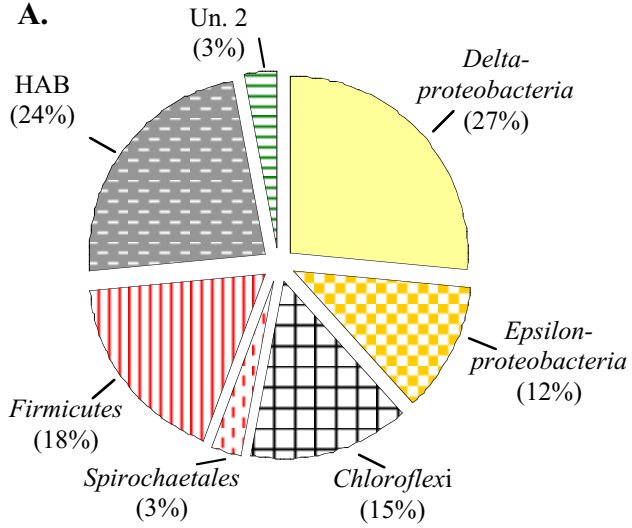

B.

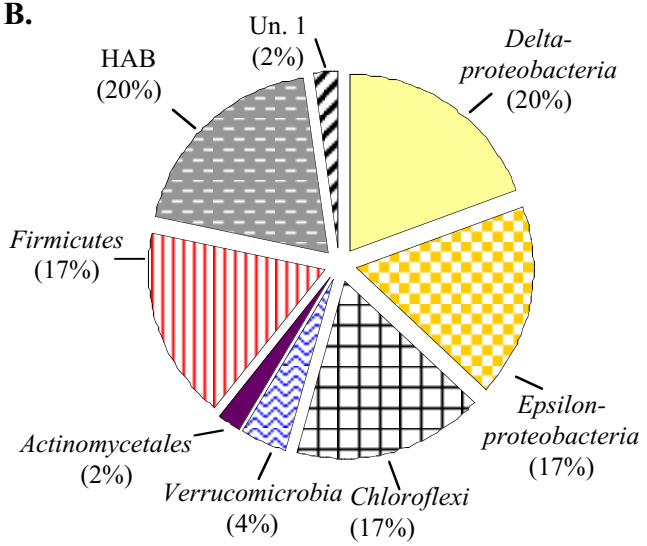

RNA-derived

C.

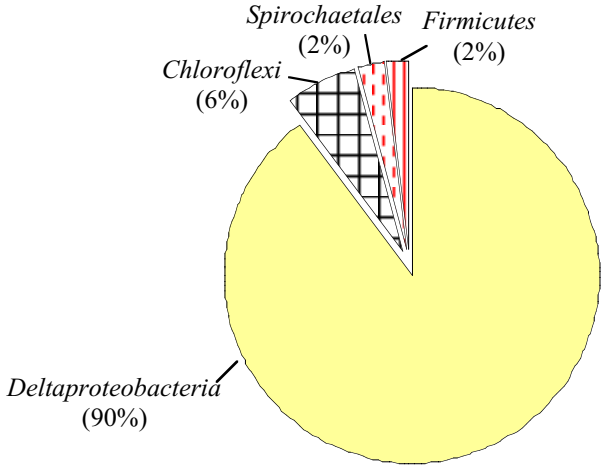

D.

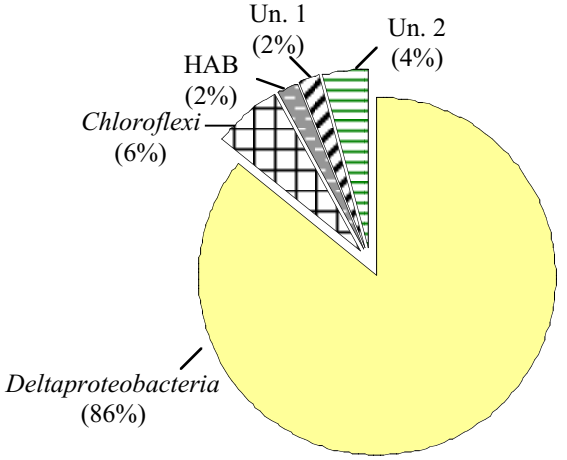

Figure 3.3 Frequency of bacterial phylogenetic lineages detected in 16S rRNA gene and 16S crDNA clone libraries derived SEH and IH samples. Calculations were made based on the total number of clones associated with phylotypes from which a representative clone had been sequenced. Charts A and B are representative of DNA-derived clone libraries. Charts C and D are representative of RNA-derived clone libraries. Each chart represents approximately 50 clones.

With the exception of the *Firmicutes*-related phylotype GoM HDB-21, detected 2.5-fold more frequently in the IH layer, the majority of *Firmicutes*-related clones exhibited a similar spatial pattern (Table 3.3). In contrast, the *Firmicutes*-related clones as a group, representing 18% of the total DNA-derived *Bacteria* library, were detected at similar percentages in both hydrate layers (Figure 3.3). Comparable observations were not possible in the *Spirochaetales* and *Actinomycetales* lineages as each of these taxonomic groups was represented by single phylotypes, incorporating one clone each (Table 3.3).

3.4.3 Determination of the metabolically active fraction of the *Bacteria* community

Analysis of the 95 16S crDNA *Bacteria* clones revealed a greater diversity relative to the *Archaea* clone libraries (Table 3.2) and predominately, included sequences most related to uncultured bacterial lineages (Table 3.4). A total of 30 distinct RFLP patterns were detected with clones representing five phylogenetic lineages (Table 3.4, Figure 3.1 and 3.2). A majority of the *Bacteria* crDNA clones from the SEH (90%) and IH (86%) layers were related to the class *δ-Proteobacteria* (Figure 3.3). However, only three of the twenty *δ-Proteobacteria*-related phylotypes, i.e., clones GoM IRB-06, GoM HRB-10 and GoM IRB-21 (Table 3.4), comprised more than 10% of the RNA-derived library. Interestingly, while nine phylotypes contained clones isolated from both hydrate layers (Table 3.4), the *δ*-related phylotype GoM IRB-16 was the only phylotype with more than two members isolated only from one hydrate layer. In addition, GoM IRB-06 and GoM HRB-10 phylotypes appeared at a greater frequency in a single hydrate layer (i.e., two- and three-fold more prevalent in the SEH or IH, respectively; Table 3.4).

Table 3.4

Summary of 16S crDNA sequences from sediment entrained hydrate and interior hydrate *Bacteria* clone libraries.

Clone	Total Number of Related Clones	Sediment Entrained Hydrate	Interior Hydrate	Nearest Relative	Phylogenetic Group	Similarity (%)
GoM IRB-06	12	8	4	GoM Clone AT425 EubF5	*Deltaproteobacteria*	89
GoM IRB-10	5	3	2	GoM Clone AT425 EubF5	*Deltaproteobacteria*	89
GoM HRB-23	2	0	2	GoM Clone AT425 EubF5	*Deltaproteobacteria*	89
GoM HRB-21	1	0	1	GoM Clone AT425 EubF5	*Deltaproteobacteria*	89
GoM IRB-11	8	4	4	CM Clone Hyd89-52	*Deltaproteobacteria*	99
GoM HRB-18	1	0	1	CM Clone Hyd89-52	*Deltaproteobacteria*	98
GoM HRB-32	1	0	1	CM Clone Hyd89-52	*Deltaproteobacteria*	98
GoM HRB-10	12	3	9	ER Isolate Eel-36e1H6	*Deltaproteobacteria*	92
GoM IRB-08	2	2	0	ER Isolate Eel-36e1H6	*Deltaproteobacteria*	91
GoM IRB-21	10	5	5	*Desulfobacter postgatei* DSM 2034	*Deltaproteobacteria*	94
GoM IRB-17	6	3	3	*Desulfobacter postgatei* DSM 2034	*Deltaproteobacteria*	94
GoM IRB-16	8	8	0	SC Clone NS-01	*Deltaproteobacteria*	88
GoM HRB-49	1	0	1	SC Clone NS-01	*Deltaproteobacteria*	88
GoM IRB-27	6	3	3	ER Clone Eel-BE1B3	*Deltaproteobacteria*	91
GoM HRB-16	4	1	3	AC Clone SJA-63	*Deltaproteobacteria*	89
GoM HRB-02	2	1	1	GB Clone B01R011	*Deltaproteobacteria*	96
GoM IRB-18	1	1	0	SS Clone Sva0081	*Deltaproteobacteria*	92
GoM IRB-03	1	1	0	DV Clone 33-PA95B98	*Deltaproteobacteria*	96
GoM HRB-03	1	0	1	MC Clone UASB TL12	*Deltaproteobacteria*	92
GoM HRB-05	1	0	1	CM Clone Hyd89-63	*Deltaproteobacteria*	91
GoM HRB-12	2	1	1	YS Clone OPB11	*Chloroflexi*	91

Table 3.4 (continued)

GoM IRB-02	1	1	0	HI Clone LAS-B16N	*Chloroflexi*	93
GoM IRB-04	1	1	0	GB Clone a2b046	*Chloroflexi*	94
GoM HRB-19	1	0	1	GB Clone a2b046	*Chloroflexi*	95
GoM HRB-30	1	0	1	GoM GC185 546E	*Chloroflexi*	98
GoM IRB-39	1	1	0	*Spirocaeta* sp. BHI80-158	*Spirochaetales*	85
GoM IRB-26	1	1	0	*Syntrophospora bryantii*	*Firmicutes*	90
GoM HRB-39	1	0	1	HS Clone GCA025	HAB	99
GoM HRB-14	1	0	1	RS Clone LBS21	Un. 1	88
GoM HRB-07	2	0	2	MS Clone ca39	Un. 2	89

The remaining 12 16S crDNA clone sequences were most related to non-*Proteobacteria* lineages including *Chloroflexi*, *Firmicutes* and *Spirochaetes* and groups including HAB and Unclassified *Bacteria* group 1 and 2 (Table 3.4, Figure 3.2). Five *Chloroflexi*-related phylotypes were identified (n=6) and detected at a similar frequency in both layers (Figure 3.3). Each of the remaining two lineages and three phylogenetic groups were represented by a single phylotype. Of these, Unclassified *Bacteria* group 2 was the only phylotype that contained more than one clone (n=2; Table 3.4).

3.4.4 *Archaea* community structure based on 16S rRNA gene sequence analyses

A total of 100 *Archaea* 16S rRNA gene clones obtained from the SEH and IH layers were grouped into 20 distinct RFLP patterns (data not shown). The 20 phylotypes were most closely related to *Crenarchaeota* and 6 lineages of *Euryarchaeota* including *Methanosarcinales*, *Methanomicrobiales*, *Thermoplasmales*, ANME-1, ANME-2 and one putatively novel clade denoted Unclassified *Euryarchaeota* (Figure 3.4). Sixteen of the 20 phylotypes were most closely related to cloned sequences previously identified from the archaeal community extant in sediments overlying gas hydrate (108) (Table 3.5; Figure 3.4). The majority of the *Archaea* 16S rRNA gene clones (58% of the total clones; Table 3.5) isolated from the SEH and IH layers were most related (>99% similar) to uncultured ANME-1 clones. The ANME-1-related phylotype represented by clone GoM IDA-34 was the numerically dominant phylotype for this library (n=24) and was predominately isolated from the SEH (23 of 24 clones; Table 3.5). The second most numerically dominant clone type in this DNA-derived library, the ANME-1-related

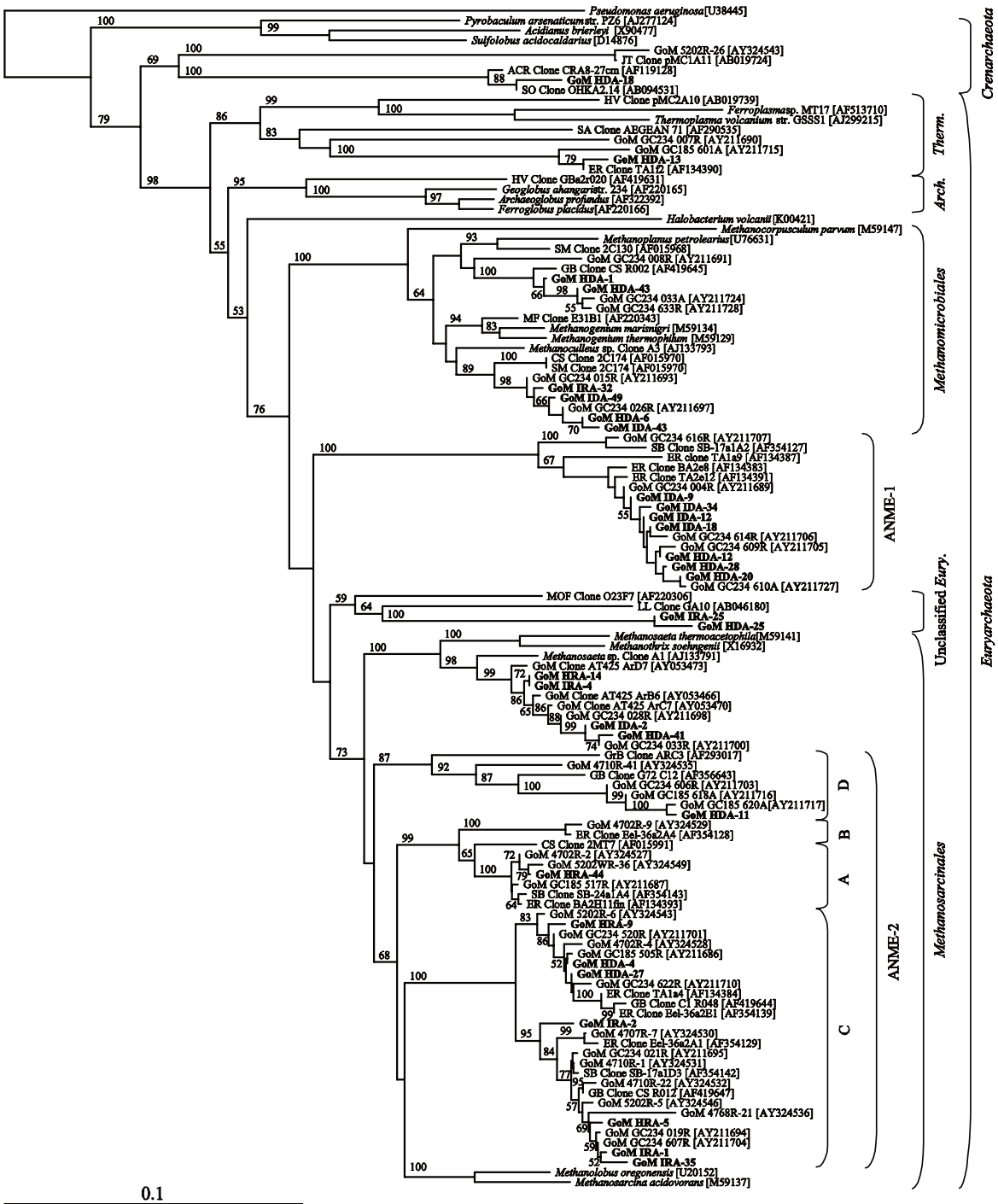
Pseudomonas aeruginosa[U38445]
Pyrobaculum arsenaticum str. PZ6 [AJ277124]
Acidianus brierleyi [X90477]
Sulfolobus acidocaldarius [D14876]
GoM 5202R-26 [AY324543]
JT Clone pMC1A11 [AB019724]
ACR Clone CRA8-27cm [AF119128]
GoM HDA-18
SO Clone OHKA2.14 [AB094531]
HV Clone pMC2A10 [AB019739]
Ferroplasma sp. MT17 [AF513710]
Thermoplasma volcanium str. GSS1 [AJ299215]
SA Clone AEGEAN 71 [AF290535]
GoM GC234 007R [AY211690]
GoM GC185 601A [AY211715]
GoM HDA-13
ER Clone TA1f2 [AF134390]
HV Clone GBa2r020 [AF419631]
Geoglobus ahangari str. 234 [AF220165]
Archaeoglobus profundus [AF322392]
Ferroglobus placidus [AF220166]
Halobacterium volcanii [K00421]
Methanocorpusculum parvum [M59147]
Methanoplanus petrolearius [U76631]
SM Clone 2C130 [AF015968]
GoM GC234 008R [AY211691]
GB Clone CS R002 [AF419645]
GoM HDA-1
GoM HDA-43
GoM GC234 033A [AY211724]
GoM GC234 633R [AY211728]
MF Clone E31B1 [AF220343]
Methanogenium marisnigri [M59134]
Methanogenium thermophilum [M59129]
Methanoculleus sp. Clone A3 [AJ133793]
CS Clone 2C174 [AF015970]
SM Clone 2C174 [AF015970]
GoM GC234 015R [AY211693]
GoM HRA-32
GoM HDA-49
GoM GC234 026R [AY211697]
GoM HDA-6
GoM HDA-43
GoM GC234 616R [AY211707]
SB Clone SB-17a1A2 [AF354127]
ER clone TA1a9 [AF134387]
ER Clone BA2e8 [AF134383]
ER Clone TA2e12 [AF134391]
GoM GC234 004R [AY211689]
GoM HDA-9
GoM HDA-34
GoM HDA-12
GoM HDA-18
GoM GC234 614R [AY211706]
GoM GC234 609R [AY211705]
GoM HDA-12
GoM HDA-28
GoM HDA-20
GoM GC234 610A [AY211727]
MOF Clone O23F7 [AF220306]
LL Clone GA10 [AB046180]
GoM HRA-25
GoM HDA-25
Methanosaeta thermoacetophila [M59141]
Methanothrix soehngenii [X16932]
Methanosaeta sp. Clone A1 [AJ133791]
GoM Clone AT425 ArD7 [AY053473]
GoM HRA-14
GoM HRA-4
GoM Clone AT425 ArB6 [AY053466]
GoM Clone AT425 ArC7 [AY053470]
GoM GC234 028R [AY211698]
GoM HDA-2
GoM HDA-41
GoM GC234 033R [AY211700]
GrB Clone ARC3 [AF293017]
GoM 4710R-41 [AY324535]
GB Clone G72 C12 [AF356643]
GoM GC234 606R [AY211703]
GoM GC185 618A [AY211716]
GoM GC185 620A [AY211717]
GoM HDA-11
GoM 4702R-9 [AY324529]
ER Clone Eel-36a2A4 [AF354128]
CS Clone 2MT7 [AF015991]
GoM 4702R-2 [AY324527]
GoM 5202WR-36 [AY324549]
GoM HRA-44
GoM GC185 517R [AY211687]
SB Clone SB-24a1A4 [AF354143]
ER Clone BA2H11fin [AF134393]
GoM 5202R-6 [AY324543]
GoM HRA-9
GoM GC234 520R [AY211701]
GoM 4702R-4 [AY324528]
GoM GC185 505R [AY211686]
GoM HDA-4
GoM HDA-27
GoM GC234 622R [AY211710]
ER Clone TA1a4 [AF134384]
GB Clone C1 R048 [AF419644]
ER Clone Eel-36a2E1 [AF354139]
GoM HRA-2
GoM 4707R-7 [AY324530]
ER Clone Eel-36e2A1 [AF354129]
GoM GC234 021R [AY211695]
GoM 4710R-1 [AY324531]
SB Clone SB-17a1D3 [AF354142]
GoM 4710R-22 [AY324532]
GB Clone CS R012 [AF419647]
GoM 5202R-5 [AY324546]
GoM 4768R-21 [AY324536]
GoM HRA-5
GoM GC234 019R [AY211694]
GoM GC234 607R [AY211704]
GoM HRA-1
GoM HRA-35
Methanolobus oregonensis [U20152]
Methanosarcina acidovorans [M59137]
0.1
Therm.
Arch.
Crenarchaeota
Methanomicrobiales
ANME-1
Unclassified Eury.
Euryarchaeota
Methanosarcinales
ANME-2
A
B
C
D

Figure 3.4 Phylogenetic tree of relationships of 16S rRNA gene and 16S crDNA archaeal clone sequences, as determined by distance Jukes-Cantor analysis, from Gulf of Mexico GC234 SEH and IH samples (in boldface) to selected cultured isolates and environmental clones. *Pseudomonas aeruginosa* was used as the outgroup. Genbank accession numbers are in parentheses. One thousand bootstrap analyses were conducted and percentages greater than 50% are reported. The scale bar represents the expected number of changes per nucleotide position.

Sediment-Entrained Hydrate

Interior Hydrate

DNA-derived

A.

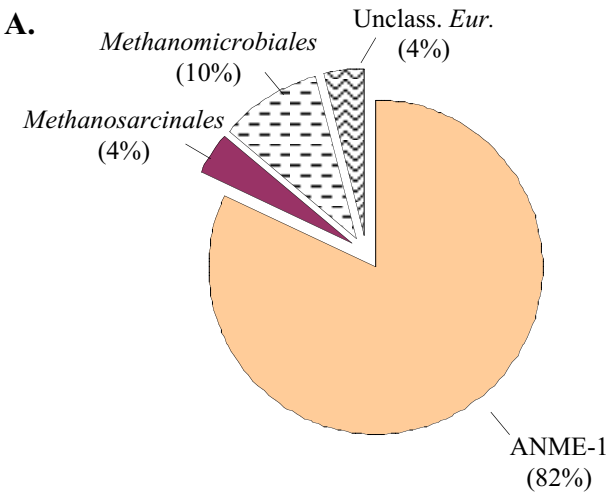

B.

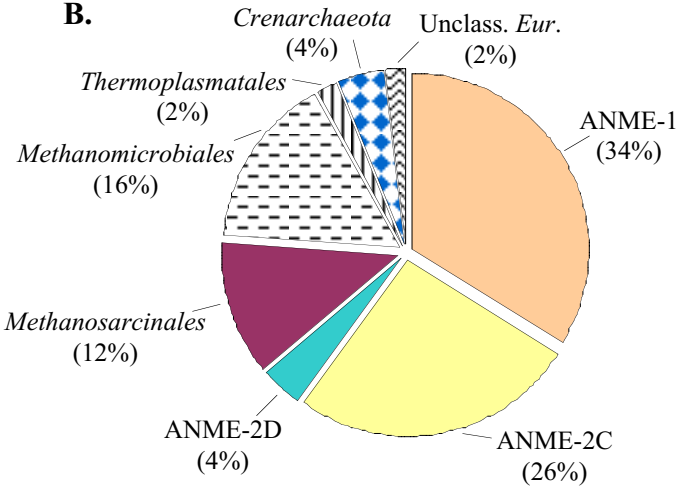

RNA-derived

C.

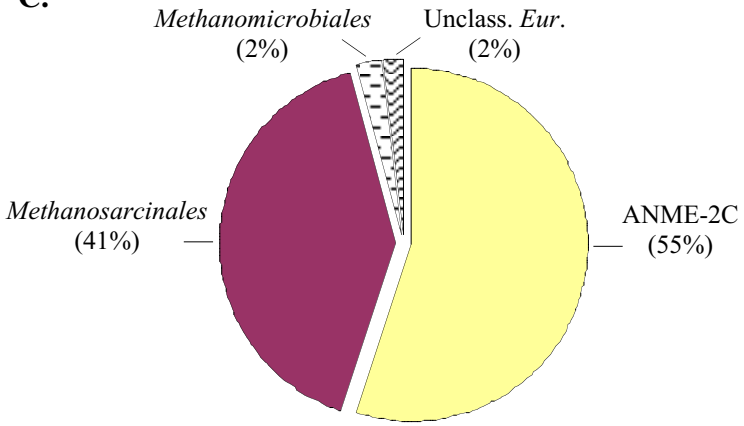

D.

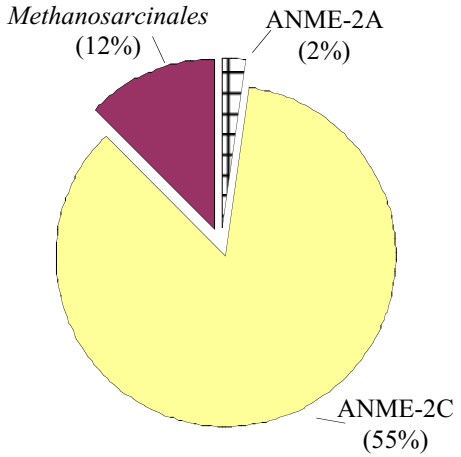

Figure 3.5 Frequency of archaeal phylogenetic lineages detected in 16S rRNA gene and 16S crDNA clone libraries derived from SEH and IH samples. Calculations were made based on the total number of clones associated with phylotypes from which a representative clone had been sequenced. Charts A and B are representative of DNA-derived clone libraries. Charts C and D are representative of RNA-derived clone libraries. Each chart represents approximately 50 clones.

Table 3.5

Summary of 16S rRNA gene sequences from sediment entrained hydrate and interior hydrate *Archaea* clone libraries.

Clone	Total Number of Related Clones	Sediment Entrained Hydrate	Interior Hydrate	Nearest Relative	Phylogenetic Group	Similarity (%)
GoM IDA-34	24	23	1	GoM GC234 609R	ANME-1	99
GoM HDA-28	9	0	9	GoM GC234 609R	ANME-1	99
GoM HDA-12	7	2	5	GoM GC234 609R	ANME-1	99
GoM IDA-09	14	14	0	GoM GC234 610A	ANME-1	99
GoM HDA-20	2	0	2	GoM GC234 610A	ANME-1	99
GoM IDA-18	1	1	0	GoM GC234 610A	ANME-1	99
GoM IDA-12	1	1	0	GoM GC234 614R	ANME-1	99
GoM HDA-27	8	0	8	GoM GC234 622R	ANME-2C	99
GoM HDA-04	5	0	5	GoM GC234 622R	ANME-2C	99
GoM HDA-11	2	0	2	GoM GC234 606R	ANME-2D	99
GoM HDA-41	7	1	6	GoM GC234 033R	*Methanosarcinales*	99
GoM IDA-02	1	1	0	GoM GC234 033R	*Methanosarcinales*	99
GoM HDA-06	6	1	5	GoM GC234 026R	*Methanomicrobiales*	99
GoM IDA-49	1	1	0	GoM GC234 026R	*Methanomicrobiales*	99
GoM IDA-43	1	1	0	GoM GC234 026R	*Methanomicrobiales*	99
GoM HDA-43	3	1	2	GoM GC234 633A	*Methanomicrobiales*	99
GoM HDA-01	2	1	1	GB Clone CS R002	*Methanomicrobiales*	98
GoM HDA-13	1	0	1	ER Clone TA1f2	*Thermoplasmatales*	99
GoM HDA-18	2	0	2	SO Clone OHKA2.14	*Crenarchaeota*	96
GoM HDA-25	3	2	1	LL Clone GA10	Unclass. *Eury.*	83

phylotype GoM IDA-09, was only detected in the SEH (Table 3.5). As a group, the ANME-1-related clones were detected nearly three-fold less frequently in the IH (Figure 3.5). However, phylotype GoM HDA-28, comprising 16% of the ANME-1-related clones, was only detected in the IH (Table 3.5). In addition, the ANME-2C- and 2D-related phylotypes were also only detected to the IH layer (Figure 3.5) and most similar to previously identified uncultured GoM clones [(108); Figure 3.4].

The remaining 27% of the *Archaea* 16S rRNA gene library consisted of 10 phylotypes related to two methanogenic *Euryarchaeota* (*Methanosarcinales* and *Methanomicrobiales*), two non-methanogenic *Euryarchaeota* (*Thermoplasmales* and an unclassified group) and one *Crenarchaeota* lineage (Figure 3.4). Although each of the 5 *Methanomicrobiales*-related phylotypes had at least one clone isolated from the SEH layer (Table 3.5), the three numerically dominant *Methanomicrobiales*-related phylotypes (i.e., GoM HDA-06, GoM HDA-43 and GoM HDA-01) were more frequently detected in the IH (8 of 11 clones; Table 3.5). Similarly, the *Methanosarcinales*-, *Thermoplasmales*- and *Crenarchaeota*-related phylotypes occurred more frequently in the IH library (Figure 3.5). Phylotype GoM HDA-25 may represent a novel lineage, designated herein as Unclassified *Euryarchaeota*, due to low similarity to previously sequenced clones (83%; Table 3.5) and deep phylogenetic branching (Figure 3.4).

3.4.5 Determination of the metabolically active fraction of the *Archaea* community

A total of 97 *Archaea* 16S crDNA clones obtained from the SEH and IH layers were grouped into 7 distinct RFLP patterns. Clones grouped into 5 phylogenetic lineages

Table 3.6

Summary of 16S crDNA sequences from sediment entrained hydrate and interior hydrate *Archaea* clone libraries.

Clone	Total Number of Related Clones	Sediment Entrained Hydrate	Interior Hydrate	Nearest Relative	Phylogenetic Group	Similarity (%)
GoM HRA-44	1	0	1	GoM 5210WR-36	ANME-2a	99
GoM HRA-09	40	7	33	GoM GC185 505R	ANME-2c	99
GoM HRA-05	26	18	8	GoM GC234 607R	ANME-2c	99
GoM IRA-35	2	2	0	GoM GC234 607R	ANME-2c	99
GoM IRA-04	26	20	6	GoM GC234 028R	*Methanosarcinales*	99
GoM IRA-32	1	1	0	GoM GC234 026R	*Methanomicrobiales*	99
GoM IRA-25	1	1	0	MF Clone 023F7	Unclass. *Eury.*	85

including *Methanomicrobiales*, *Methanosarcinales*, two groups of ANME-2 and one putatively novel clade denoted Unclassified *Euryarchaeota* (Table 3.6, Figure 3.4). The majority of the 16S crDNA *Archaea* clones (70%) were related to ANME-2C (Table 3.6). A large percentage of the ANME-2C clones (59%) grouped into a phylotype denoted GoM HRA-9 and were most related (99% similar; Table 3.6) to an environmental clone originally isolated from the overlying sediment on a GoM gas hydrate mound (108). Although this phylotype was almost five-fold more numerically abundant in the IH library (Figure 3.5), a second ANME-2C-related phylotype, represented by clone GoM HRA-05, was over two-fold more numerically abundant in the SEH library (Figure 3.5).

The remaining 28 clones were most related to *Methanosarcinales* and *Methanomicrobiales* lineages and one uncharacterized group. A single *Methanosarcinales*-related phylotype, denoted GoM IRA-4, comprised 26 of the 28 clones and were detected three-fold more frequently in the SEH library (Figure 3.5). A single *Methanomicrobiales*-related clone, GoM IRA-32, isolated from the SEH, was most closely related (99%) to a previously sequenced GoM GC234 clone from the overlying sediment [(108); Figure 3.4]. Interestingly, one additional phylotype isolated from the SEH, denoted Unclassified *Euryarchaeota* GoM IRA-25, was the only phylotype not closely related to a clone previously identified from the GoM.

3.5 Discussion

Microbial communities resident in cold seep environments have been the focus of several characterization studies (62, 88, 108, 122). To date, fluorescent in situ

hybridization (FISH) has been one of more widely used techniques to identify the presumptively metabolically active fraction of the microbial community. This technique, however, does not provide an in-depth characterization of the overall microbial diversity nor can it detect novel lineages without prior clone sequence information. The present study is the first to extract RNA directly from gas hydrate and to delineate the metabolically active *Bacteria* and *Archaea* fraction of the gas hydrate microbial community. In addition, DNA-derived libraries were created to compare these two different molecular-based approaches for community analyses. Several putatively novel microbial (*Bacteria* and *Archaea)* lineages were detected in the different hydrate layers sampled in this study. Geochemical and rate measurement data from the same sample layers have been previously reported (121) and provide a linkage to gas hydrate microbial community structure and function.

3.5.1 Detection of metabolically active microbes associated with GoM gas hydrates

Discrete sampling of GoM gas hydrate (i.e., the SEH and IH layers) and subsequent isolation of ribosomal RNA enables characterization of the presumptively metabolically active fraction of the microbial assemblages. Gas hydrate samples can be collected via manned submersible or from shipboard using piston or gravity cores. Our method of collection, by submersible, provided us unprecedented opportunity to accurately sample the distinct GoM hydrate ecosystem. Thus, sufficient amounts of hydrate materials were retrieved, providing the necessary volumes, which yielded suitable concentrations (quantity and quality) of RNA needed for molecular analyses.

To date, few studies have shown the presence of metabolically active microbial communities within gas hydrates. One line of evidence for the presence of active microbial fractions in GoM gas hydrates is our finding of a 4- and 10-fold higher RNA:DNA ratio and total RNA concentration [Table 3.1; (32)], respectively, across the distinct hydrates layers. Phylogenetic analysis of RNA-derived clones revealed a total of 30 distinct *Bacteria* and 7 distinct *Archaea* phylotypes between the SEH and IH libraries. Rarefaction data and percent coverage calculations suggest that the bacterial 16S rRNA gene libraries from both layers did not reach saturation. This was in contrast to the calculations obtained for the archaeal libraries. Although additional sampling of bacterial clones would be needed to determine the full extent of the *Bacteria* community diversity, we did obtain several numerically dominant lineages. We theorized that additional sampling of these libraries would not likely alter the existing bacterial phylotype percent distribution patterns reported herein.

Geochemical data measured from the same hydrate samples used in this study provide a second line of compelling evidence for the presence of metabolically active microbial populations (121). Although AOM and SR rates were higher in the overlying sediment, i.e., 0.60 and 76.2 nmol cm^{-3} day^{-1}, respectively, active anaerobic methane oxidizing and sulfate reducing populations were detected in the IH layer, i.e., 0.28 and 3.2 nmol cm^{-3} day^{-1}, respectively (121). Interestingly, within the hydrate layers, the highest SR rates did not correspond to the same layer in which the highest rates of AOM were detected. Orcutt et al. (121) describe this surprising finding as a result of a "loose coupling between SR and AOM". Regardless, the combined geochemical data and RNA-based phylogenetic identification of microbial populations within intact gas hydrate and

across boundary layers suggest active microbial habitation of this extreme environment by diverse lineages of *Bacteria* and *Archaea*.

3.5.2 Putative phylotype niche specificity

Although similar distribution of phylotypes was observed between the SEH and the IH *Bacteria* and *Archaea* clone libraries, we hypothesized that some phylotypes may be restricted (or only detected) in a single hydrate layer. As SEH and IH samples were collected from the same piece of solid gas hydrate, the potential for heterogeneity was minimized. The geochemistry and rate measurements (121) differed by several fold between the SEH and IH layers even though the sampled layers were in close proximity (~2-4 cm apart) to each other. Moreover, several phylotypes, especially those related to the lineages *Chloroflexi*, δ-*Proteobacteria*, ANME-1 and ANME-2C, were detected at higher frequencies from only one layer. The differences in chemistry, metabolic activity, and clone frequency suggest the presence of two distinct hydrate-associated habitats (Tables 3.2, 3.3 and 3.4).

While statistical estimations of the *Archaea* clone sequences supported the presence of two hydrate habitats, the same analyses of *Bacteria* sequences did not. Specifically, ten different statistical indices were applied to the eight DNA- and RNA-derived clone libraries constructed from the SEH and IH layers. Although the Sorensen's index indicated little overlap between *Bacteria* phylotypes from the SEH and IH, all other indices revealed few differences between these two layers. Insignificant F_{ST} and P tests suggest that the *Bacteria* sequences from the SEH and IH were from similar lineage distributions and were indistinguishable from the combined communities (101).

Therefore, although differences in individual phylotype distributions were observed between the two layers, these differences were not large enough to indicate two distinct bacterial communities. Lineage-per-time plots indicated an excess of highly divergent lineages, suggesting that selection factors affecting both hydrate layers maintain high diversity in the bacterial community (101). In contrast, plots that show an excess of closely related lineages are indicative of a recent selection event resulting in the speciation of a few surviving or newly colonizing species (101). In this study the *Archaea* libraries had lineage-per-time plots in close proximity to the plot lines indicative of constant lineage births and deaths (101). This result suggests that relative to the *Bacteria*, the *Archaea* are less divergent and may possibly have experienced a more recent selection event. Additionally, the statistical indices applied to the *Archaea* libraries, including F_{ST} and P tests, suggest a significant difference between the SEH and IH *Archaea* communities. Mills et al. (109) reported a similar trend in *Archaea* community phylotype frequency variances across a depth profile in sediments associated with GoM microbial mats while *Bacteria* phylotype frequencies were relatively less depth specific. Therefore, it is tempting to speculate that the archaeal populations are more specialized for specific environmental conditions and perhaps less able to tolerate environmental fluctuations than the bacterial populations.

Differences in lineage frequency were detected between the RNA- and DNA-derived libraries within individual hydrate layers. The utilization of PCR techniques to construct clone libraries is inherently biased by the concentration of template available for amplification. DNA-derived clone libraries are based on a constant number of 16S rRNA genes per cell and can potentially detect dead or quiescent cells. In contrast, the

concentration of ribosomal RNA present in a cell is thought to be proportional to the metabolic activity of the cell and therefore can alter the detection frequency of phylotypes relative to the DNA-derived clone libraries (32). Whereas absolute quantification of resident populations is not possible by analyzing the DNA- and RNA-derived clone libraries, the relative proportions between the total population and the active fraction of the population can be determined. Thus, *ε-Proteobacteria*- and ANME-1-related lineages may be present in the hydrate-associated samples, but are either not metabolically active or are active at a level below our detection limits. In contrast, *δ-Proteobacteria*- and ANME-2C-related lineages appear to be less abundant in the total population then in the active metabolic fraction of the community. Discrepancies between 16S rRNA gene and 16S crDNA libraries demonstrate the necessity of generating DNA- and RNA-derived libraries when possible to gain a more comprehensive analysis of the extant microbial communities.

3.5.3 Detection of novel microbial lineages

Molecular characterization of microbial communities from extreme environments has provided evidence for numerous new taxonomic groups with no known closely related culturable isolates (62, 108, 122). In this study, several potentially novel clones grouped into four distinct clades, i.e., three from the *Bacteria* library and one from the *Archaea* library, that were distantly related to cultured isolates. Recent reports have indicated a new clade within the *Chloroflexi* lineage specific to hydrocarbon seeps (68). This clade, denoted as "Hydrocarbon Associated Bacteria", lacks a cultivated isolate and therefore the specific physiology is unknown. However, clones related to this clade,

along with a closely related second branch within the *Chloroflexi* lineage, were identified in our RNA-derived *Bacteria* clone library from the IH layer providing the first described environment in which this lineage appears to be metabolically active.

Two additional clades, denoted in this study as "Unclassified *Bacteria* Group 1" and "Unclassified *Bacteria* Group 2", were less than 90% similar to the nearest cultivated relative. Interestingly, both groups contained RNA- and DNA-derived clones, thus providing evidence for this group not only being present, but also metabolically active in hydrate-associated habitats. Similarly, the novel *Archaea* cluster, denoted "Unclassified *Euryarchaeota*" group, was detected in both the 16S rRNA gene and 16S crDNA library. The data presented herein provides further evidence of the potential habitat range for each of these novel lineages, as well as other previously characterized lineages. However, we readily acknowledge that our present study lacks a temporal component. Thus there is a need to confirm that similar results would be obtained in future GoM hydrate samplings. Additionally, attempts will be made to cultivate these and other microbes identified within these GoM clone libraries to determine their specific physiology and if they possess any potential medical or economical benefit.

3.6 Acknowledgements

This work was supported by National Science Foundation LExEn grant OCE-0085549 to P.A.S. We thank C. Fisher for invaluable sampling and study site information.

CHAPTER 4

IDENTIFICATION OF MEMBERS OF THE METABOLICALLY ACTIVE MICROBIAL POPULATIONS ASSOCIATED WITH *BEGGIATOA* SP. MAT COMMUNITIES FROM GULF OF MEXICO COLD SEEP SEDIMENTS

4.1 Abstract

In this study, the composition of the metabolically active fraction of the microbial community occurring in Gulf of Mexico marine sediments (water depth 550-575 m) with overlying filamentous bacterial mats was determined. The mats were mainly composed of either orange- or white-pigmented *Beggiatoa* spp. Complementary 16S rDNA (crDNA) was obtained from ribosomal RNA extracted from three different sediment depths (0-2, 6-8 and 10-12 cm) that had been subjected to reverse transcription-PCR amplification. Domain-specific 16S PCR primers were used to construct 12 different 16S crDNA libraries containing 333 *Archaea* and 329 *Bacteria* clones. Analysis of the *Archaea* clones indicated that all sediment depths associated with overlying orange- and white-pigmented microbial mats were almost exclusively dominated by ANME-2 (95% of total *Archaea* clones), a lineage related to the methanogenic order *Methanosarcinales*. In contrast, bacterial diversity was considerably higher with the dominant phylotype varying by sediment depth. An equivalent number of clones detected at 0-2 cm, representing a total of 93%, were related to the γ and δ classes of *Proteobacteria*, whereas clones related to δ-*Proteobacteria* dominated the metabolically active fraction of the bacterial

community occurring at 6-8 cm (79%) and 10-12 cm (85%). This is the first phylogenetic-based evaluation of the presumptive metabolically active fraction of the *Bacteria* and *Archaea* community structure investigated along a sediment depth profile in the northern GoM, a hydrocarbon-rich cold seep region.

4.2 Introduction

The GoM is a dynamic environment containing active venting and seepage of hydrocarbons. The upward thrust of salt diapirs forms faults that act as conduits from subsurface oil and gas reservoirs through the sediment layers (150, 183). Faults reaching the surface can facilitate the formation of surface-breaching gas hydrate mounds [reviewed in (15)] and actively venting hydrocarbon plumes (21, 41, 139, 143). In contrast to hydrothermal seeps, these features are collectively known as cold seeps due to low-level geological heating. Owing to the extensive oil and gas reserves, a primary focus of long-term research in the GoM has been the characterization of the physical geology of the system (106, 139). Surprisingly, GoM cold seep chemosynthetic-based ecosystems were not reported until 1989 (96) and the ecosystem's primary energy source (i.e., CH_4) was not linked to gas hydrate decomposition until 1994 (16).

A more thorough characterization of an ecosystem, however, requires identification of the mechanisms and biota responsible for energy transfer and the cycling of nutrients. Owing to the water depth at GoM cold seeps, chemosynthesis rather than photosynthesis predominates (145). As has been shown for hydrothermal seep ecosystems, energy transfer from chemosynthetic microorganisms to higher trophic levels

is mediated by primary consumers including symbiont-containing macrofauna and free-living heterotrophic microorganisms (36, 38, 42, 116). Whereas numerous reports characterizing tubeworm and mussel symbiotic associations with chemoautotrophic microbes have been described (18, 38, 82), the portion of the chemosynthetic-based community in the GoM comprised of non-symbiotic and free-living microbes has been much less studied (88, 108, 189). For example, vast aggregations of dense microbial mats on the sediment surface are readily visible to the naked eye. These mats are mainly composed of large [cell diameter, 12-160 μm; (48, 103)], pigmented (orange and white) and unpigmented vacuolate sulfur bacteria, e.g., *Beggiatoa* sp. (2, 116, 180). Such mat- and sediment-associated microbial communities have been shown to support high rates of sulfate reduction (10, 74, 126, 180) and oxidation (90, 126, 164), nitrate reduction (126, 151, 164) and anaerobic methane oxidation (10, 74). Interestingly, as potentially critical as these microbial communities are to GoM cold seep ecosystem productivity, no detailed information describing the composition of the metabolically active microbes and their spatial and/or temporal structures is available.

In this present study, depth profiles of sediments with two different overlying types of microbial mats, composed mainly of orange- or white-pigmented *Beggiatoa* spp., were collected from a manned submersible at two different cold seep locations (550–575 m water depth). The primary objective in this study was to characterize the metabolically active fraction of the sediment microbial communities associated with the microbial mats. Total rRNA was extracted from three sediment depths (0-2, 6-8 and 10-12 cm) and subjected to reverse transcription-polymerase chain reaction (RT-PCR) with primers specific for the *Bacteria* and *Archaea* domains. This is among the first phylogenetic

surveys to be conducted on GoM seep sediment microbial communities directly associated with overlying microbial mats and the first survey describing the metabolically active fraction of the microbial communities in GoM sedimentary habitats.

4.3 Materials and methods

4.3.1 Gulf of Mexico site description and sample collection

The study sites are located in the northern GoM continental slope province. The sites, GC185 (Bush Hill; 550 m depth) and GC234 (575 m depth) are located at 27°46'N, 91°30'W and 27°44'N, 91°13'W, respectively. Both of these locales contained visible oil and gas seepage, surface breaching gas hydrate, and extensive (i.e., extending several meters in diameter) microbial mats. Sediment cores from both sites were obtained from areas containing mainly either orange- or white-pigmented *Beggiatoa* sp. mats with the manned-submersible *Johnson Sea Link* during July 2002. Sediment cores (7.2 cm ID, 15-20 cm average length) were immediately sectioned at 2 cm intervals and stored in liquid N_2 until further processing. Direct cell counts were performed on aliquots (0.5 g wet wt) as previously described (131).

4.3.2 Preparation of reagents and materials used for RNA extractions

Prior to nucleic acid extraction, RNases were removed from solutions and solids by treating stock solutions and water with 0.1% diethylpyrocarbonate (DEPC) overnight at 37^{o}C and autoclaving. All glassware and non-plastics were baked at 250^{o}C for 24 h.

All surfaces and plastics were cleaned with RNase Erase (ICN Biomedicals Inc., Aurora, OH) to remove contaminating RNases during shipboard and laboratory manipulations.

4.3.3 RNA isolation

Total ribonucleic acids were extracted as described in Hurt et al. (66) from 10 g (wet weight) of sediment sampled in triplicate from each sediment depth (0-2, 6-8 and 10-12 cm). In brief, sediment samples stored in liquid N_2 were repeatedly thawed by physical grinding in the presence of a denaturing solution (4 M guanidine isothiocyanate, 10 mM Tris-HCl [pH 7.0], 1 mM EDTA, 0.5% 2-mercaptoethanol) and refrozen by immersion in liquid N_2. The sediment samples were incubated 30 min at 65^{o}C in pH 7.0 extraction buffer (100 mM sodium phosphate [pH 7.0], 100 mM Tris-HCl [pH 7.0], 100 mM EDTA [pH 8.0], 1.5 M NaCl, 1% hexadecyltrimethylammonium bromide [CTAB], and 2% SDS) and centrifuged (1,800 × g for 10 min). The supernatants from three separate extractions were pooled, extracted with 24:1 (v/v) chloroform-isoamyl alcohol and centrifuged (1,800 × g for 20 min). The nucleic acids were precipitated at room temperature with isopropanol (30 min), pelleted by centrifugation (16,000 × g for 20 min), resuspended in DEPC-treated water and subsequently purified into RNA-only aliquots (66).

4.3.4 Reverse transcription and amplification of ribosomal RNA

Aliquots of ribosomal RNA were reverse transcribed (RT) using MMLV reverse transcriptase according to manufacturer's instructions (Invitrogen, CA). RNA was initially denatured by heating (65^{o}C) for 10 min. The RT reaction mix consisted of 5 μM

of a 16S rRNA reverse primer amplifying either domain-specific *Bacteria*, i.e., DXR518 (5'-CGTATTACCGCGGCTGCTGG-3') (120) or *Archaea*, i.e., Ar958r (5'-YCCGGCGTTGAMTCCAATTT-3') (33), 50-100 ng of denatured RNA and 200 μM dNTP. The mix was incubated for 5 min at 65^{o}C and 2 min at 4^{o}C followed by addition of 1× 1st Strand Buffer (50 mM Tris-HCl [pH 8.3], 75 mM KCl, 3 mM $MgCl_2$) and 75 U RNase inhibitor and heating at 37^{o}C for 2 min. A 200 U aliquot of MMLV reverse transcriptase was added prior to a 50 min incubation at 37^{o}C that resulted in transcription of the RNA into crDNA. The crDNA end product was used as template for a standard PCR reaction. Possible DNA contamination of RNA templates was routinely monitored by PCR amplification of aliquots of RNA that were not reverse-transcribed. No contaminating DNA was detected in any of these reactions. The primers used for standard PCR amplification included the above reverse primers (DXR518 and Ar958r) and 16S rRNA gene forward domain-specific *Bacteria*, i.e., 27F (5'-AGAGTTTGATCCTGGCTCAG-3'), and *Archaea*, i.e., A341f (5'-CCTAIGGGGIGCAICAG-3') (179) primers. The PCR reaction mix contained 10-50 ng crDNA, 1× PCR buffer (Stratagene, CA), 1.5 mM $MgCl_2$, 200 μM of each deoxynucleoside triphosphate, 1 pmol of each forward and reverse primer, and 0.025 U μl^{-1} *TaKaRa Taq*^{TM} (TaKaRa, Japan). Amplicons were analyzed on 1.0% agarose gels run in TBE buffer stained with ethidium bromide and UV illuminated.

4.3.5 Environmental clone library construction

Purified pooled amplicons representing 16S crDNA sequences were cloned into the TOPO TA cloning vector pCR2.1 according to manufacturer's instructions

(Invitrogen, CA). Clones denoted in Tables 1 and 2 by either "WB" or "B" were obtained from sediments with overlying white- or orange-pigmented mats, respectively. In addition, clones designated with either "47" or "52" denote sites GoM GC185 and GC234, respectively, and "02", "68" or "10" denotes 0-2, 6-8 and 10-12 cm depths, respectively. Inserts were subsequently PCR-amplified from lysed colonies with the following primers specific for either the vector, i.e., M13F (5'-GTAAAACGACGGCCAG-3') and M13R (5'-CAGGAAACAGCTATGAC-3') or the *Archaea* amplicons, i.e, A341f (179) and Ar958r (33). Vector specific M13F/R primers were used to amplify inserts from bacterial clones obtained with 27F and DXR518 primers to prevent amplification of the *Escherichia coli* host 16S rRNA gene. PCR products of bacterial clones were digested (2 h, 37^{o}C) with *Msp*I and *Hha*I and with *Hha*I and *Rsa*I for archaeal clones. Clones were grouped according to restriction fragment length polymorphism (RFLP) banding patterns and representative clones sequenced as previously described (108). RFLP groups containing two or more members had representative clones sequenced. Multiple representative clones were sequenced from RFLP groups containing five or more members to verify group integrity. A limited number of clones from those RFLP groups containing a single member were also sequenced. All calculations were based upon the number of clones incorporated in RFLP groups that had representative clones sequenced. Sequencing was performed at the Georgia Institute of Technology core DNA facility using a BigDye Terminator v3.1 Cycle sequencing kit on an automated capillary sequencer (model 3100 Gene Analyzer, Applied Biosystems, CA). Inserts were sequenced multiple times on each strand. Prior to

comparative sequence analysis, vector sequences flanking the bacterial 16S crDNA insert were manually removed.

4.3.6 Phylogenetic and rarefaction analysis

Sequence analysis was preformed as previously described (108). Multiple sequences of individual inserts were initially aligned using the program 'BLAST 2 Sequences' (167) available through the National Center for Biotechnology Information and assembled with the program BioEdit v5.0.9 (57). Sequences were checked for chimeras using Chimera Check from Ribosomal Database Project II (99). Sequences from this study and reference sequences, as determined by BLAST analysis, were subsequently aligned using CLUSTALX v1.81 (171). An average of 500 (*Bacteria* clones) to 600 (*Archaea* clones) nucleotides were included in the final phylogenetic analyses. Neighbor-Joining trees were created from the shortened sequence alignments. The bootstrap data represents 1,000 samplings. The final trees were viewed using NJPlot (130) and TreeView v1.6.6 available at http://taxonomy.zoology.gla.ac.uk/rod/treeview.html. Rarefaction analysis was performed using equations as described in Heck et al. (60). Standard calculations were used to produce the curve using the total number of clones obtained compared to the number of clones representing each unique RFLP pattern. The percentage coverage (C) of the clone libraries was calculated according to the equation $C = [1- (n_1/N)] \times 100$ (54, 111), where n_1 is the number of unique clones as determined by RFLP analysis and N is the total number of clones in the given library.

4.3.7 Nucleotide sequence accession numbers

The 61 16S crDNA gene nucleotide sequences have been deposited in the GenBank database under accession numbers AY324490–AY324550.

4.4 Results

RNA was extracted from three different sediment depths (0-2, 6-8, and 10-12 cm) from sites with either overlying orange- or white-pigmented microbial mats from gas hydrate-bearing cold seep locations in the Gulf of Mexico (GoM). The purified RNA was of sufficient quality and quantity to be reverse transcribed, amplified with 16S domain-specific PCR primers and cloned. Microbial cell numbers in sediments with overlying orange- and white-pigment mats were quantified by direct microscopy. Cell counts per gram sediment, of the orange-pigmented microbial mats samples were 1.1×10^8 (0-2 cm), 4.6×10^7 (6-8 cm) and 4.4×10^7 (10-12 cm), and 1.9×10^7 (0-2 cm), 7.3×10^6 (6-8 cm) and 1.7×10^7 (10-12 cm) for the white-pigmented microbial mats samples. Direct microscopic examination of individual giant filaments from orange- and white-pigmented mats revealed few if any gross morphological differences (data not shown). These observations were consistent with previous assignments of these filamentous bacteria to the genus *Beggiatoa* (116). It should be noted, however, that while *Beggiatoa* spp. dominated these mats, other as yet unidentified microorganism(s) were also present.

4.4.1 RFLP and rarefaction analyses of 16S crDNA libraries

A total of 185 *Bacteria* and 185 *Archaea* 16S complementary rDNA (crDNA) sequences from sediments with overlying orange-pigmented mats and 144 *Bacteria* and 148 *Archaea* clones from sediments with white-pigmented mats were grouped according to restriction fragment length polymorphism (RFLP) patterns (data not shown). Rarefaction analysis (Figure 4.1) and percent coverage calculated to determine if a sufficient number of clones were examined to estimate diversity within each of the clone libraries sampled. Curves generated for crDNA clones obtained from both mat communities with *Bacteria* primer sets did not indicate saturation (Figure 4.1), while percent coverage was determined to be 92.4% and 89.6% for the orange- and white-pigmented mat libraries respectively (54). Although additional sampling of clones would be necessary to reveal the full extent of diversity, numerically dominant RFLP groups were obtained (Table 4.1). Specifically, one dominant bacterial phylotype from the white-pigmented mat (i.e., clone GoM 4702B-09) and orange-pigmented mat (i.e., clone GoM 5268WB-5) libraries comprised 15 and 18% of all clones, respectively (Table 4.1). In contrast, for those libraries obtained from both microbial mat types with *Archaea* specific primers, the curves indicated saturation and the percent coverage was 94.6% and 97.3% for orange-and white-pigmented mats respectively. Thus, a sufficient number of clones were sampled representative of the archaeal diversity in these libraries (Figure 4.1). Numerically dominant phylotypes, containing 16% to 44% of all archaeal clones, were also obtained for each of these libraries (Table 4.2).

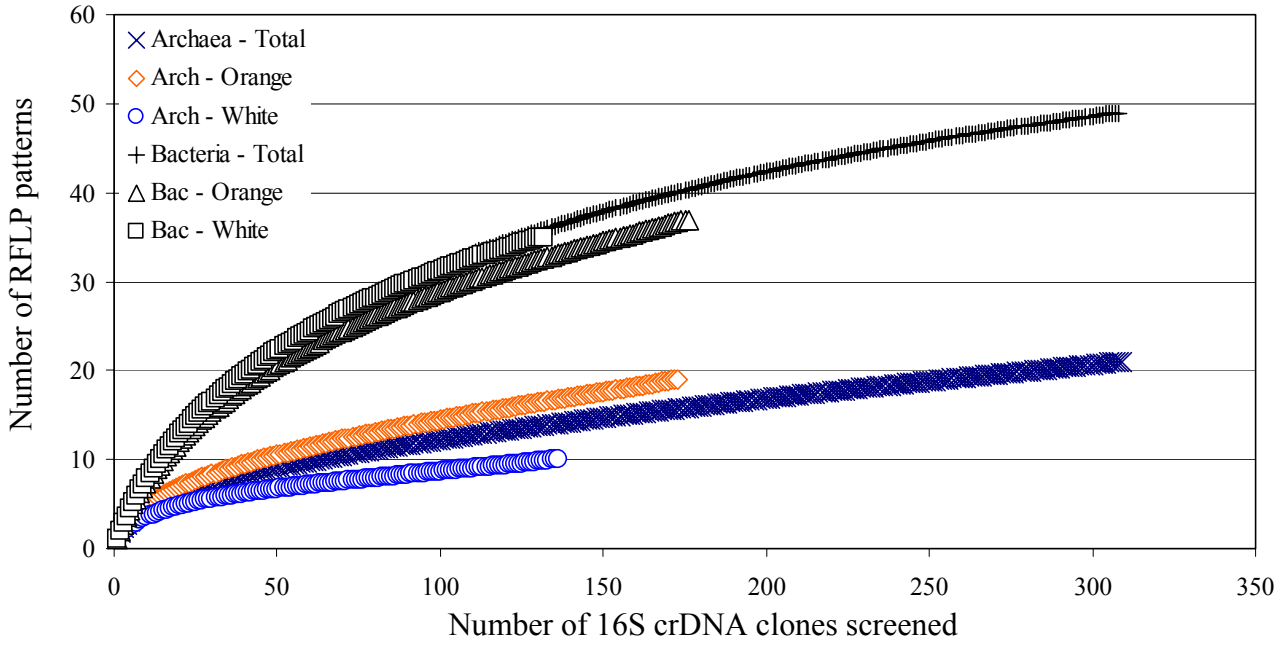

Figure 4.1 Rarefaction curves determined for the different RFLP patterns of 16S crDNA gene clone libraries. *Bacteria* clones were grouped to represent the total library (+), and those associated with either the orange- (△), or white-pigmented (□) *Beggiatoa* sp. mats. *Archaea* clones were also grouped to represent the total library (X), and those associated with either the orange- (◊), or white-pigmented (○) *Beggiatoa* sp. mats. The number of different RFLP patterns was determined after digestion with restriction endonucleases *Hha*I and *Msp*I for *Bacteria* clones and *Hha*I and *Rsa*I for *Archaea* clones.

Table 4.1

Summary of 16S crDNA sequences from *Beggiatoa* sp. mat-associated sediment *Bacteria* clone libraries.

Clone	Number of related clones	RFLP Group	Nearest Relative	Phylogenetic Group	Similarity (%)
4702B-03	11	Delta-1	CM Clone 8-42	δ-*Proteobacteria*	98
4702B-06	9	Delta-2	SS Clone Sva0081	δ-*Proteobacteria*	91
4702B-09	51	Delta-3	CM Clone Hyd89-52	δ-*Proteobacteria*	99
4702B-12	4	Delta-4	SB Clone SB-24e1D6	δ-*Proteobacteria*	99
5268WB-5	37	Delta-5	CM Clone Hyd89-52	δ-*Proteobacteria*	99
5268WB-15	12	Delta-6	CM Clone Hyd24-08	δ-*Proteobacteria*	94
5202B-4	6	Delta-7	SB Clone SB-24e1D6	δ-*Proteobacteria*	92
4702B-30	3	Delta-8	AS Clone SB1_46	δ-*Proteobacteria*	94
4702B-37	19	Delta-9	ER Isolate Eel-36e1H1	δ-*Proteobacteria*	99
5202B-2	7	Delta-10	SS Clone Sva0863	δ-*Proteobacteria*	99
4710B-2	3	Delta-11	CM Clone Hyd89-61	δ-*Proteobacteria*	99
5210WB-1	19	Delta-12	CM Clone Hyd89-21	δ-*Proteobacteria*	98
4710B-20	2	Delta-13	CM Clone Hyd89-22	δ-*Proteobacteria*	92
4768B-3	3	Delta-14	CM Clone Hyd89-52	δ-*Proteobacteria*	98
4768B-7	1	Delta-15	CM Clone Hyd89-52	δ-*Proteobacteria*	98

Table 4.1 (continued)

5210WB-16	2	Delta-16	ER Isolate Eel-36e1H1	δ-*Proteobacteria*	97
5268WB-3	6	Epsilon-1	CS Clone CS060	ε-*Proteobacteria*	97
4702B-14	6	Epsilon-2	JT Clone CS2.28	ε-*Proteobacteria*	98
4702B-07	16	Gamma-1	*Beggiatoa* sp. 'Monterey Canyon'	γ-*Proteobacteria*	97
4702B-18	22	Gamma-2	Sulfur-Oxidizing endosymbiont	γ-*Proteobacteria*	93
5202B-21	6	Gamma-3	*Beggiatoa* sp. 'Monterey Canyon'	γ-*Proteobacteria*	93
5202B-31	13	Gamma-4	*Beggiatoa* sp. 'Monterey Canyon'	γ-*Proteobacteria*	99
5202WB-40	4	Gamma-5	LS Methanotrophic Gill Symbiant	γ-*Proteobacteria*	94
4702B-10	3	Plancto-1	NC Clone wb1 E15	*Planctomycetales*	91
5268WB-14	2	Plancto-2	FB Clone MB-C2-147	*Planctomycetales*	88
5268WB-34	2	Plancto-3	NA Clone NS-G61	*Planctomycetales*	93
5210WB-37	2	Plancto-4	FB Clone MB-C2-105	*Planctomycetales*	89
5202B-40	3	Verruco-1	MS Clone LD1-PA15	*Verrucomicrobia*	86
4710B-36	5	Cloro-1	HS Clone BPC110	GNS, *Cloroflexi*	99
5268WB-9	2	Sphingo-1	WS Clone KM93	*Sphingobacterales*	94

Table 4.2

Summary of 16S crDNA sequences from *Beggiatoa* sp. mat-associated sediments *Archaea* clone library.

Clone	Number of Related Clones	RFLP Group	Nearest Relative	Phylogenetic Group	Similarity (%)
4702R-2	145	ANME-2A-1	MS Clone BA2H11fin	ANME-2A	99
4710R-40	1	ANME-2A-2	MS Clone BA2H11fin	ANME-2A	99
4768R-34	1	ANME-2A-3	MS Clone BA2H11fin	ANME-2A	96
5202WR-36	1	ANME-2A-4	MS Clone BA2H11fin	ANME-2A	98
5210WR-16	1	ANME-2A-5	MS Clone BA2H11fin	ANME-2A	99
4702R-9	34	ANME-2B-1	ER Clone Eel-36a2A4	ANME-2B	99
4702R-4	75	ANME-2C-1	ER Clone Eel-36a2E1	ANME-2C	99
4702R-7	31	ANME-2C-2	ER Clone Eel-36a2A1	ANME-2C	98
5202R-5	2	ANME-2C-3	GB Clone CS_R012	ANME-2C	99
4710R-22	5	ANME-2C-4	GB Clone CS_R012	ANME-2C	99
4710R-24	1	ANME-2C-5	GB Clone CS_R012	ANME-2C	99
5202R-6	1	ANME-2C-6	ER Clone Eel-36a2E1	ANME-2C	95
4768R-21	1	ANME-2C-7	GB Clone CS_R012	ANME-2C	96
4702R-17	6	ANME-2D-1	GB Clone G72_C61	ANME-2D	96
4710R-41	13	ANME-2D-2	GB Clone G72_C61	ANME-2D	92
5202R-25	9	Cren-1	NS Clone TS235C306	*Crenarchaeota*	99

Table 4.2 (continued)

5202R-15	2	Cren-2	HF Clone pCIRA-X	*Crenarchaeota*	86
5202R-20	1	Cren-3	MA Clone 74A4	*Crenarchaeota*	96
5202R-23	1	Cren-4	HF Clone pCIRA-X	*Crenarchaeota*	86
5202R-26	1	Cren-5	JT Clone pMC1A11	*Crenarchaeota*	97
5202R-43	1	Cren-6	JT Clone pMC1A11	*Crenarchaeota*	99

4.4.2 Phylogenetic diversity of metabolically active *Bacteria*

Analysis of the 329 rRNA-derived *Bacteria* clones representing all three sediment depths associated with overlying orange- and white-pigmented microbial mat samples indicated a greater diversity relative to the *Archaea* clone libraries (Figure 4.1). *Bacteria* clones were most similar to as yet uncultured bacterial lineages (Table 4.1). A total of 49 distinct RFLP patterns (data not shown) representing seven phylogenetic lineages were detected (Table 4.1). A considerable majority of the clones (93%) were representative of the phylum *Proteobacteria* (Figure 4.2).

4.4.2.1 *δ-Proteobacteria*

A total of 72% of all bacterial clones examined were most closely related to the class *δ-Proteobacteria*. Included was the most numerically dominant phylotype in the bacterial clone library, designated Delta-3 (15% of the total library; Table 4.1). The Delta-3 phylotype, most similar (99%) to a non-cultured microorganism initially identified from the Cascadia Margin, was detected more frequently at the 6-8 cm and 10-12 cm depths (Figure 4.4) regardless of mat type (Figure 4.3). In contrast to Delta-3, the phylotypes Delta-9 and Delta-5 (Table 4.1) occurred 3- to 5-fold more frequently in sediments covered with orange-pigmented mats relative to clones from white-pigmented mats (Figure 4.3). Phylotype Delta-4 was found exclusively associated with the orange-pigmented mat (Figure 4.3) and only at the upper (0-2 cm) depth (Figure 4.4).

Whereas the highest incidence of metabolically active Delta-4, Delta-5 and Delta-9 phylotypes occurred in sediments associated with the orange-pigmented mats, phylotypes Delta-1, Delta-6, and Delta-12 were most dominant in sediments associated

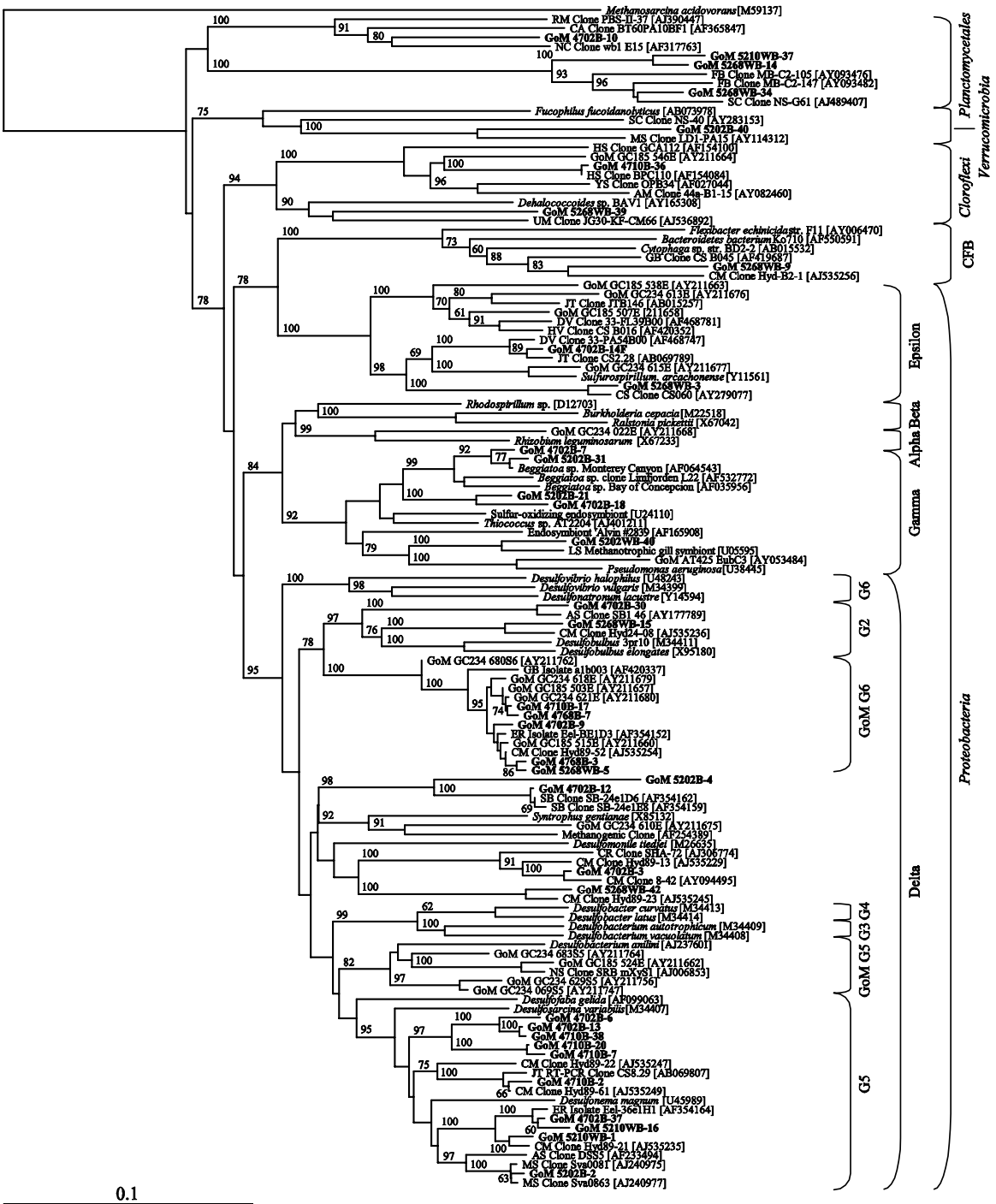
Methanosarcina acidovorans [M59137]
RM Clone PBS-II-37 [AJ390447]
CA Clone BT60PA10BF1 [AF365847]
GoM 4702B-10
NC Clone wb1 E15 [AF317763]
GoM 5210WB-37
GoM 5268WB-14
FB Clone MB-C2-105 [AY093476]
FB Clone MB-C2-147 [AY093482]
GoM 5268WB-34
SC Clone NS-G61 [AJ489407]
Fucophilus fucoidanolyticus [AB073978]
SC Clone NS-40 [AY283153]
GoM 5202B-40
MS Clone LD1-PA15 [AY114312]
HS Clone GCA112 [AF154100]
GoM GC185 546E [AY211664]
GoM 4710B-36
HS Clone BPC110 [AF154084]
YS Clone OPB24 [AF027044]
AM Clone 44a-B1-15 [AY082460]
Dehalococcoides sp. BAV1 [AY165308]
GoM 5268WB-39
UM Clone JG30-KF-CM66 [AJ536892]
Flexibacter echinicidasts. F11 [AY006470]
Bacteroidetes bacterium Ko710 [AF550591]
Cytophaga sp. str. BD2-2 [AB015332]
GB Clone CS B045 [AF419687]
GoM 5268WB-9
CM Clone Hyd-B2-1 [AJ535256]
GoM GC185 538E [AY211663]
GoM GC234 613E [AY211676]
JT Clone JTB146 [AB015257]
GoM GC185 507E [211658]
DV Clone 33-FL39300 [AF468781]
HV Clone CS B016 [AF420352]
DV Clone 32-2A54B00 [AF468747]
GoM 4702B-14F
JT Clone CS2.28 [AB069789]
GoM GC234 615E [AY211677]
Sulfurospirillum. arcachonense [Y11561]
GoM 5268WB-3
CS Clone CS060 [AY279077]
Rhodospirillum sp. [D12703]
Burkholderia cepacia [M22518]
Ralstonia pickettii [X67042]
GoM GC234 022E [AY211668]
Rhizobium leguminosarum [X67233]
GoM 4702B-7
GoM 5202B-31
Beggiatoa sp. Monterey Canyon [AF064543]
Beggiatoa sp. clone Limnorden L22 [AF532772]
Beggiatoa sp. Bay of Concepcion [AF035956]
GoM 5202B-21
GoM 4702B-18
Sulfur-oxidizing endosymbiont [U24110]
Thiococcus sp. AT2204 [AJ401211]
Endosymbiont 'Alvin #2839' [AF165908]
GoM 5202WB-40
LS Methanotrophic gill symbiont [U05595]
GoM AT425 BubC3 [AY053484]
Pseudomonas aeruginosa [U38445]
Desulfovibrio halophilus [U48243]
Desulfovibrio vulgaris [M34399]
Desulfonatronum lacustre [Y14594]
GoM 4702B-30
AS Clone SB1 46 [AY177789]
GoM 5268WB-15
CM Clone Hyd24-08 [AJ535236]
Desulfobulbus sp. [M34411]
Desulfobulbus elongates [X95180]
GoM GC234 680S6 [AY211762]
GB Isolate a1b003 [AF420337]
GoM GC234 618E [AY211679]
GoM GC185 503E [AY211657]
GoM GC234 621E [AY211680]
GoM 4710B-17
GoM 4768B-7
GoM 4702B-9
ER Isolate Eel-BE1D3 [AF354152]
GoM GC185 515E [AY211660]
CM Clone Hyd89-52 [AJ535254]
GoM 4768B-3
GoM 5268WB-5
GoM 5202B-4
GoM 4702B-12
SB Clone SB-24e1D6 [AF354162]
SB Clone SB-24e1E8 [AF354159]
Syntrophus gentianae [X85132]
GoM GC234 610E [AY211675]
Methanogenic Clone [AF254389]
Desulfomonile tiedjei [M26635]
CR Clone SHA-72 [AJ306774]
CM Clone Hyd89-13 [AJ535229]
GoM 4702B-3
CM Clone 8-42 [AY094495]
GoM 5268WB-42
CM Clone Hyd89-23 [AJ535245]
Desulfobacter curvatus [M34413]
Desulfobacter latus [M34414]
Desulfobacterium autotrophicum [M34409]
Desulfobacterium vacuolatum [M34408]
Desulfobacterium anilini [AJ237601]
GoM GC234 683S5 [AY211764]
GoM GC185 524E [AY211662]
NS Clone SRB mXyS1 [AJ006853]
GoM GC234 629S5 [AY211756]
GoM GC234 069S5 [AY211747]
Desulfofaba gelida [AF090063]
Desulfosarcina variabilis [M34407]
GoM 4702B-6
GoM 4702B-13
GoM 4710B-38
GoM 4710B-20
GoM 4710B-7
CM Clone Hyd89-22 [AJ535247]
JT RT-PCR Clone CS8.29 [AB069807]
GoM 4710B-2
CM Clone Hyd89-61 [AJ535249]
Desulfonema magnum [U45989]
ER Isolate Eel-36e1H1 [AF354164]
GoM 4702B-37
GoM 5210WB-16
GoM 5210WB-1
CM Clone Hyd89-21 [AJ535235]
AS Clone DSS3 [AF253494]
MS Clone Sva0081 [AJ240975]
GoM 5202B-2
MS Clone Sva0863 [AJ240977]
0.1
Planctomycetales
Verrucomicrobia
Cloroflexi
CFB
Epsilon
Alpha Beta
Gamma
Delta
Proteobacteria
G6
G2
GoM G6
G3 G4
GoM G5
G5

Figure 4.2 Phylogenetic tree of relationships of 16S crDNA bacterial clone sequences, as determined by distance Jukes-Cantor analysis, from GoM GC185 and GC234 seep sediments associated with orange- and white-pigmented microbial mats (in boldface) to selected cultured isolates and environmental clones. Designations of environmental clone sequences are AM, acid mine; AS, anoxic sediment; CA, coral-associated; CM, Cascadia Margin; CR, Chlorinated compound reduction; CS, continental slope; DV, Deep-sea volcano; ER, Eel River; FB, Forearc Basin; GB, Guaymus Basin; GoM, Gulf of Mexico; HS, hydrocarbon seep; HV, hydrothermal vent; JT, Japan Trench; LS, Louisiana Slope; MS, marine sediments; NC, Nullarbor Cave, Australia; NS, North Sea; RM, rice microcosms; SB, Santa Barbara Basin; SC, South China Sea; UM, uranium mine; YS, Yellowstone hot springs.

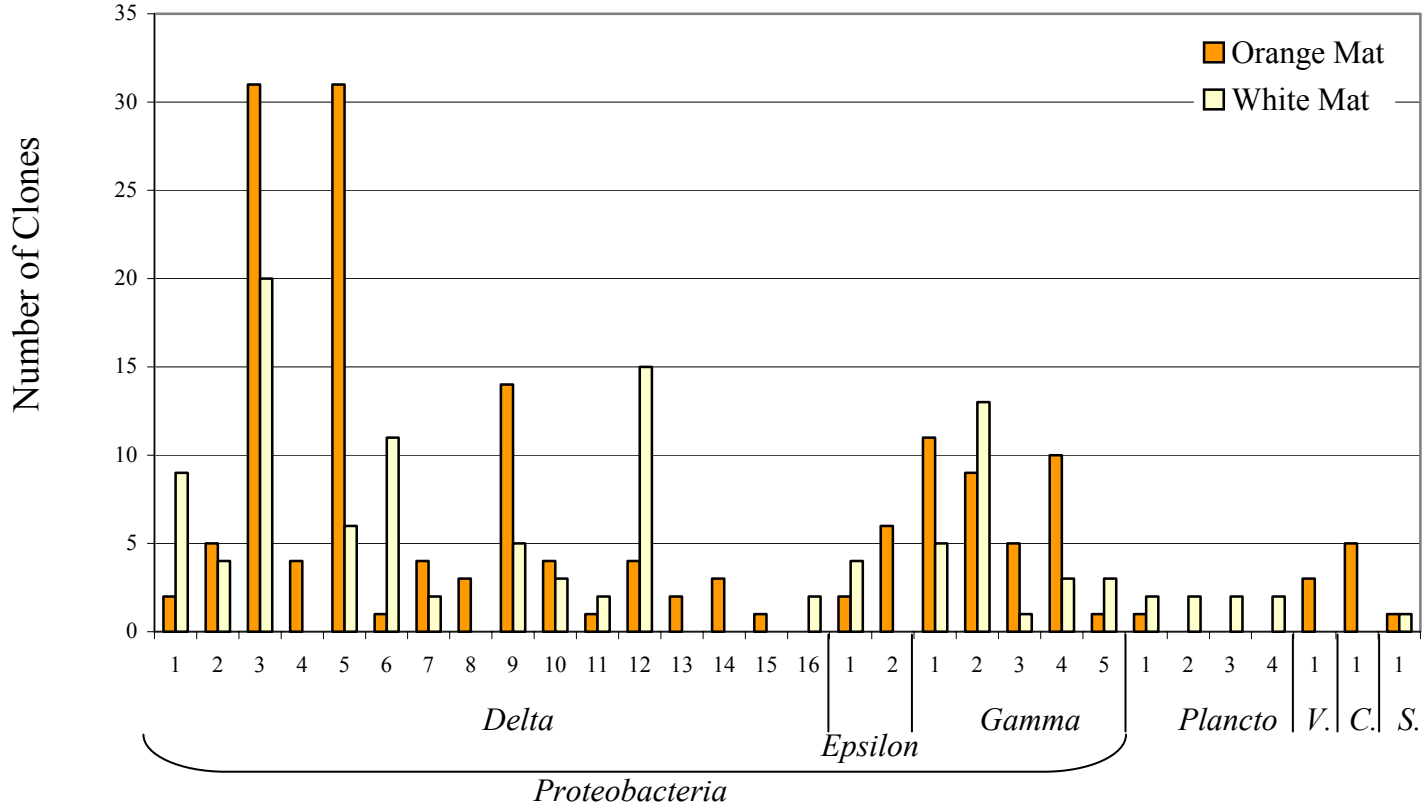

Figure 4.3 Comparison between 16S crDNA *Bacteria* clones obtained from sediments associated with either orange- or white-pigmented *Beggiatoa* sp mats. Clones are phylogenetically grouped according to sequence analysis data. Numbers along the abscissa denote unique phylotypes as determined by RFLP analysis and are consistent with the phylotype names in Table 4.1. Abbreviations: *Plancto., Planctomycetales*; *V., Verrucomycrobia*; *C., Chloroflexi*; *S., Sphingobacteria*.

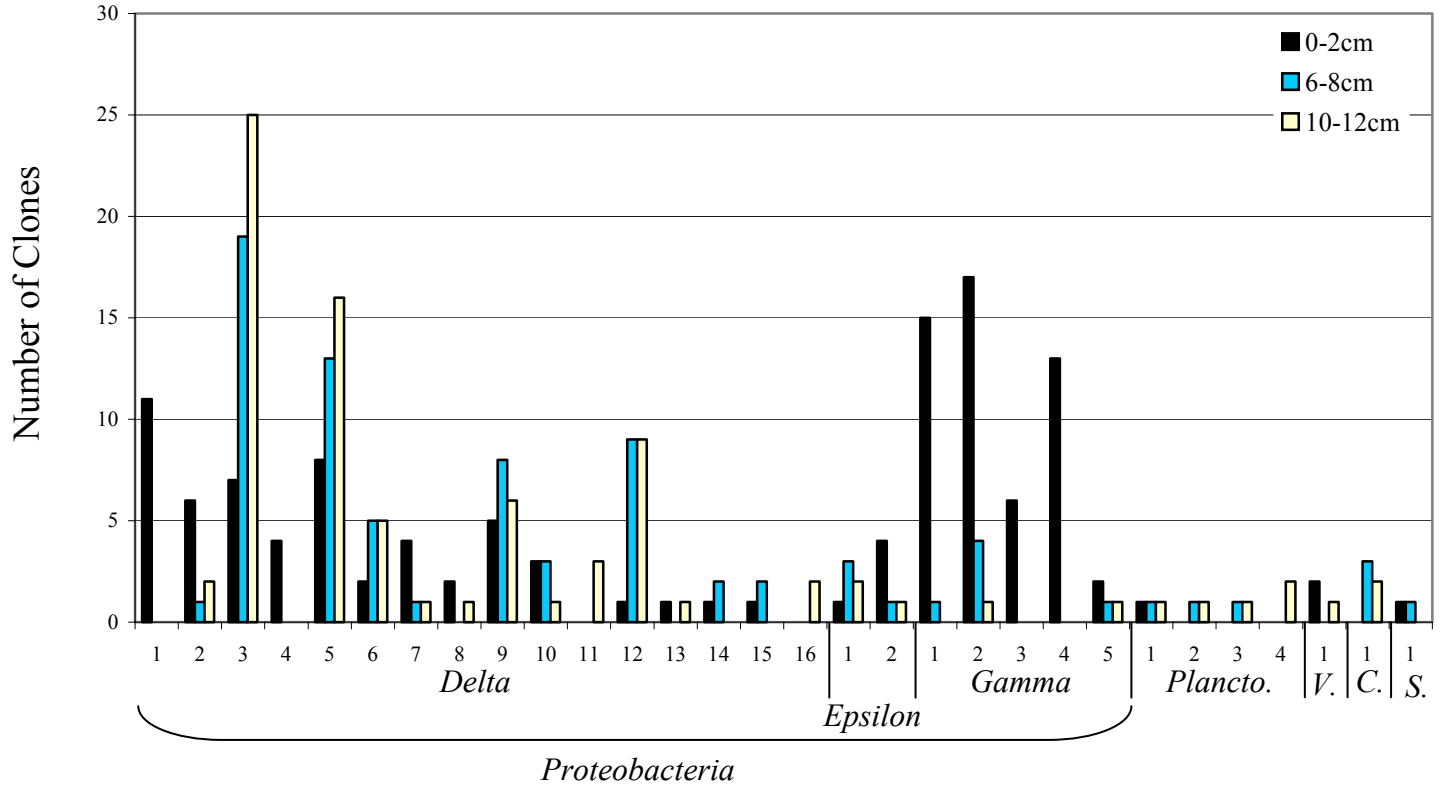

Figure 4.4 Comparison between 16S crDNA *Bacteria* clones obtained from specific depths in sediments associated with both orange- and white-pigmented *Beggiatoa* sp mats. Clones are phylogenetically grouped according to sequence analysis data. Numbers along the abscissa denote unique phylotypes as determined by RFLP analysis and are consistent with the phylotype names in Table 4.1. Abbreviations: *Plancto., Planctomycetales*; *V., Verrucomycrobia*; *C., Chloroflexi*; *S., Sphingobacteria*.

with the white-pigmented mats (Figure 4.3). These phylotypes exhibited a 3.8-fold to 11-fold greater incidence in sediments associated with white-pigmented mats relative to clones associated with overlying orange mats. While Delta-1 was exclusively detected at the 0-2 cm depth (Figure 4.4), phylotypes Delta-6 and Delta-12 were most frequently detected (5- and 18-fold respectively) at the lower depths (6-8 and 10-12 cm; Figure 4.4).

4.4.2.2 *γ-Proteobacteria*

The second most dominant group of bacterial phylotypes was most similar to several non-cultured microorganisms, including *Beggiatoa* sp. 'Monterey Canyon' (2) (Figure 4.2), all clustering within the class *γ-Proteobacteria* (22% of all clones; Table 4.1). The phylotypes associated with the overlying orange-pigmented mat most closely related to the *Beggiatoa* sp. 'Monterey Canyon' were either predominantly (i.e., Gamma-1) or exclusively (i.e., Gamma-3 and Gamma-4) located at the 0-2 cm depth (Figure 4.3 and Figure 4.4). In contrast, phylotypes Gamma-2 and Gamma-5 (Figure 4.3) were more frequently detected in sediments covered with white-pigmented mats and were most similar to clones previously characterized as mussel endosymbionts (Table 4.1). These were the only metabolically active *γ-Proteobacteria*-related clones detected at the 10-12 cm depth (Figure 4.4). Phylotypes Gamma-2 and Gamma-3 were most related (98% similar) to each other (Figure 4.2). However, BLAST results indicated these phylotypes were 93% similar to two different environmental clones (Table 4.1).

4.4.2.3 *ε-Proteobacteria.*

The remaining *Proteobacteria*-related clones were located in two different clades within the class *ε-Proteobacteria* (Figure 4.2). Epsilon-1 phylotype, highly similar (97%) to a previously identified cold seep clone (Table 4.1), occurred in sediments covered with orange- and white-pigmented mats and was not detected any more frequently at any particular depth (Figure 4.3 and Figure 4.4). In contrast, the Epsilon-2 phylotype, 98% similar to an uncultured clone first isolated from the Japan Trench which had also been obtained by RT-PCR (67) (Table 4.1), was exclusively obtained from sediments associated with the overlying orange-pigmented mat (Figure 4.3) and predominately from 0-2 cm (4 of 6 clones; Figure 4.4).

4.4.2.4 Non-proteobacterial lineages

In contrast to numerous *Proteobacteria*-related phylotypes, clones exhibiting similarity to the classes *Planctomycetacia*, *Verrucomicrobia*, and *Cloroflexi* appeared to exhibit potential mat specificity. For example, *Planctomycetacia*-related clones, represented by four distinct phylotypes (n=9; Table 4.1), were detected almost exclusively at lower sediment depths covered with white-pigmented mats (Figure 4.3 and Figure 4.4). The *Verrucomicrobia*- (n=3) and *Cloroflexi*-related (n=5) clones were detected at varying sediment depths and associated exclusively with the overlying orange-pigmented mat (Figrue 4.3 and Figure 4.4). Clones from each of these three classes were most closely related to environmental clones (Table 4.1) that have only been previously obtained from DNA-derived clone libraries. The remaining non-proteobacterial-related clones were most similar to the class *Sphingobacteria*, and were

detected in sediments covered with orange- and white-pigmented mats at the 0-2 cm and 6-8 cm depths, respectively (Figure 4.3 and Figure 4.4).

4.4.3 Phylogenetic diversity of metabolically active *Archaea*.

A total of 333 rRNA-derived *Archaea* clones, obtained from sediments with overlying orange- and white-pigmented microbial mats, grouped into 21 distinct RFLP patterns (data not shown) and representative clones from all patterns sequenced (Table 4.2). Interestingly, these 21 RFLP groups represented only two phylogenetic lineages, i.e. *Crenarcheota* and the Euryarchaeotal ANME-2 cluster of the order *Methanosarcinales*.

4.4.3.1 ANME-2

The majority of *Archaea* clones (95%; Table 4.2) were related to a distinct clade of *Methanosarcinales* known as ANME-2 (122). Members of this cluster have been previously detected in methane seep environments with sediment profiles indicative of anaerobic methane oxidation activity (62, 88, 122, 169). The ANME-2 cluster has been divided into four distinct subgroups designated A, B, C and D (Figure 4.5) (108, 122). Clones representing all four of these subgroups were detected in this current study (Figure 4.5). Subgroup A was numerically dominant in the clone library (n=145), while subgroup C exhibited the greatest intraclade genetic diversity (n=7) relative to the other ANME-2 subgroups (Table 4.2). The phylotype ANME-2A-1, comprised 43% of the total *Archaea* library (Table 4.2), was most frequently detected in sediments covered with white-pigmented mats. We also observed a significantly greater ($P < 0.05$) number of ANME-2A-1 clones at the 0-2 cm depth (Figure 4.7). In contrast, a comparable number

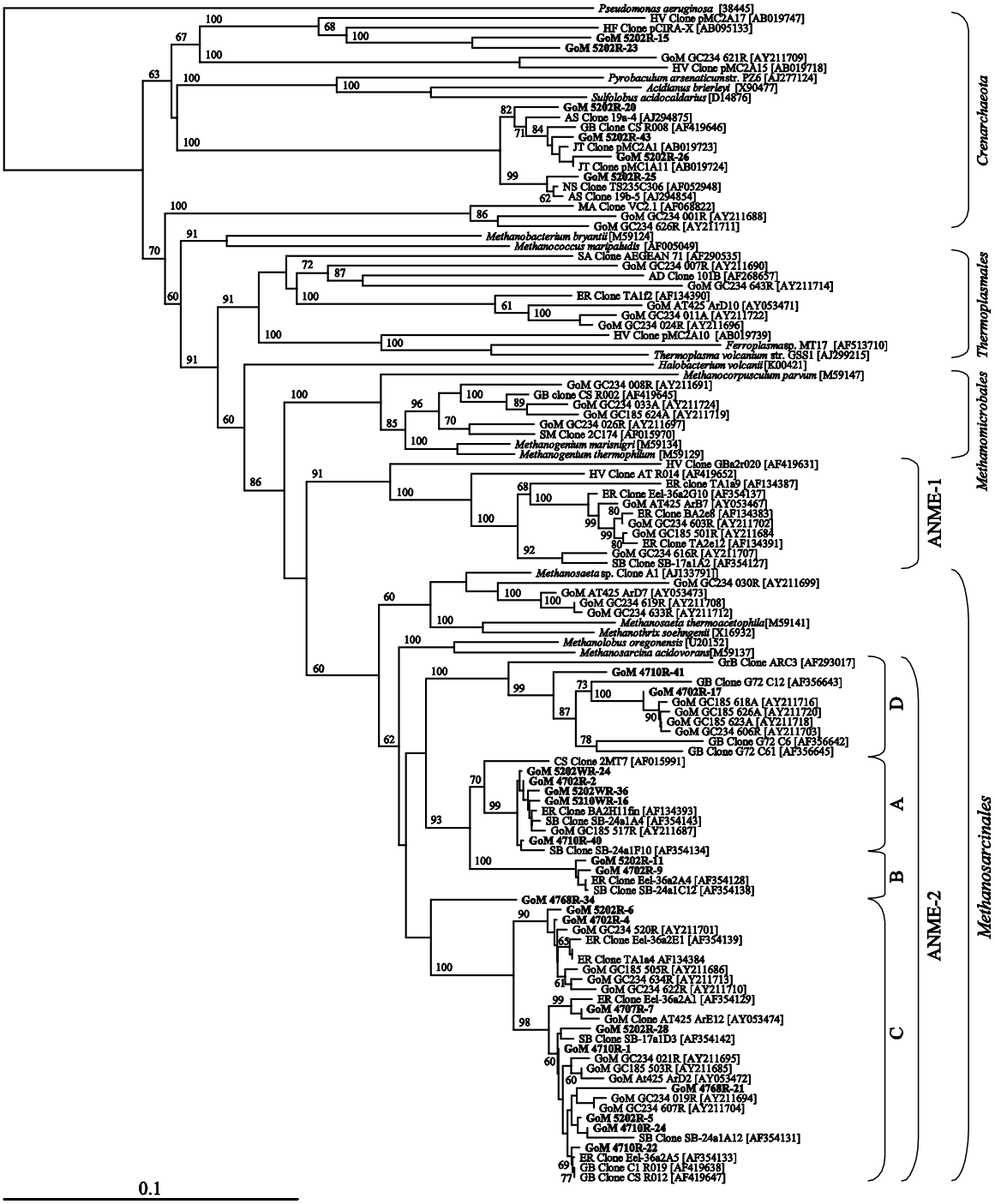
Pseudomonas aeruginosa [38445]
HV Clone pMC2A17 [AB019747]
HF Clone pCIRA-X [AB095133]
GoM 5202R-15
GoM 5202R-23
GoM GC234 621R [AY211709]
HV Clone pMC2A15 [AB019718]
Pyrobaculum arsenaticumstr. PZ6 [AJ277124]
Acidianus brierleyi [X90477]
Sulfolobus acidocaldarius [D14876]
GoM 5202R-20
AS Clone 19a-4 [AJ294875]
GB Clone CS R008 [AF419646]
GoM 5202R-43
JT Clone pMC2A1 [AB019723]
GoM 5202R-26
JT Clone pMC1A11 [AB019724]
GoM 5202R-25
NS Clone TS235C306 [AF052948]
AS Clone 19b-5 [AJ294854]
MA Clone VC2.1 [AF068822]
GoM GC234 001R [AY211688]
GoM GC234 626R [AY211711]
Methanobacterium bryantii [M59124]
Methanococcus maripaludis [AF005049]
SA Clone AEGEAN 71 [AF290535]
GoM GC234 007R [AY211690]
AD Clone 101B [AF268657]
GoM GC234 643R [AY211714]
ER Clone TA1f2 [AF134390]
GoM AT425 ArD10 [AY053471]
GoM GC234 011A [AY211722]
GoM GC234 024R [AY211696]
HV Clone pMC2A10 [AB019739]
Ferroplasmasp. MT17 [AF513710]
Thermoplasma volcanium str. GSS1 [AJ299215]
Halobacterium volcanii [K00421]
Methanocorpusculum parvum [M59147]
GoM GC234 008R [AY211691]
GB clone CS R002 [AF419645]
GoM GC234 033A [AY211724]
GoM GC185 624A [AY211719]
GoM GC234 026R [AY211697]
SM Clone 2C174 [AF015970]
Methanogenium marinigri [M59134]
Methanogenium thermophilum [M59129]
HV Clone GBa2r020 [AF419631]
HV Clone AT R014 [AF419652]
ER clone TA1a9 [AF134387]
ER Clone Eel-36a2G10 [AF354137]
GoM AT425 ArB7 [AY053467]
ER Clone BA2e8 [AF134383]
GoM GC234 603R [AY211702]
GoM GC185 501R [AY211684]
ER Clone TA2e12 [AF134391]
GoM GC234 616R [AY211707]
SB Clone SB-17a1A2 [AF354127]
Methanosaeta sp. Clone A1 [AJ133791]
GoM GC234 030R [AY211699]
GoM AT425 ArD7 [AY053473]
GoM GC234 619R [AY211708]
GoM GC234 633R [AY211712]
Methanosaeta thermoacetophila [M59141]
Methanothrix soehngenii [X16932]
Methanolobus oregonensis [U20152]
Methanosarcina acidovorans [M59137]
GrB Clone ARC3 [AF293017]
GoM 4710R-41
GB Clone G72 C12 [AF356643]
GoM 4702R-17
GoM GC185 618A [AY211716]
GoM GC185 626A [AY211720]
GoM GC185 623A [AY211718]
GoM GC234 606R [AY211703]
GB Clone G72 C6 [AF356642]
GB Clone G72 C61 [AF356645]
CS Clone 2MT7 [AF015991]
GoM 5202WR-24
GoM 4702R-2
GoM 5202WR-36
GoM 5210WR-16
ER Clone BA2H11fin [AF134393]
SB Clone SB-24a1A4 [AF354143]
GoM GC185 517R [AY211687]
GoM 4710R-40
SB Clone SB-24a1F10 [AF354134]
GoM 5202R-11
GoM 4702R-9
ER Clone Eel-36a2A4 [AF354128]
SB Clone SB-24a1C12 [AF354138]
GoM 4768R-34
GoM 5202R-6
GoM 4702R-4
GoM GC234 520R [AY211701]
ER Clone Eel-36a2E1 [AF354139]
ER Clone TA1a4 AF134384
GoM GC185 505R [AY211686]
GoM GC234 634R [AY211713]
GoM GC234 622R [AY211710]
ER Clone Eel-36a2A1 [AF354129]
GoM 4707R-7
GoM Clone AT425 ArE12 [AY053474]
GoM 5202R-28
SB Clone SB-17a1D3 [AF354142]
GoM 4710R-1
GoM GC234 021R [AY211695]
GoM GC185 503R [AY211685]
GoM At425 ArD2 [AY053472]
GoM 4768R-21
GoM GC234 019R [AY211694]
GoM GC234 607R [AY211704]
GoM 5202R-5
GoM 4710R-24
SB Clone SB-24a1A12 [AF354131]
GoM 4710R-22
ER Clone Eel-36a2A5 [AF354133]
GB Clone C1 R019 [AF419638]
GB Clone CS R012 [AF419647]
0.1
Crenarchaeota
Thermoplasmales
Methanomicrobales
ANME-1
ANME-2
Methanosarcinales
D
A
B
C

Figure 4.5 Phylogenetic tree of relationships of 16S crDNA archaeal clone sequences, as determined by distance Jukes-Cantor analysis, from GoM GC185 and GC234 seep sediments associated with orange- and white-pigmented mats (in boldface) to selected cultured isolates and environmental clones. Designations of environmental clone sequences are AD, Anaerobic digester; AS, Anoxic sediment; CS, continental slope; ER, Eel River; GB, Guaymus Basin; GoM, Gulf of Mexico; GrB, Green Bay; HF, hydrothermal field; HV, Hydrothermal vent; JT, Japan Trench; MA, Mid-Atlantic ridge; NS, North Sea; SB, Santa Barbara Basin; SM, Salt marsh.

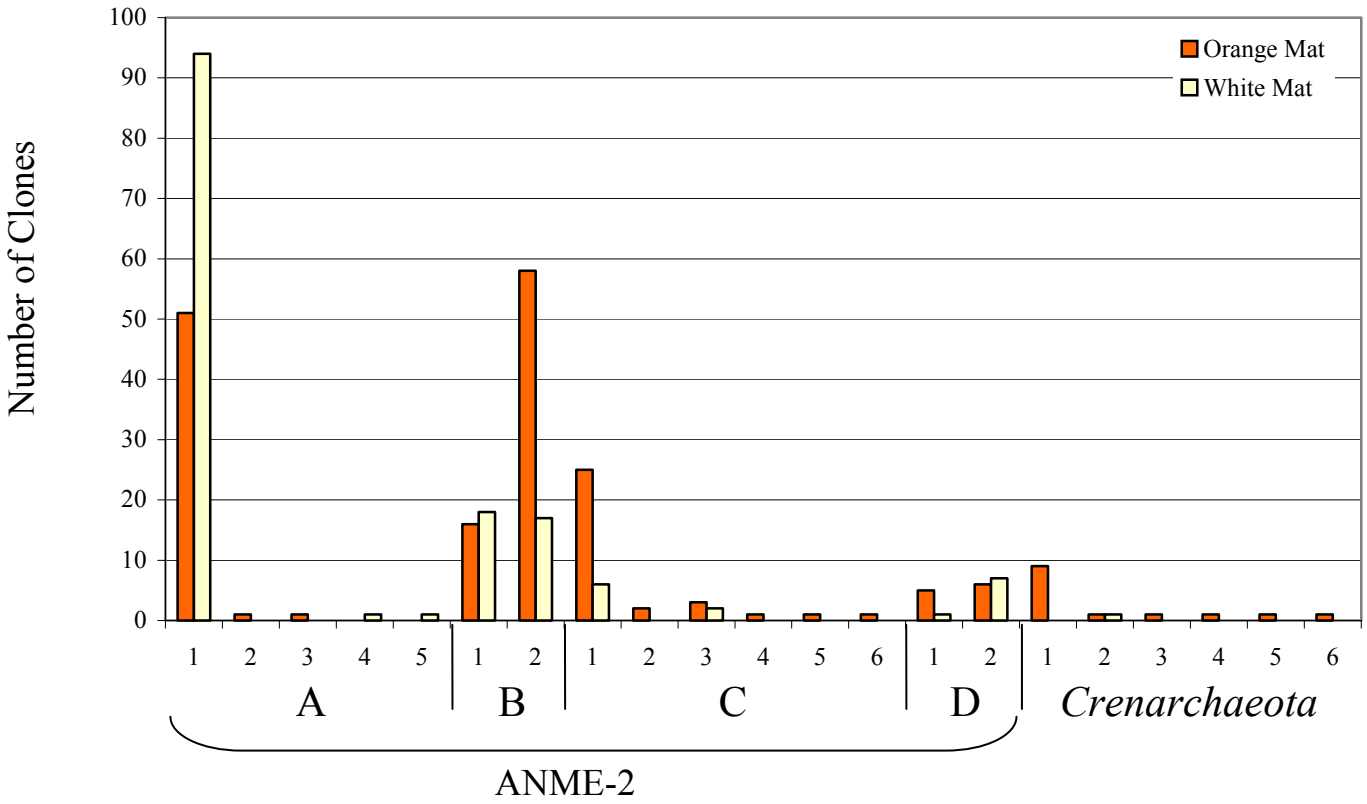

Figure 4.6 Comparison between 16S crDNA *Archaea* clones obtained from sediments associated with either orange- or white-pigmented *Beggiatoa* sp mats. Clones are phylogenetically grouped according to sequence analysis data. Numbers along the abscissa denote unique phylotypes as determined by RFLP analysis and are consistent with the phylotype names in Table 4.2.

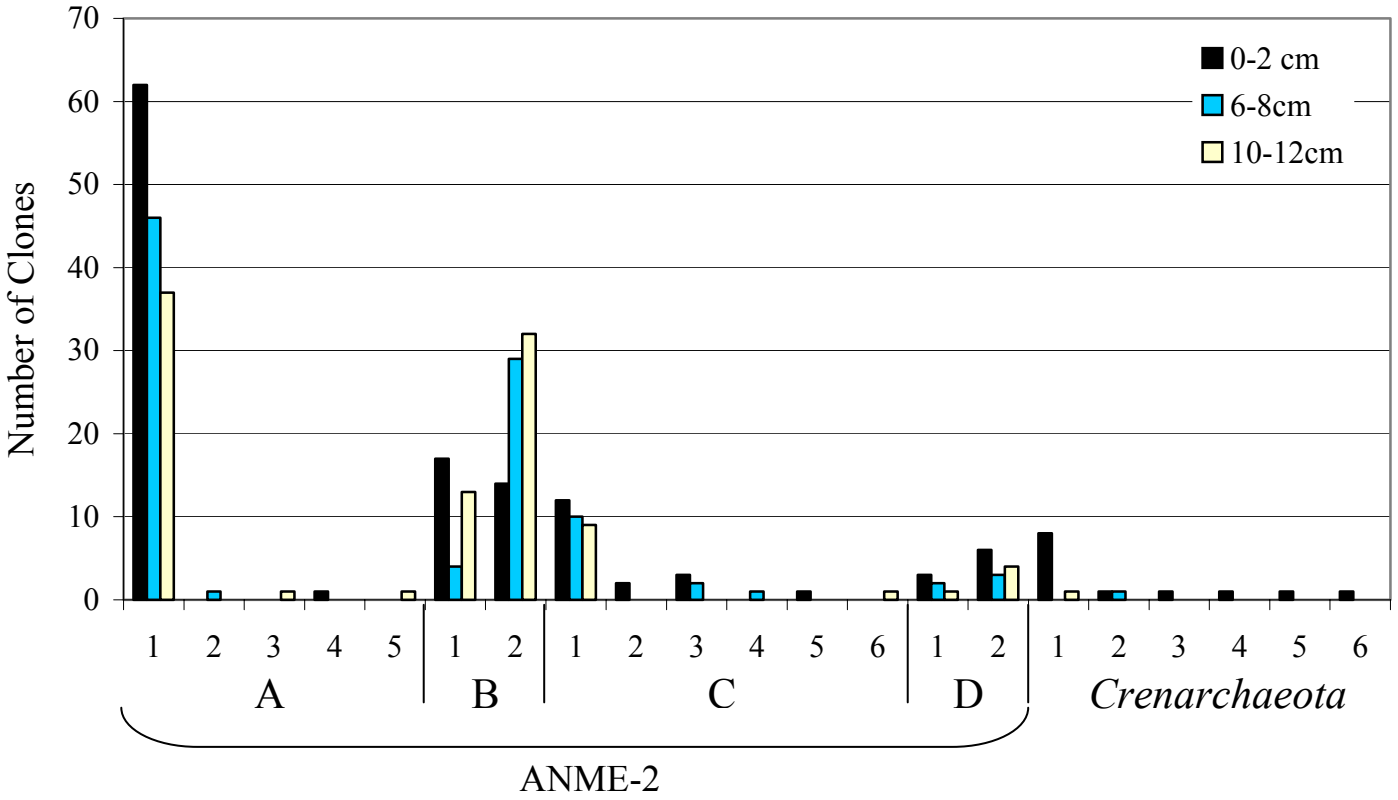

Figure 4.7 Comparison between 16S crDNA *Archaea* clones obtained from specific depths in sediments associated with both orange- and white-pigmented *Beggiatoa* sp mats. Clones are phylogenetically grouped according to sequence analysis data. Numbers along the abscissa denote unique phylotypes as determined by RFLP analysis and are consistent with the phylotype names in Table 4.2.

of ANME-2B-1 clones, related to ANME-2 subgroup B, were detected in sediments covered with both mat types (Figure 4.6). This phylotype was recovered from sediments associated with orange-pigmented mats and only detected at 0-2 cm, while clones obtained from white-mat covered sediments predominated at 10-12 cm (13 of 18 clones; Figure 4.7). Therefore, this metabolically active phylotype appeared to exhibit depth specificity relative to mat type. Clones related to the subgroup ANME-2C were dominated by two phylotypes, ANME-2C-1 and ANME-2C-2 (Table 4.2) and were most related to environmental clones previously isolated from a cold methane seep locale in the Eel River Basin (122). Both of these phylotypes were more frequently detected in sediments associated with overlying orange-pigmented mats (Figure 4.6) and were metabolically active at all sampled sediment depths (Figure 4.7). However, ANME-2C-1 was significantly ($P < 0.05$) more active at the lower depths sampled (6-8 and 10-12 cm; Figure 4.7). The remaining five ANME-2C-related phylotypes were detected at a low frequency (10 of 333) and were predominately metabolically active at the 0-2 and 6-8 cm depths (Figure 4.7). The fourth ANME-2 subgroup, designated ANME-2D, was first observed in *Archaea*-specific 16S rRNA gene libraries derived from total DNA extracted from sediments directly associated with surface breaching gas hydrate (108). In the present study, two distinct phylotypes from this subgroup were identified (Figure 4.5). The phylotype denoted ANME-2D-1 was closely related (99.8% similar) to the dominant ANME-2D phylotype reported by Mills et al. (108) and was most frequently (i.e., 5-fold) detected in orange-mat covered sediments (Figure 4.6). However, the ANME-2D-2 phylotype was genetically divergent, having only 92% sequence similarity to GoM GC234 606R (108) (Figure 4.5) and was not specific to any particular mat type.

4.4.3.2 *Crenarchaeota*

The remaining 5% of the archaeal clones (n=15) were grouped into 6 distinct RFLP patterns (data not shown) forming three clades within the *Crenarchaeota* lineage (Figure 4.5). Clones representing these 6 phylotypes were most similar to sequences obtained from non-cultured microorganisms (Table 4.2 and Figure 4.5). Phylotype Cren-1 represented a majority of the *Crenarchaeota*-related clones (9 of 15), and was most related (99% similar) to a 16S rRNA gene sequence isolated from surface sediments in the North Sea (175) (Figure 4.5). In addition, phylotype Cren-1 was predominately active only at the 0-2 cm sediment depth (8 of 9) and exclusively associated with the overlying orange-pigmented mat. Interestingly, with the exception of the single clone associated with the Cren-2 phylotype, all other *Crenarchaeota*-related clones obtained in the present study, were isolated from orange mat covered sediments (Figure 4.6).

4.5 Discussion

This study is the first to report the composition of the metabolically active members of the archaeal and bacterial communities in gas hydrate sedimentary systems in the Gulf of Mexico. Moreover, to the best of our knowledge, this is also one of the first characterizations of metabolically active *Archaea* from marine environments as determined by rRNA analysis and one of the first microbial community depth profiles of sediments associated with overlying microbial mats in cold seep habitats. Inagaki et al. (21) recently reported that ε- and δ-*Proteobacteria* phylotypes dominated the

metabolically active fraction of the bacterial community in cold seep sediments beneath a *Calyptogena* colony at the Sanriku Escarpment (Japan Trench, 5343 m water depth). We have also previously shown, by DNA-based phylogenetic analyses, that in GoM sediments directly above gas hydrate mounds lacking microbial mats, *ε-Proteobacteria* dominated the bacterial clone libraries (108). However, in the present study, fewer than 4% of the metabolically active phylotypes detected at the 0-2 cm depth belonged to *ε-Proteobacteria*. Instead, the 0-2 cm *Bacteria* clone library was dominated by *γ-Proteobacteria* and *δ-Proteobacteria* (45% and 48% respectively) while the 6-8 cm and 10-12 cm libraries were dominated by *δ-Proteobacteria.*

All *γ*-proteobacterial-related clones derived from sediments covered with either orange- or white-pigmented microbial mats were most similar to either *Beggiatoa* sp. or macrofaunal endosymbionts (93% to 99% similar). Surprisingly, all of the *Beggiatoa*-related clones were most similar to *Beggiatoa* sp. 'Monterey Canyon' (2) providing a possible biogeographical link between these two distinct cold seep environments. As geologic evidence has shown that the presence of a deep water current flowing between the Gulf of Mexico and the Eastern Pacific was disrupted 4.6 Mya as a result of the rise of the Isthmus of Panama (59), it is tempting to speculate that these *Beggiatoa* populations originated from common ancestor(s) separated by this event. The occurrence of other *γ*–proteobacterial phylotypes related to previously identified endosymbiont clone sequences may be explained by the presence of numerous juvenile clams and shrimp observed during microscopic examination of intact, unprocessed sediments (i.e., 0-2 cm). Whether these endosymbionts are free-living in the sediment or were detected as a result

of disruption/breakage of the juvenile clams and shrimp cannot be determined in this study.

While the vast majority of the metabolically active *γ-Proteobacteria* phylotypes detected in this study appeared to be constrained to the 0-2 cm depth, four distinct clades of active *δ-Proteobacteria* remained numerically dominant at all three depths. As many members of the *δ-Proteobacteria* are known sulfate-reducing bacteria, these clades are likely to be important players in S cycling. Although not determined in this present study, previously measured porewater sulfate concentrations (>25 mM) from GoM site GC234 sediments associated with overlying microbial mats did not exceed sulfate concentrations in sediments lacking mats (74). The rates of sulfate reduction in sediments covered with mats, however, were several orders of magnitude greater along a 0-12 cm depth profile relative to comparable sediments lacking microbial mats (74). A corresponding increase in H_2S concentration was detected as sulfate concentrations decreased with increasing sediment depth (74). Such concentrations and rates are similar to previously characterized *Beggiatoa* sp. mat-associated sediment porewater from other cold seep environments (10, 122) as well as a GoM study conducted at GC185 (1). We hypothesize that the predominance of active *δ-Proteobacteria* detected at the lower depths may be explained by two different mechanisms. First, upward flow of subsurface fluids channeled around microbial mats may result in a downward fluid flux through the mat (180). Sulfate-rich seawater is pumped deeper into the mat-covered sediments than surrounding sediments lacking mats. Thus, the microbial mats would provide a localized increased concentration of sulfate at lower depths facilitating overall higher rates of sulfate reduction. Secondly, anaerobic sulfur oxidation due to *Beggiatoa* sp. activity

would replenish sulfate throughout the sediment profile. Although there was a 7-fold increase in the total number of metabolically active *Beggiatoa* sp. clones detected at 0-2 cm, *Beggiatoa*-related clones were also detected at 6-8 cm and 10-12 cm. Such results were perhaps not surprising, as previous reports have demonstrated the ability of *Beggiatoa* spp. to migrate below 10 cm to reach elevated concentrations of H_2S (2, 116).

Planctomycetales-related clones were more frequently detected at the lower depths (i.e., 6-8 cm and 10-12 cm) in sediments covered with orange- and white-pigmented microbial mat communities. Previous studies have demonstrated the breadth of physiological characteristics of this phylum (50, 92, 152) including a possible link between some members of the *Planctomycetales* to the anaerobic oxidation of ammonia (153, 161). This process, known as ANAMMOX and described by a metabolic pathway first reported by Van de Graaf et al. (174), requires ammonia and nitrite in an anaerobic environment to produce dinitrogen gas (162, 163). Ammonium concentrations in previously characterized porewater from one of our study sites (i.e., GoM GC234) were 4-fold higher in *Beggiatoa* spp. mat-covered sediments at 10-12 cm (>30 μM) relative to sediments lacking microbial mats (5 μM) (74). Although nitrite concentrations were not determined, nitrate concentrations in porewater from GC234 sediments with microbial mats were highest at the surface (>20 μM) and decreasing to less than 2 μM below 2 cm (74). The nitrite source, required for ANAMMOX, may be derived from either the incomplete reduction of nitrate or from the advective flow of nitrite-bearing seawater through the *Beggiatoa*-covered sediment as has been reported by Weber and Jorgensen (180). Therefore, an increased concentration of nitrite and ammonia may be attributed to the presence of *Beggiatoa* sp. mats. Thus, we theorize that the *Planctomycetale*-related

clones detected in this study are dependant on the presence of the *Beggiatoa* sp. mat community.

Methane concentrations and anaerobic oxidation of methane (AOM) rates previously determined for GC234 sediments covered with *Beggiatoa* sp. mats have been shown to be several orders of magnitude higher than control sediments lacking microbial mats (74). In the present study, the vast majority (95%) of *Archaea* clones obtained from the three sediment depths also sampled from GoM sites GC234 and GC185 were phylogenetically related to the ANME-2 group of the order *Methanosarcinales*, proposed candidates for AOM. ANME-2-related sequences have been isolated from total DNA extracted from other cold seep environments (62, 88, 108, 122), but have never represented such a majority of the sequences as obtained in this study. This study also represents the first archaeal clone library containing sequences related to all four ANME-2 subdivisions [i.e. A, B, C and D; (108, 122)]. Interestingly, the ANME-2C-related clones do not form a GoM specific cluster as was observed in other phylogenetic analyses of GoM hydrate-associated sediments (88, 108). However, one of the two ANME-2D-related phylotypes was only 92% similar to previously identified ANME-2D sequences from the GoM (108) and thus may represent a novel lineage within the ANME-2D clade. The uniqueness of the *Archaea* clone libraries constructed in this study may be a result of the environmental conditions associated with an overlying microbial mat community or due to this study being the first to characterize metabolically active archaea communities from a cold seep locale. A PCR primer bias seems less likely as the primers employed in this study have been used in another GoM study that resulted in more diverse libraries

that included sequences related to *Methanomicrobiales*, *Archaeglobus*, non-ANME-2 *Methanosarcinales* and *Crenarchaeota* (109).

Based on our current findings characterizing the metabolically active fraction of the bacterial and archaeal community in conjunction with recent geochemical data and microbial rate measurements from *Beggiatoa*-covered sediments (74), we propose the following. *Beggiatoa* sp. serve as a keystone member of the seep community owing to their ability to (directly and indirectly) influence the metabolic activity of *δ–Proteobacteria*, *Planctomycetales*, and ANME archaea. The end products of *Beggiatoa*-mediated anaerobic sulfur oxidation (i.e. sulfate and ammonia) and an increase in advective flow rate into the mat (180) would result in higher concentrations of reactants available for *δ-Proteobacteria* and *Planctomycetales*. Recent findings by Joye et. al (74) lend support to this hypothesis as they detected an increase in sulfate and ammonium concentrations, and microbial sulfate reduction rates in GoM GC234 sediments with overlying microbial mats. In addition, the increased rate of sulfate reduction and advective flow of organic material into the sediment can promote a more conducive environment for AOM [reviewed in (173)]. The predominance of ANME-related clones (regardless of sediment depth) and reported high rates of AOM (74) support this general hypothesis. In conclusion, this study represents some of the first molecular phylogenetic data describing the fraction of the metabolically active *Bacteria* and *Archaea* communities in GoM cold seep habitats. Such information provides insights into the interconnection and interdependency of the microbial populations residing in sediments associated with overlying mat communities dominated mainly by *Beggiatoa* spp.

4.6 Acknowledgements

This work was supported by National Science Foundation LExEn grant OCE-0085549. Support for submersible operations was provided by NOAA NURP and DOE NETL. We thank Captain, George Gunther, Craig Caddigan and the crews of the JSL submersible and R.V. *Seward Johnson II* for their invaluable assistance in sample collections. We also thank Cassie Hodges for excellent technical assistance.

CHAPTER 5

CONCLUSIONS

The northern Gulf of Mexico continental slope margin is an active geologic region that supports diverse chemosynthetic communities. Faults formed by rising subsurface salt diapirs provide conduits for gas and oil migration into the upper sediments and water column. The resulting cold seeps provide the necessary geochemistry to support diverse chemosynthetic communities. Located below the photic zone, the primary producers in this extreme environment ecosystem are symbiotic and free-living chemoautotrophic bacteria. Symbiotic thiotrophs and methanotrophs have been well characterized within the tissues of tube worms (*Lamellibrachia* sp. and *Escarpia* sp.) and mussels (*Bathymodiolus* sp.), respectively. However, to gain a better understanding of the microbial community extant at GoM cold seeps, the free living chemoautotrophic, as well as the heterotrophic microbial communities must be identified.

The focus of this study was to characterize the microbial community structure associated with GoM cold seeps. Two locales on the GoM continental slope were selected, GC185 and GC234. Both sites contained surface breaching gas hydrate mounds and orange- and white-pigmented microbial mats. Hydrate and microbial mat associated sediment samples were obtained on two separate research cruises, both utilizing the manned submersible *Johnson Sea Link*. The submersible provided the ability to obtain discrete samples using a specially designed hydrate drill and sediment push cores. These samples were utilized to complete one of the first molecular characterizations of the total microbial community and the first characterization of the active fraction of the microbial

community within three distinct layers of a surface breaching hydrate mound. In addition, this study is the first to characterize the active fraction of the microbial community down a depth profile in sediments associated with orange- and white-pigmented microbial mats. The archaeal clone libraries obtained from these samples make up one of the first reports of metabolically active *Archaea* from marine sediments. This study was also the first to utilize a hydrate drill to obtain stratified cores of surface-breeching gas hydrate.

All hydrate samples were recovered using a specially designed hydrate recovery chamber and a hydrate stabilization chamber. The hydrate recovery chamber (HRC) maintained ambient bottom water temperature (~7^{o}C) and pressure (~50 atm) to reduce the rapid dissociation of hydrates common to shipboard gravity and piston coring techniques. The hydrate stabilization chamber (HSC) provided a work platform with a surface temperature of <-30^{o}C, thus maintaining hydrate integrity during core dissection. Stabilized intact hydrate cores provided access to microbial communities at the three different hydrate layers. The large volume of sample obtained in the HRC allowed the extraction sufficient quality and quantity of RNA from intact interior hydrate.

The nineteen clone libraries obtained in this study have identified several unique clades with no closely related previously cultured isolates. In particular, the ANME-2 subdivision, within the order *Methanosarcinales,* was originally divided into three subgroups by Orphan et al. (122). Clone libraries from both the gas hydrate- and *Beggiatoa* sp. mat-associated sediments indicated a fourth subgroup denoted ANME-2D (108). This group was identified in both DNA- and RNA-derived libraries indicating both presence and metabolic activity of this group. Three additional groups of clones, denoted Unclassified *Euryarchaeota*, Unclassified *Bacteria* 1 and Unclassified *Bacteria* 2, were

detected within the sediment entrained hydrate and interior hydrate layers. In contrast to the ANME-2D subgroup, these clades were too distantly related to any previously identified group to provide supporting data to determine their role in the community. Such groups could be future bioprospecting targets to determine if resulting isolates are unique to the Gulf of Mexico or if they have any practical medical or industrial application.

Numerous cloned sequences obtained in this study were closely related to sequences previously identified from cold seeps at Eel River and Santa Barbara Basins and Cascadia Margin, and hydrothermal vents at Guaymus Basin. However, there were clones and clades that were unique to the Gulf of Mexico. Molecular analysis of *Beggiatoa* sp.-related clones indicated a potential divergence between GoM *Beggiatoa* sp. and Monterey Canyon *Beggiatoa* sp. corresponding to the rise of the Isthmus of Panama (109). In addition, novel clades, i.e, ANME-2D (108), Unclassified *Euryarchaeota*, Unclassified *Bacteria* 1 and Unclassified *Bacteria* 2, and distinct clusters, GoM SRB Group 5 and GoM SRB Group 6 (108), were reported in both archaeal and bacterial clone libraries from RNA- and DNA-derived clones. There is a current trend to assign biogeographical parameters to newly characterized microbial communities. Microbial biogeography attempts to identify microbes that are unique to a specific location. Whereas numerous clades and phylotypes appear to be GoM specific, more sequence comparisons using additional genes are required to begin to speculate on the potential GoM biogeography.

The purpose of this study was to characterize the microbial communities extant within GoM cold seep gas hydrates and microbial mat associated sediments. The latest

molecular techniques were used to isolate DNA and RNA, and subsequently construct and characterize clone libraries. As a result, novel clades and phylotypes in addition to well-characterized lineages were identified, providing a better understanding of the microbial community structure.

While insight was gained into the microbial component of the cold seep ecosystem, future research directions were identified that will guide studies in this and other extreme environments. Data presented in this study represented a single time point at two seep sites in the GoM. Additional sample dates and locations will determine if these microbial communities are subject to temporal and spatial variations. Clone libraries are inherently qualitative; therefore, using real time-PCR, or quantitative PCR, will provide data on the cell concentrations in the community within the individual lineages identified in this study. Additionally, attempts to cultivate and characterize representatives from the novel clades identified in this study will potentially determine their role in the community. Additionally, representatives from these novel clades could possess new metabolic processes potentially usefully in medical or industrial applications.

REFERENCES

[1] **Aharon, P. and B. Fu.** 2000. Microbial sulfate reduction rates and sulfur and oxygen isotope fractionations at oil and gas seeps in deepwater Gulf of Mexico. Geochim. Cosmochim. Acta. **64**:233-246.

[2] **Ahmad, A., J. P. Barry and D. C. Nelson.** 1999. Phylogenetic affinity of a wide, vacuolate, nitrate- accumulatlng *Beggiatoa* sp. from Monterey Canyon, California, with *Thioploca* spp. Appl. Environ. Microbiol. **65**:270-277.

[3] **Amann, R. I., W. Ludwig and K. H. Schleifer.** 1995. Phylogenetic identification and in situ detection of individual microbial cells without cultivation. Microbiol. Rev. **59**:143-169.

[4] **Andreassen, K., K. Hogstad and K. Berteussen.** 1990. Gas hydrate in the southern Barents Sea indicated by a shallow seismic anomaly. First Break **8**:235-245.

[5] **Baker, V. R., R. G. Strom, V. C. Gulick, J. S. Kargel, G. Komatsu and V. S. Kale.** 1991. Ancient oceans, ice sheets and the hydrological cycle on mars. Nature **352**:589-594.

[6] **Barry, J. P., H. G. Greene, D. L. Orange, C. H. Baxter and a. others.** 1996. Biologic and geologic characteristics of cold seeps in Monterey Bay, California. Deep-sea Res. I **43**:1739-1762.

[7] **Baud, R. D., R. H. Peterson, G. Doyle and G. Richardson**. 2000. Deepwater Gulf of Mexico: America's emerging frontier. US Department of the Interior,

Mineral Management Service, Gulf of Mexico OCS Regional Office. OCS Report MMS 2000-022, New Orleans.

[8] **Bergquist, D. C., F. M. Williams and C. R. Fisher.** 2000. Longevity record for deep-sea invertebrate - The growth rate of a marine tubeworm is tailored to different environments. Nature **403**:499-500.

[9] **Bidle, K. A., M. Kastner and D. H. Bartlett.** 1999. A phylogenetic analysis of microbial communities associated with methane hydrate containing marine fluids and sediments in the Cascadia margin (ODP site 892B). FEMS Microbiol. Lett. **177**:101-8.

[10] **Boetius, A., K. Ravenschlag, C. J. Schubert, D. Rickert, F. Widdel, A. Gieseke, R. Amann, B. B. Jorgensen, U. Witte and O. Pfannkuche.** 2000. A marine microbial consortium apparently mediating anaerobic oxidation of methane. Nature **407**:623-626.

[11] **Boone, D. R., I. M. Mathrani, Y. T. Liu, J. Menaia, R. A. Mah and J. E. Boone.** 1993. Isolation and characterization of *Methanohalophilus portucalensis* sp nov and DNA reassociation study of the genus *Methanohalophilus*. Int. J. Syst. Bacteriol. **43**:867-867.

[12] **Brooks, J. M., H. B. Cox, W. R. Bryant, M. C. Kennicutt, R. G. Mann and T. J. McDonald.** 1986. Association of gas hydrates and oil seepage in the Gulf of Mexico. Org. Geochem. **10**:221-234.

[13] **Brooks, J. M., M. C. Kennicutt, R. R. Fay, T. J. McDonald and R. Sassen.** 1984. Thermogenic gas hydrates in the Gulf of Mexico. Science **225**:409-411.

[14] **Brooks, J. M., M. C. Kennicutt, C. R. Fisher, S. A. Macko, K. Cole, J. J. Childress, R. R. Bidigare and R. D. Vetter.** 1987. Deep-sea hydrocarbon seep communities - evidence for energy and nutritional carbon sources. Science **238**:1138-1142.

[15] **Buffett, B. A.** 2000. Clathrate hydrates. Annu. Rev. Earth Planet. Sci. **28**:477-507.

[16] **Carney, R. S.** 1994. Consideration of the oasis analogy for chemosynthetic communities at Gulf of Mexico. Organ. Geochem. **10**:221-234.

[17] **Cary, S. C., C. R. Fisher and H. Felbeck.** 1988. Mussel growth supported by methane as sole carbon and energy-source. Science **240**:78-80.

[18] **Cavanaugh, C. M., S. L. Gardiner, M. L. Jones, H. W. Jannasch and J. B. Waterbury.** 1981. Prokaryotic cells in the hydrothermal vent tube worm *Riftia pachyptila* Jones - possible chemoautotrophic symbionts. Science **213**:340-342.

[19] **Chand, S. and T. A. Minshull.** 2003. Seismic constraints on the effects of gas hydrate on sediment physical properties and fluid flow: a review. Geofluids **3**:275-289.

[20] **Chao, A.** 1987. Estimating the population size for capture-recapture data with unequal catchability. **43**:783-791.

[21] **Charlou, J. L., J. P. Donval, T. Zitter, N. Roy, P. Jean-Baptiste, J. P. Foucher and J. Woodside.** 2003. Evidence of methane venting and geochemistry of brines on mud volcanoes of the eastern Mediterranean Sea. Deep-sea Res. I **50**:941-958.

[22] **Childress, J. J., C. R. Fisher, J. M. Brooks, M. C. Kennicutt, R. Bidigare and A. E. Anderson.** 1986. A methanotrophic marine molluscan (*Bivalvia*, *Mytilidae*) symbiosis - mussels fueled by gas. Science **233**:1306-1308.

[23] **Clennell, M. B., M. Hovland, J. S. Booth, P. Henry and W. J. Winters.** 1999. Formation of natural gas hydrates in marine sediments I. Conceptual model of gas hydrate growth conditioned by host sediment properties. J. Geophys. Res. **104**:22985-23003.

[24] **Coleman, D. D., J. B. Risatti and M. Schoell.** 1981. Fractionation of carbon and hydrogen isotopes by methane-oxidizing bacteria. Geochim. Cosmo. Acta. **45**:1033-1037.

[25] **Collett, T. S.** 1997. Resource potential of marine and permafrost associated gas hydrates, p. 51 *In* Oceanic gas hydrate: guidance for research and parogrammatic development at the Naval Research Laboratory, Max, M.D., Pallenbarg, R.E. and Rath, B.B. (eds.), Proceedings Workshop Naval Research Laboratory Gas Hydr. Research Progress. Washington, D.C.

[26] **Colwell, R. K.** 1997. EstimateS: Statistical estimation of species richness and shared species from samples. Version 5. User's Guide and application published at: http://viceroy.eeb.uconn.edu/estimates.

[27] **Colwell, R. K. and J. A. Coddington.** 1994. Estimating terrestrial biodiversity through extrapolation. **345**:101-118.

[28] **Conway, N. M., M. C. Kennicutt and C. L. Van Dover**. 1994. Stable isotopes in the study of marine chemosynthetic-based ecosystems., p. 158-186 *In* Stable

Isotopes in Ecology and Environmental Science, Lajtha, K. and Michener, R.H. (eds.), Blackwell, Oxford.

[29] **Daly, K., R. J. Sharp and A. J. McCarthy.** 2000. Development of oligonucleotide probes and PCR primers for detecting phylogenetic subgroups of sulfate-reducing bacteria. Microbiol. **146**:1693-705.

[30] **Dando, P. R., M. C. Austen, R. A. Burke, M. A. Kendall, M. C. Kennicutt, A. G. Judd, D. C. Moore, S. C. M. Ohara, R. Schmaljohann and A. J. Southward.** 1991. Ecology of a North Sea pockmark with an active methane seep. Mar. Ecol. Prog. Ser. **70**:49-63.

[31] **De Beukelaer, S. M., I. R. MacDonald, N. L. Guinasso and J. A. Murray.** 2003. Distinct side-scan sonar, RADARSAT SAR, and acoustic profiler signatures of gas and oil seeps on the Gulf of Mexico slope. Geo-Mar. Lett. **23**:177-186.

[32] **Dell'anno, A., M. Fabiano, G. C. A. Duineveld, A. Kok and R. Danovaro.** 1998. Nucleic acid (DNA, RNA) quantification and RNA/DNA ratio determination in marine sediment: Comparison of spectophotometric, fluorometric, and high performance liquid chromatography methods and estimation of detrital DNA. Appl Environ Microbiol **64**:3238-3245.

[33] **DeLong, E. F.** 1992. Archaea in coastal marine environments. Proc. Natl. Acad. Sci. USA **89**:5685-5689.

[34] **Derakshani, M., T. Lukow and W. Liesack.** 2001. Novel bacterial lineages at the (sub)division level as detected by signature nucleotide-targeted recovery of

16S rRNA genes from bulk soil and rice roots of flooded rice microcosms. Appl. Environ. Microbiol. **67**:623-631.

[35] **Devereux, R., M. D. Kane, J. Winfrey and D. A. Stahl.** 1992. Genus- and group-specfic hybridization probes for determinative and environmental studies of sulfate-reducing bacteria. Appl Environ Microbiol **15**:601-609.

[36] **Di Meo, C. A., A. E. Wilbur, W. E. Holben, R. A. Feldman, R. C. Vrijenhoek and S. C. Cary.** 2000. Genetic variation among endosymbionts of widely distributed vestimentiferan tubeworms. Appl. Environ. Microbiol. **66**:651-658.

[37] **Dickens, G. R., C. K. Paull and P. Wallace.** 1997. Direct measurement of in situ methane quantities in a large gas-hydrate reservoir. Nature **385**:426-428.

[38] **Distel, D. L., H. Felbeck and C. M. Cavanaugh.** 1994. Evidence for phylogenetic congruence among sulfur-oxidizing chemoautotrophic bacterial endosymbionts and their bivalve hosts. J. Bacteriol. **38**:533-542.

[39] **Dobrynin, V. M., Y. P. Korotajev and D. V. Plyuschev**. 1981. Gas hydrates - a possible energy resource. p. 727-729 *In* Long-Term Energy Resources., Meyer, R.F. and Olson, J.C. (eds.), Pitman, Boston.

[40] **Eggen, R., H. Harmsen, A. Geerling and W. M. Devos.** 1989. Nucleotide sequence of a 16s ribosomal-RNA encoding gene from the *Archaebacterium methanothrix-soehngenii*. Nucleic Acids Res. **17**:9469-9469.

[41] **Eichhubl, P., H. G. Greene, T. Naehr and N. Maher.** 2000. Structural control of fluid flow: offshore fluid seepage in the Santa Barbara Basin, California. J. Geochem. Explor. **69**:545-549.

[42] **Felbeck, H., J. J. Childress and G. N. Somero.** 1981. Calvin-Benson cycle and sulfide oxidation enzymes in animals from sulfide-rich habitats. Nature (London) **293**:291-293.

[43] **Fisher, C. R.** 1990. Chemoautotrophic and methanotrophic symbioses in marine invertebrates. Rev. Aquatic Sci. **2**:399-436.

[44] **Fisher, C. R. and J. J. Childress.** 1992. Organic carbon transfer from methanotrophic symbionts to the host hydrocarbon seep mussel. Symbiosis **12**:221-235.

[45] **Fisher, C. R., I. R. MacDonald, R. Sassen, C. M. Young, S. A. Macko, S. Hourdez, R. S. Carney, S. Joye and E. McMullin.** 2000. Methane ice worms: *Hesiocaeca methanicola* colonizing fossil fuel reserves. **87**:184-187.

[46] **Fisher, C. R., I. A. Urcuyo, M. A. Simpkins and E. R. Nix.** 1996. Mar. Ecol. **18**:83-94.

[47] **Formolo, M. J., T. W. Lyons, C. L. Zhang, C. Kelley, R. Sassen, J. Horita and D. R. Cole.** 2004. Quantifying carbon sources in the formation of authigenic carbonates at gas hydrate sites in the Gulf of Mexico. **205**:253-264.

[48] **Fossing, H., V. A. Gallardo, B. B. Jorgensen, M. Huttel, L. P. Nielsen, H. Schulz, D. E. Canfield, S. Forster, R. N. Glud, J. K. Gundersen, J. Kuver, N. B. Ramsing, A. Teske, B. Thamdrup and O. Ulloa.** 1995. Concentration and transport of nitrate by the mat-forming sulfur bacterium *Thioploca*. Nature **374**:713-715.

[49] **Freytag, J. K., P. R. Girguis, D. C. Bergquist, J. P. Andras, J. J. Childress and C. R. Fisher.** 2001. A paradox resolved: Sulfide acquisition by roots of seep

tubeworms sustains net chemoautotrophy. Proc. Nat. Acad. Sci. USA **98**:13408-13413.

[50] **Fuerst, J. A.** 1995. The *Planctomycetes* - Emerging models for microbial ecology, evolution and cell biology. Microbiol. UK **141**:1493-1506.

[51] **Fujiwara, Y., C. Kato, N. Masui, K. Fujikura and S. Kojima.** 2001. Dual symbiosis in the cold-seep thyasirid clam *Maorithyas hadalis* from the hadal zone in the Japan Trench, western Pacific. Mar. Ecol.-Prog. Ser. **214**:151-159.

[52] **Gei, D. and J. M. Carcione.** 2003. Acoustic properties of sediments saturated with gas hydrate, free gas and water. Geophys. Prospect. **51**:141-157.

[53] **Goldhaber, M. B. and I. R. Kaplan.** 1974. The sulfur cycle. The Sea **5**:569-655.

[54] **Good, I. J.** 1953. The population frequencies of species and the estimation of population parameters. Biometrika **40**:237-264.

[55] **Grauls, D.** 2001. Gas hydrates: importance and applications in petroleum exploration. Mar. Petrol. Geol. **18**:519-523.

[56] **Gustafson, R. G., R. D. Turner, R. A. Lutz and R. C. Vrijenhoek.** 1998. A new genus and five new species of mussels (*Bivalvia*, *Mytilidae*) from deep-sea sulfide/hydrocarbon seeps in the Gulf of Mexico. Malacologia **40**:63-112.

[57] **Hall, T. A.** 1999. BioEdit: a user-friendly biological sequence alignment editor and analysis program for Windows 95/98/NT. Nucl. Acids Symp. Ser. **41**:95-98.

[58] **Handa, Y. P., M. Zakrzewski and C. Fairbridge.** 1992. Effect of restricted geometries on the structure and thermodynamic properties of ice. J. Chem. Phys. **96**:8594-8599.

[59] **Haug, G. H. and R. Tiedemann.** 1998. Effect of the formation of the Isthmus of Panama on Atlantic Ocean thermohaline circulation. Nature **393**:673-676.

[60] **Heck, K. L., G. v. Belle and D. Simberloff.** 1975. Explict calculation of the rarefaction diversity measurement and the determination of sufficient sample size. Ecol. **56**:1459-1461.

[61] **Hernandez-Eugenio, G., M. L. Fardeau, J. L. A. Cayol, B. K. C. Patel, P. Thomas, H. Macarie, J. L. Garcia and B. Ollivier.** 2002. *Clostridium thiosulfatireducens* sp. nov., a proteolytic, thiosulfate- and sulfur-reducing bacterium isolated from an upflow anaerobic sludge blanket (UASB) reactor. Int. J. Syst. Evol. Microbiol. **52**:1461-1468.

[62] **Hinrichs, K. U., J. M. Hayes, S. P. Sylva, P. G. Brewer and E. F. DeLong.** 1999. Methane-consuming archaebacteria in marine sediments. Nature **398**:802-805.

[63] **Hoehler, T. M., M. J. Alperin, D. B. Albert and C. S. Martens.** 1994. Field and laboratory studies of methane oxidation in an anoxic marine sediment - evidence for a methanogen-sulfate reducer consortium. Glob. Biogeochem. Cycle **8**:451-463.

[64] **Holder, G. D. and J. H. Hand.** 1982. Multiple phase equilibria in hydrates from methane, ethane, propane and water mixtures. Aiche J. **28**:440-447.

[65] **Huber, J. A., D. A. Butterfield and J. A. Baross.** 2002. Temporal changes in archaeal diversity and chemistry in a mid-ocean ridge subseafloor habitat. Appl. Environ. Microbiol. **68**:1585-94.

[66] **Hurt, R. A., X. Y. Qiu, L. Y. Wu, Y. Roh, A. V. Palumbo, J. M. Tiedje and J. H. Zhou.** 2001. Simultaneous recovery of RNA and DNA from soils and sediments. Appl. Environ. Microbiol. **67**:4495-4503.

[67] **Inagaki, F., Y. Sakihama, A. Inoue, C. Kato and K. Horikoshi.** 2002. Molecular phylogenetic analyses of reverse-transcribed bacterial rRNA obtained from deep-sea cold seep sediments. Environ. Microbiol. **4**:277-286.

[68] **Inagaki, F., M. Suzuki, K. Takai, H. Oida, T. Sakamoto, K. Aoki, K. H. Nealson and K. Horikoshi.** 2003. Microbial communities associated with geological horizons in coastal subseafloor sediments from the Sea of Okhotsk. Appl. Environ. Microbiol. **69**:7224-7235.

[69] **Iversen, N. and B. B. Jorgensen.** 1985. Anaerobic methane oxidation rates at the sulfate-methane transition sediments from the Kattegat and Skagerrack (Denmark). Limnol. Oceanogr. **30**:944-955.

[70] **Jakobsen, M., T. A. Johansen and B. O. Ruud.** 2001. Modeled velocity and reflectivity properties of anisotropic hydrated sediments. J. Comp. Acoustics **9**:1507-1522.

[71] **James, A. T. and B. J. Burns.** 1984. Microbial alteration of subsurface natural gas accumulations. Aapg Bull. Amer. Assoc. Petrol. Geologists **68**:957-960.

[72] **Jeffery, G. A. and R. K. McMullan.** 1967. The clatherate hydrates. Prog. Inorg. Chem. **8**:43-108.

[73] **Johnson, J. L.** 1994. Similarity analysis of rRNAs, p. 683-700 *In* Methods for general and molecular bacteriology, Gerhardt, P., Murray, R.G.E., Wood, W.A. and Krieg, N.R. (eds.), American Society for Microbiology, Washington, D.C.

[74] **Joye, S. B., A. Boetius, B. N. Orcutt, J. P. Montoya, H. Schulz, M. J. Erickson and S. K. Lugo.** 2004. The anaerobic oxidation of methane and sulfate reduction in sediments from Gulf of Mexico cold seeps. Chem. Geol. **205**:219-238.

[75] **Julian, D., F. Gaill, E. Wood, A. J. Arp and C. R. Fisher.** 1999. Roots as a site of hydrogen sulfide uptake in the hydrocarbon seep vestimentiferan *Lamellibrachia* sp. J. Exper. Biol. **202**:2245-2257.

[76] **Kastner, M., K. A. Kvenvolden and T. D. Lorenson.** 1998. Chemistry, isotopic composition, and origin of a methane-hydrogen sulfide hydrate at the Cascadia subduction zone. Earth Planet. Sci. Lett. **156**:173-183.

[77] **Katz, D. L., R. Cornell, R. Kobayashi, F. H. Poettmann, J. A. Vary, J. R. Elenblass and C. G. Weinaug**. 1959. Handbook of Natural Gas Engineering. McGraw-Hill, New York.

[78] **Kennicutt, M. C., J. M. Brooks, R. R. Bidigare, R. R. Fay, T. L. Wade and T. J. McDonald.** 1985. Vent type taxa in a hydrocarbon seep region on the Louisiana Slope. Nature **317**:351-353.

[79] **Kennicutt, M. C., J. M. Brooks and G. J. Denoux.** 1988. Leakage of deep, reservoired petroleum to the near surface on the Gulf of Mexico continental slope. Mar. Chem. **24**:39-59.

[80] **Khokhar, A. A., J. S. Gudmundsson and E. D. Sloan.** 1998. Gas storage in structure H hydrates. Fluid Phase Equil. **151**:383-392.

[81] **Kochevar, R. E., J. J. Childress, C. R. Fisher and E. Minnich.** 1992. The methane mussel - Roles of symbiont and host in the metabolic utilization of methane. Mar. Biol. **112**:389-401.

[82] **Kojima, S., T. Hashimoto, M. Hasegawa, S. Murata, S. Ohta, H. Seki and N. Okada.** 1993. Close phylogenetic relationship between *Vestimentifera* (Tube Worms) and *Annelida* revealed by the amino acid sequence of Elongation Factor-1-Alpha. J. Mol. Evol. **37**:66-70.

[83] **Krason, J., P. Finley and B. Rudloff**. 1985. Geological evolution and analysis of confirmed or suspected gas hydrate localities. *In* Basin Analysis, Formation and Stability of Gas Hydrates in the Western Gulf of Mexico.(eds.), US Department of Energy, Washington.

[84] **Kvenvolden, K. A.** 1988. Methane hydrate - a major reservoir of carbon in the shallow geosphere. Chem. Geol. **71**:41-51.

[85] **Kvenvolden, K. A.** 1993. Gas hydrates - Geological perspective and global shange. Rev. Geophys. **31**:173-187.

[86] **Kvenvolden, K. A.** 1999. Potential effects of gas hydrate on human welfare. PNAS USA **96**:3420-3426.

[87] **Kvenvolden, K. A., P. R. Carlson, A. Warden and C. N. Threlkeld.** 1998. Carbon isotopic comparisons of oil products used in the developmental history of Alaska. Chem. Geol. **152**:73-84.

[88] **Lanoil, B. D., R. Sassen, M. T. La Duc, S. T. Sweet and K. H. Nealson.** 2001. *Bacteria* and *Archaea* physically associated with Gulf of Mexico gas hydrates. Appl. Environ. Microbiol. **67**:5143-5153.

[89] **Larkin, J., P. Aharon and M. C. Henk.** 1994. *Beggiatoa* in microbial mats at hydrocarbon vents in the Gulf of Mexico and warm mineral spring, Florida. Geo-Mar. Lett. **14**:97-103.

[90] **Larkin, J. M. and W. R. Strohl.** 1983. *Beggiatoa*, *Thiothrix*, and *Thioploca*. Ann. Rev. Microbiol. **37**:341-367.

[91] **Lashof, D. A. and D. R. Ahuja.** 1990. Relative contributions of greenhouse gas emissions to global warming. Nature **344**:529-531.

[92] **Liesack, W. and E. Stackebrandt.** 1992. Occurrence of novel groups of the domain *Bacteria* as revealed by analysis of genetic material isolated from an Australian terrestrial environment. J. Bacteriol. **174**:5072-5078.

[93] **Lorenson, T. D. and T. S. Collett.** 2000. Gas content and compostion of gas hydrate from sediments of the southeastern North American continental margin. Proc. Ocean Drill. Prog., Sci. Results **164**:37-46.

[94] **Lunine, J. I. and D. J. Stevenson.** 1987. Clathrate and ammonia hydrates at high-pressure - Application to the origin of methane on Titan. Icarus **70**:61-77.

[95] **MacAvoy, S. E., S. A. Macko and S. B. Joye.** 2002. Fatty acid carbon isotope signatures in chemosynthetic mussels and tube worms from Gulf of Mexico hydrdocarbon seep communities. Chem. Geol. **185**:1-8.

[96] **MacDonald, I. R., G. S. Boland, J. S. Baker, J. M. Brooks, M. C. Kennicutt and R. R. Bidigare.** 1989. Gulf of Mexico hydrocarbon seep communities II. Spatial distribution of seep organisms and hydrocarbons at Bush Hill. Mar. Biol. **101**:235-247.

[97] **MacDonald, I. R., N. L. Guinasso, R. Sassen, J. M. Brooks, L. Lee and K. T. Scott.** 1994. Gas hydrate that breaches the sea-floor on the continental slope of the Gulf of Mexico. Geology **22**:699-702.

[98] **MacDonald, I. R., J. F. Reilly, N. L. Guinasso, J. M. Brooks, R. S. Carney, W. A. Bryant and T. J. Bright.** 1990. Chemosynthetic mussels at a brine-filled pockmark in the northern Gulf of Mexico. Science **248**:1096-1099.

[99] **Maidak, B. L., J. R. Cole, C. T. Parker Jr., G. M. Garrity, N. Larsen, B. Li, T. G. Lilburn, M. J. McCaughey, G. J. Olsen, R. Overbeek, S. Pramanik, T. M. Schmidt, J. M. Tiedje and C. R. Woese.** 1999. A new version of the RDP (Ribosomal Database Project). Nucleic Acids Res. **27**:171-173.

[100] **Marchesi, J. R., A. J. Weightman, B. A. Cragg, R. J. Parkes and J. C. Fry.** 2001. Methanogen and bacterial diversity and distribution in deep gas hydrate sediments from the Cascadia Margin as revealed by 16S rRNA molecular analysis. FEMS Microbiol. Ecol. **34**:221-228.

[101] **Martin, A. P.** 2002. Phylogenetic approaches for describing and comparing the diversity of microbial communities. **68**:3673-3682.

[102] **Masuzawa, T., N. Handa, H. Kitagawa and M. Kusakabe.** 1992. Sulfate reduction using methane in sediments beneath a *Bathyal* cold seep giant clam community off Hatsushima Island, Sagami Bay, Japan. Earth Planet. Sci. Lett. **110**:39-50.

[103] **McHatton, S. C., J. P. Barry, H. W. Jannasch and D. C. Nelson.** 1996. High nitrate concentrations in vacuolate, autotrophic marine *Beggiatoa* spp. Appl. Environ. Microbiol. **62**:954-958.

[104] **Mechichi, T., M. L. Fardeau, M. Labat, J. L. Garcia, F. Verhe and B. K. C. Patel.** 2000. *Clostridium peptidivorans* sp. nov., a peptide-fermenting bacterium

from an olive mill wastewater treatment digester. Int. J. Syst. Evol. Microbiol. **50**:1259-1264.

[105] **Milkov, A. V. and R. Sassen.** 2000. Thickness of the gas hydrate stability zone, Gulf of Mexico continental slope. Mar. Pet. Geol. **17**:981-991.

[106] **Milkov, A. V. and R. Sassen.** 2001. Estimate of gas hydrate resource, northwestern Gulf of Mexico continental slope. Mar. Geol. **179**:71-83.

[107] **Miller, D. N., J. E. Bryant, E. L. Madsen and W. C. Ghiorse.** 1999. Evaluation and optimization of DNA extraction and purification procedures for soil and sediment samples. Appl. Environ. Microbiol. **65**:4715-24.

[108] **Mills, H. J., C. Hodges, K. Wilson, I. R. MacDonald and P. A. Sobecky.** 2003. Microbial diversity in sediments associated with surface-breaching gas hydrate mounds in the Gulf of Mexico. FEMS Microbiol. Ecol. **46**:39-52.

[109] **Mills, H. J., R. M. Martinez, S. Story and P. Sobecky.** 2004. Phylogenetic analysis of active microbial populations associated with exposed gas hydrate in the Gulf of Mexico. Appl. Environ. Microbiol. In press.

[110] **Moeseneder, M. M., C. Winter, J. M. Arrieta and G. J. Herndl.** 2001. Terminal-restriction fragment length polymorphism (T-RFLP) screening of a marine archaeal clone library to determine the different phylotypes. J. Microbiol. Meth. **44**:159-172.

[111] **Mullins, T. D., T. B. Britschgi, R. I. Krest and S. J. Giovannoni.** 1995. Genetic comparisons reveal the same unknown bacterial lineages in Atlantic and Pacific bacterioplankton communities. Limnol. Oceano. **40**:148-158.

[112] **Munson, M. A., D. B. Nedwell and T. M. Embley.** 1997. Phylogenetic diversity of *Archaea* in sediment samples from a coastal salt marsh. Appl. Environ. Microbiol. **63**:4729-4733.

[113] **Nei, M.** 1987. Molecular Evolutionary Genetics. Columbia University Press, New York.

[114] **Nelson, D. C. and C. R. Fisher**. 1995. Chemoautotrophic and methanotrophic endosymbiotic bacteria at deep-sea vent and seeps, p. 125-167 *In* The microbiology of deep-sea hydrothermal vents, Karl, D.M. (eds.), CRC Press. Boca Raton, FL.

[115] **Nelson, D. C., C. O. Wirsen and H. W. Jannasch.** 1989. Characterization of large, autotrophic *Beggiatoa* spp abundant at hydrothermal vents of the Guaymas Basin. Appl. Microbiol. Ecol. **55**:2909-2917.

[116] **Nikolaus, R., J. W. Ammerman and I. R. MacDonald.** 2003. Distinct pigmentation and trophic modes in *Beggiatoa* from hydrocarbon seeps in the Gulf of Mexico. Aquatic Micro. Ecol. **32**:85-93.

[117] **Nisbet, E. G.** 1990. The end of the ice-age. Can. J. Earth Sci. **27**:148-157.

[118] **Nisbet, E. G.** 1992. Sources of atmospheric CH_4 in early postglacial time. J. Geophys. Res.-Atmos. **97**:12859-12867.

[119] **Nix, E. R., C. R. Fisher, J. Vodenichar and K. M. Scott.** 1995. Physiological ecology of a mussel with methanotrophic endosymbionts at 3 hydrocarbon seep sites in the Gulf of Mexico. **122**:605-617.

[120] **Nogales, B., E. R. B. Moore, W.-R. Abraham and K. N. Timmis.** 1999. Identification of the metabolically active members of a bacterial community in a polychlorinated biphenyl-polluted moorland soil. Environ. Microbiol. **1**:199-212.

[121] **Orcutt, B. N., A. Boetius, S. K. Lugo, I. R. Macdonald, V. A. Samarkin and S. Joye.** 2004. Life at the edge of methane ice: microbial cycling of carbon and sulfur in Gulf of Mexico gas hydrates. Chem. Geol. **205**:239-251.

[122] **Orphan, V. J., K. U. Hinrichs, W. Ussler, 3rd, C. K. Paull, L. T. Taylor, S. P. Sylva, J. M. Hayes and E. F. Delong.** 2001. Comparative analysis of methane-oxidizing archaea and sulfate-reducing bacteria in anoxic marine sediments. Appl. Environ. Microbiol. **67**:1922-1934.

[123] **Orphan, V. J., C. H. House, K. U. Hinrichs, K. D. McKeegan and E. F. DeLong.** 2001. Methane-consuming archaea revealed by directly coupled isotopic and phylogenetic analysis. Science **293**:484-7.

[124] **Orphan, V. J., C. H. House, K. U. Hinrichs, K. D. McKeegan and E. F. DeLong.** 2002. Direct phylogenetic and isotopic evidence for multiple groups of archaea involved in the anaerobic oxidation of methane. Geochim. Cosmochim. Acta **66**:A571-A571.

[125] **Orphan, V. J., C. H. House, K. U. Hinrichs, K. D. McKeegan and E. F. DeLong.** 2002. Multiple archaeal groups mediate methane oxidation in anoxic cold seep sediments. Proc. Natl. Acad. Sci. U.S.A. **99**:7663-7668.

[126] **Otte, S., J. G. Kuenen, L. P. Nielsen, H. W. Paerl, J. Zopfi, H. N. Schulz, A. Teske, B. Strotmann, V. A. Gallardo and B. B. Jorgensen.** 1999. Nitrogen,

carbon, and sulfur metabolism in natural *Thioploca* samples. Appl. Environ. Microbiol. **65**:3148-3157.

[127] **Paull, C. K., W. J. Buelow, W. Ussler and W. S. Borowski.** 1996. Increased continental-margin slumping frequency during sea-level lowstands above gas hydrate-bearing sediments. Geol. **24**:143-146.

[128] **Paull, C. K., W. Ussler and W. P. Dillon.** 1991. Is the extent of glaciation limited by marine gas hydrates. Geophys. Res. Lett. **18**:432-434.

[129] **Peel, F. J., C. J. Travis and J. R. Hossack**. 1995. Genetic structural provinces and salt tectonics of the Cenozoic offshore US Gulf of Mexico: a preliminary analysis. p. 153-175 *In* Salt Tectonics: A Global Perspecitive, Jackson, M.P.A., Roberts, D.G. and Snelson, S. (eds.), Am. Assoc. Pet. Geol. Mem. Washington.

[130] **Perriere, G. and M. Gouy.** 1996. WWW-query: an on-line retrieval system for biological sequence banks. Biochimie **78**:364-369.

[131] **Powers, L. G., H. J. Mills, A. V. Palumbo, C. L. Zhang, K. Delaney and P. Sobecky.** 2002. Introduction of a plasmid-encoded *phoA* gene for constitutive overproduction of alkaline phosphatase in three subsurface *Pseudomonas* isolates. FEMS Microbiol. Ecol. **41**:115-123.

[132] **Radjasa, O. K., H. Urakawa, K. Kita-Tsukamoto and K. Ohwada.** 2001. Characterization of psychrotrophic bacteria in the surface and deep-sea waters from the northwestern Pacific Ocean based on 16S ribosomal DNA analysis. Mar. Biotechnol. **3**:454-462.

[133] **Reeburgh, W. S.** 1980. Anaerobic methane oxidation - Rate depth distributions in Skan Bay sediments. Earth Planet. Sci. Lett **47**:345-352.

[134] **Reed, D. W., Y. Fujita, M. E. Delwiche, D. B. Blackwelder, P. P. Sheridan, T. Uchida and F. S. Colwell.** 2002. Microbial communities from methane hydrate-bearing deep marine sediments in a forearc basin. Appl. Environ. Microbiol. **68**:3759-3770.

[135] **Reysenbach, A. L., K. Longnecker and J. Kirshtein.** 2000. Novel bacterial and archaeal lineages from an in situ growth chamber deployed at a Mid-Atlantic Ridge hydrothermal vent. Appl. Environ. Microbiol. **66**:3798-806.

[136] **Ripmeester, J. A., J. S. Tse, C. I. Ratcliffe and B. M. Powell.** 1987. A new clathrate hydrate structure. Nature **325**:135.

[137] **Rothwell, R. G., J. Thomson and G. Kahler.** 1998. Low-sea-level emplacement of a very large Late Pleistocene 'megaturbidite' in the western Mediterranean Sea. Nature **392**:377-380.

[138] **Rowan, M. G., M. P. A. Jackson and B. D. Trudgill.** 1999. Salt-related fault families and fault welds in the northern Gulf of Mexico. Aapg Bull. Amer. Assoc. Petrol. Geologists **83**:1454-1484.

[139] **Sager, W. W., C. S. Lee, I. R. Macdonald and W. W. Schroeder.** 1999. High-frequency near-bottom acoustic reflection signatures of hydrocarbon seeps on the Northern Gulf of Mexico continental slope. Geo-Mar. Lett. **18**:267-276.

[140] **Salvador, A.** 1987. Late Triassic-Jurassic paleogeography and origin of Gulf of Mexico Basin. Aapg Bull.-Amer. Assoc. Petrol. Geologists **71**:419-451.

[141] **Sassen, R., J. M. Brooks, M. C. Kennicutt, I. R. Macdonald and N. L. Guinasso.** 1993. How oil seeps, discoveries relate in deep-water Gulf of Mexico. Oil Gas J. **91**:64-69.

[142] **Sassen, R., S. Joye, S. T. Sweet, D. A. DeFreitas, A. V. Milkov and I. R. MacDonald.** 1999. Thermogenic gas hydrates and hydrocarbon gases in complex chemosynthetic communities, Gulf of Mexico continental slope. Organ. Geochem. **30**:485-497.

[143] **Sassen, R., S. L. Losh, L. Cathles III, H. H. Roberts, J. K. Whelan, A. V. Milkov, S. T. Sweet and D. A. DeFreitas.** 2001. Massive vein-filling hydrate: relation to ongoing gas migration from the deep subsurface in the Gulf of Mexico. Mar. Pet. Geol. **18**:551-560.

[144] **Sassen, R. and I. R. MacDonald.** 1997. Hydrocarbons of experimental and natural gas hydrates, Gulf of Mexico continental slope. Org. Geochem. **26**:289-293.

[145] **Sassen, R., I. R. MacDonald, N. L. Guinasso, S. Joye, A. G. Requejo, S. T. Sweet, J. Alcala-Herrera, D. DeFreitas and D. R. Schink.** 1998. Bacterial methane oxidation in sea-floor gas hydrate: Significance to life in extreme environments. Geol. **26**:851-854.

[146] **Sassen, R., I. R. MacDonald, A. G. Requejo, N. L. Guinasso, M. C. Kennicutt, S. T. Sweet and J. M. Brooks.** 1994. Organic geochemistry of sediments from chemosynthetic communities, Gulf of Mexico slope. **14**:110-119.

[147] **Sassen, R., A. V. Milkov, H. H. Roberts, S. T. Sweet and D. A. DeFreitas.** 2003. Geochemical evidence of rapid hydrocarbon venting from a seafloor-piercing mud diapir, Gulf of Mexico continental shelf. Mar. Geol. **198**:319-329.

[148] **Sassen, R., H. H. Roberts, P. Aharon, J. Larkin, E. W. Chinn and R. Carney.** 1993. Chemosynthetic bacterial mats at cold hydrocarbon seeps, Gulf of Mexico continental slope. Organ. Geochem. **20**:77-78.

[149] **Sassen, R., S. T. Sweet, A. V. Milkov, D. A. DeFreitas and M. C. Kennicutt.** 2001. Thermogenic vent gas and gas hydrate in the Gulf of Mexico slope: Is gas hydrate decomposition significant? Geol. **29**:107-110.

[150] **Sassen, R., S. T. Sweet, A. V. Milkov, D. A. DeFreitas, G. G. Salata and E. C. McDade.** 1999. Geology and geochemistry of gas hydrates, central Gulf of Mexico continental slope. Trans. Gulf Coast Assoc. Geol. Soc. **49**:462-468.

[151] **Sayama, M.** 2001. Presence of nitrate-accumulating sulfur bacteria and their influence on nitrogen cycling in a shallow coastal marine sediment. Appl. Environ. Microbiol. **67**:3481-3487.

[152] **Schlesner, H.** 1994. The development of media suitable for the microorganisms morphologically resembling *Planctomyces* spp, *Pirellula* spp, and other *Planctomycetales* from various aquatic habitats using dilute media. Syst. Appl. Microbiol. **17**:135-145.

[153] **Schmid, M., U. Twachtmann, M. Klein, M. Strous, S. Juretschko, M. Jetten, J. W. Metzger, K. H. Schleifer and M. Wagner.** 2000. Molecular evidence for genus level diversity of bacteria capable of catalyzing anaerobic ammonium oxidation. Syst. Appl. Microbiol. **23**:93-106.

[154] **Schneider, S., D. Roessli and L. Excoffier**, Arlequin ver. 2.000: A software for poulation genetics data analysis. 2000, Genetics and Biometry Laboratory: University of Geneva, Switzerland.

[155] **Slatkin, M.** 1991. Inbreeding coefficients and coalescence times. **58**:167-175.

[156] **Sloan, E. D.** 1998. Clatherate Hydrates of Natural Gases. Dekker, New York.

[157] **Smith, E. B., K. M. Scott, E. R. Nix, C. Korte and C. R. Fisher.** 2000. Growth and condition of seep mussels (*Bathymodiolus childressi*) at a Gulf of Mexico brine pool. Ecol. **81**:2392-2403.

[158] **Sobecky, P. A., T. J. Mincer, M. C. Chang and D. R. Helinski.** 1997. Plasmids isolated from marine sediment microbial communities contain replication and incompatibility regions unrelated to those of known plasmid groups. **63**:888-895.

[159] **Stackebrandt, E., C. Sproer, F. A. Rainey, J. Burghardt, O. Pauker and H. Hippe.** 1997. Phylogenetic analysis of the genus *Desulfotomaculum*: Evidence for the misclassification of *Desulfotomaculum guttoideum* and description of *Desulfotomaculum orientis* as *Desulfosporosinus orientis* gen. nov., comb. nov. Int. J. Syst. Bacteriol. **47**:1134-1139.

[160] **Streams, M. E., C. R. Fisher and A. FialaMedioni.** 1997. Methanotrophic symbiont location and fate of carbon incorporated from methane in a hydrocarbon seep mussel. Mar. Biol. **129**:465-476.

[161] **Strous, M., J. A. Fuerst, E. H. M. Kramer, S. Logemann, G. Muyzer, K. T. van de Pas-Schoonen, R. Webb, J. G. Kuenen and M. S. M. Jetten.** 1999. Missing lithotroph identified as new planctomycete. Nature **400**:446-449.

[162] **Strous, M., J. G. Kuenen and M. S. M. Jetten.** 1999. Key physiology of anaerobic ammonium oxidation. Appl. Environ. Microbiol. **65**:3248-3250.

[163] **Strous, M., E. VanGerven, P. Zheng, J. G. Kuenen and M. S. M. Jetten.** 1997. Ammonium removal from concentrated waste streams with the anaerobic

ammonium oxidation (anammox) process in different reactor configurations. Water Res. **31**:1955-1962.

[164] **Sweerts, J., D. Debeer, L. P. Nielsen, H. Verdouw, J. C. Vandenheuvel, Y. Cohen and T. E. Cappenberg.** 1990. Denitrification by sulfur oxidizing *Beggiatoa* spp mats on fresh-water sediments. Nature **344**:762-763.

[165] **Tajima, F.** 1983. Evolutionary relationship of DNA sequences in finite populations. **105**:437-460.

[166] **Takai, K. and K. Horikoshi.** 1999. Genetic diversity of archaea in deep-sea hydrothermal vent environments. Genetics **152**:1285-1297.

[167] **Tatusova, T. A. and T. L. Madden.** 1999. BLAST 2 SEQUENCES, a new tool for comparing protein and nucleotide sequences (vol 174, pg 247, 1999). FEMS Microbiol. Lett. **177**:187-188.

[168] **Tebbe, C. C. and W. Vahjen.** 1993. Interference of humic acids and DNA extracted directly from soil in detection and transformation of recombinant DNA from *Bacteria* and a yeast. Appl. Environ. Microbiol. **59**:2657-2665.

[169] **Teske, A., T. Brinkhoff, G. Muyzer, D. P. Moser, J. Rethmeier and H. W. Jannasch.** 2000. Diversity of thiosulfate-oxidizing bacteria from marine sediments and hydrothermal vents. Appl. Environ. Microbiol. **66**:3125-3133.

[170] **Teske, A., K. U. Hinrichs, V. Edgcomb, A. de Vera Gomez, D. Kysela, S. P. Sylva, M. L. Sogin and H. W. Jannasch.** 2002. Microbial diversity of hydrothermal sediments in the Guaymas Basin: evidence for anaerobic methanotrophic communities. Appl. Environ. Microbiol. **68**:1994-2007.

[171] **Thompson, J. D., T. J. Gibson, F. Plewniak, F. Jeanmougin and D. G. Higgins.** 1997. The CLUSTAL_X windows interface: flexible strategies for multiple sequence alignment aided by quality analysis tools. Nucleic Acids Res. **25**:4876-82.

[172] **Thomsen, T. R., K. Finster and N. B. Ramsing.** 2001. Biogeochemical and molecular signatures of anaerobic methane oxidation in a marine sediment. Appl. Environ. Microbiol. **67**:1646-1656.

[173] **Valentine, D. L.** 2002. Biogeochemistry and microbial ecology of methane oxidation in anoxic environments: a review. Ant. von Leeuwen. **81**:271-282.

[174] **Van de Graaf, A. A., P. de Bruijn, L. A. Robertson, M. S. M. Jetten and J. G. Kuenen.** 1997. Metabolic pathway of anaerobic ammonium oxidation on basis of ^{15}N-studies in a fluidized bed reactor. Microbiol. **143**:2415-2421.

[175] **van der Maarel, M., R. R. E. Artz, R. Haanstra and L. J. Forney.** 1998. Association of marine archaea with the digestive tracts of two marine fish species. Appl. Environ. Microbiol. **64**:2894-2898.

[176] **Van Hook, A.** 1961. Crystallization: Theory and Practice. Reinhold, New York:.

[177] **von Stackelberg, M. and H. R. Muller.** 1954. Feste gashydrate. Z. fur Elektrochemie **58**:25.

[178] **Ward, D. M., C. M. Santegoeds, S. C. Nold, N. B. Ramsing, M. J. Ferris and M. M. Bateson.** 1997. Biodiversity within hot spring microbial mat communities: Molecular monitoring of enrichment cultures. Ant. von Leeuwen. **71**:143-150.

[179] **Watanabe, K., Y. Kodama, N. Hamamura and N. Kaku.** 2002. Diversity, abundance, and activity of archaeal populations in oil-contaminated groundwater

accumulated at the bottom of an underground crude oil storage cavity. Appl. Environ. Microbiol. **68**:3899-3907.

[180] **Weber, A. and B. B. Jorgensen.** 2002. Bacterial sulfate reduction in hydrothermal sediments of the Guaymas Basin, Gulf of California, Mexico. Deep-Sea Res. Part I-Oceanogr. Res. Pap. **49**:827-841.

[181] **Weimer, P., M. G. Rowan, B. C. McBride and R. Kligfield.** 1998. Evaluating the petroleum systems of the northern deep Gulf of Mexico through integrated basin analysis: An overview. Aapg Bull. **82**:865-877.

[182] **Wirsen, C. O., H. W. Jannasch and S. J. Molyneaux**. 1992. Results of studies concerning microbiota, p. *In* Chemosynthetic ecosystems study interim report, Appendix A., MacDonald, I.R. and Schroeder, W.W. (eds.), US Dept. Interior, Minerals Management Service, Gulf of Mexico, OCS Region, New Orleans.

[183] **Worrall, D. M. and S. Snelson**. 1989. Evolution of the northern Gulf of Mexico, with emphasis on Cenozoic growth faulting and the role of salt., p. 97-138 *In* The Geology of North America - An Overview, Bally, A.W. and R., P.A. (eds.), Geological Society of America, Boulder, CO.

[184] **Wu, J. H., W. T. Liu, I. C. Tseng and S. S. Cheng.** 2001. Characterization of a 4-methylbenzoate-degrading methanogenic consortium as determined by small-subunit rDNA sequence analysis. J. Biosci. Bioeng. **91**:449-455.

[185] **Zahnle, K., J. B. Pollack, D. Grinspoon and L. Dones.** 1992. Impact generated atmospheres over Titan, Ganymede, and Callisto. Icarus **95**:1-23.

[186] **Zatsepina, O. Y. and B. A. Buffett.** 1997. Phase equilibrium of gas hydrate: Implications for the formation of hydrate in the deep sea floor. Geophys. Res. Lett. **24**:1567-1570.

[187] **Zatsepina, O. Y. and B. A. Buffett.** 1998. Thermodynamic conditions for the stability of gas hydrate in the seafloor. J. Geophys. Res.- Solid Earth **103**:24127-24139.

[188] **Zhang, C. L.** 2002. Stable carbon isotopes of lipid biomarkers: analysis of metabolites and metabolic fates of environmental microorganisms. Curr. Opin. Biotechnol. **13**:25-30.

[189] **Zhang, C. L., Y. Li, J. D. Wall, L. Larsen, R. Sassen, Y. Huang, Y. Wang, A. Peacock, D. C. White, J. Horita and D. R. Cole.** 2002. Lipid and carbon isotopic evidence of methane-oxidizing and sulfate-reducing bacteria in association with gas hydrates from the Gulf of Mexico. Geol. **30**:239-242.

VITA

Heath J. Mills received his bachelors of Science degree from Duke University with a major in Biology and a certificate in Human Development. Prior to starting his graduate work at the Georgia Institute of Technology, he worked for two years as a Research Technician at Clark Atlanta University in Dr. Deena Kegler-Ebo's laboratory. While at Georgia Tech, Heath was a GAANN Fellow for three years and an IGERT Fellow for one year. In addition, he served two terms as the President of the Biology Graduate Student Association for two years and one year campus representative for *Science Next Wave*. Heath accepted a non-tenure tract Research Faculty position with the Department of Oceanography at Florida State University where he will be joining Dr. Joel Kostka's lab after graduation from Georgia Tech.